UNIVERSITY OF GHANA

COLLEGE OF BASIC AND APPLIED SCIENCES

IDENTIFICATION OF NATURAL PRODUCT-DERIVED COMPOUNDS THAT INHIBIT HIV-1 ENTRY INTO TARGET CELLS

BY

NNEKA PASCHALINE UGWU

(10640105)

THIS THESIS IS SUBMITTED TO THE UNIVERSITY OF GHANA, LEGON IN PARTIAL FULFILMENT OF THE REQUIREMENT FOR THE AWARD OF MPHIL. IN MOLECULAR CELL BIOLOGY OF INFECTIOUS DISEASE DEGREE

DEPARTMENT OF BIOCHEMISTRY, CELL AND MOLEULAR BIOLOGY

JULY 2019

DECLARATION

I, Nneka Ugwu Paschaline, do hereby declare that the work described in this dissertation is a product of my own research undertaken at the Department of Biochemistry, Cell, and Molecular Biology, University of Ghana, Legon under the supervision of Dr. Osbourne Quaye and Dr. Samuel Kojo Kwofie. I certify that no part of this dissertation has been previously submitted for a degree or any other qualification.

Signature…….. Date: 06-May-2020

Ugwu Nneka Paschaline

(Student)

Signature…… Date: 06/05/2020

Dr. Osbourne Quaye

(Supervisor)

Signature…..…… Date: 06-May-2020

Dr. Samuel Kojo Kwofie

(Co-Supervisor)

DEDICATION

I dedicate this work to my baby girl Zinachimdi, for being my greatest inspiration.

ACKNOWLEDGEMENT

I wish to express my profound gratitude to West African Centre for Cell Biology of Infectious Pathogens (WACCBIP), for the opportunity to come to Ghana and undertake my study in this prestigious institution. My utmost gratitude to my supervisors, Dr. Osbourne Quaye, Dr. Samuel Kojo Kwofie, and Dr. Edward Wright for their advice, encouragement, guidance, support, and generosity throughout this project. I am most grateful to my husband, Mr. Nnaemeka Korie for his encouragement and support during my studies. I would like to express my appreciation to all members of the virology lab of the Department of Biochemistry, Cell and Molecular Biology, University of Ghana, Legon especially Mr. Sylvester Languon for taking personal interests in the progress of my work. I would also like to thank Mr. Odame Agyapong for his immense help in the *in-silico* part of my work. I like to acknowledge my Ghanaian friends, Kwadwo Oworae and Magdalene Dogbe for always being there when I need and being the kind and generous friends.

CONTENTS **PAGE**

TABLE OF CONTENTS

LIST OF FIGURES

LIST OF TABLES

ABSTRACT

HIV-1 infection is mediated by the interaction between the host cellular CD4 receptor and co-receptors with HIV Envelope protein (Env). Inhibition of HIV entry into host cell presents a biological target for therapeutic intervention. Broadly neutralizing antibody (bNabs) are potent in neutralizing a broad range of HIV strains by binding to the Env and preventing entry into the host cell. VRC01 is a CD4 binding-site class bNabs that binds to the conserved CD4 binding region of Env. However, using antibodies as therapeutic agents pose challenges of low availability and high cost of production. Natural products that can mimic VRC01 bNabs by interacting with the conserved CD4-binding regions may serve as new generation of HIV-1 entry inhibitors, which are broadly reactive and potently neutralizing. This study aimed to identify natural products that mimic VRC01 broadly neutralizing antibody, by interacting with the CD4-bs of HIV-1 gp120 and inhibit viral entry into a target cell. A library of purchasable compounds derived from natural products was virtually screened against the HIV-1 gp120 of clade A/E recombinant 93TH057 (PDB: 3ngb) using AutoDock Vina, and LIGPLOT was used to elucidate the interactions between the compounds and the HIV-1 gp120 complexes. The compounds with the lowest binding energies were selected and further screened against gp120 of a reference HIV strain (HXB2). Pharmacological profiling of the compounds was undertaken using SwissADME. Ten selected compounds were purchased and used for cell-based antiviral infectivity inhibition assay using HXB2-env pseudotype virus. Three compounds, NP-005114, NP-008297 and NP-007382 inhibited entry of HIV HXB2 pseudotype virus into target cells, while the rest of the compounds showed no inhibitory activity against HIV entry into target cells. NP-005114, extracted from the seed of *T. chebula*, had IC_{50} of 10µg/ml. Protein-ligand interaction showed that NP-005114 had inter-molecular hydrogen bond interactions with eight and eleven amino acid residues on the CD4-

binding site of recombinant clades A/E and B HIV -1 gp120, respectively. NP-005114 had intermolecular hydrogen and hydrophobic interactions with Asp457, a critical amino acid residue in the Phe43 cavity of the HIV gp120 for recombinant clades A/E and B, respectively. Derived from the leaf of *Ginkgo biloba*, NP-008297 formed ten and four hydrogen bond interactions with amino acid residues of the CD4-binding site on HIV-1 gp120 of recombinant clades A/E and B, respectively. NP-008297 inhibited viral entry at IC_{50} of 15.5µg/ml. NP-007382 was derived from bacteria and interacted with five amino acid residues in the CD4-binding site of HIV-1 gp120 of recombinant clades A/E and B, via intermolecular hydrogen bond. The 50% inhibitory concentration of NP-007382 against viral entry into the target cell was 13.1µg/ml. These compounds inhibited the entry of HIV clade B pseudotype (HXB2) with an IC_{50} which was comparable to that of VRC01 (0.1-50 µg/ml) against HIV clade B pseudotypes and primary isolate. The interaction of the compounds with critical residues of the CD4-binding site of more than one clade of HIV-gp120 demonstrates the possibility of broad entry inhibition of other HIV clades. This is the first report of the characterization of NP-008297, NP-00738, and NP-005114 as HIV-1 entry inhibitors.

CHAPTER ONE

1.0. INTRODUCTION

Acquired Immune Deficiency Syndrome (AIDS) is a range of symptoms and diseases related to a compromised immune system that manifest in persons with the Human Immune Deficiency Virus (HIV) infection. According to UNAIDS 2016 factsheet, HIV has infected about seventy-six million people and has caused the death of 36 million individuals since the discovery of the disease (Pustil, 2016). About 1.8 million people became infected in 2016 alone (Pustil, 2016), making HIV epidemic control a global priority, as stated in the Millennium Development Goals (MDGs) (WHO, 2016). There is currently no therapeutic cure; however, early and chronic stages of HIV infection are managed with antiretrovirals (ARVs). Antiretroviral therapy (ART) is a lifelong therapy, that suppresses viral replication to undetectable levels in the plasma, allowing the CD4 cells to rebound. Highly Active Antiretroviral Therapy (HAART) has been successfully used in treating HIV infection and reduction of viremia to an undetectable level in HIV infections, thereby improving the immune system (Kaufmann & Rosenberg, 2003). HAART is a mixture of two or more classes of Anti-Retroviral (ARV) drugs that inhibit several points in the HIV-1 life cycle (Chesney, Morin, & Sherr, 2000). Currently, four classes of ARVs; Reverse Transcriptase Inhibitors (RTIs), Protease Inhibitors (PIs), Entry Inhibitors, and Integrase Inhibitors have been approved for use in the treatment of HIV-1 infection (Stolk & Lüers, 2004). While these ARVs are very useful in treating and managing the viral infection, the drugs do not entirely get rid of the HIV infection, and continuous use poses risks of toxicity, adverse side effects, and development of resistant virus strains (Broder, 2010).

HIV infection of host cells begins with entry into the host cell, followed by deposition of viral genetic material into the host cell. Once inside the host cell, the RNA genome is reverse transcribed

to cDNA and integrated into the host genome, by the viral enzymes, reverse transcriptase and integrase respectively to make the provirus. The provirus undergoes either lytic (actively replicative) or latent (dormant) cycle. In the lytic cycle, the provirus is transcribed and translated into viral RNA and proteins, respectively, which are cleaved and processed by the viral enzyme protease and packaged into new viral particles. The new viral particles bud off the host cell, taking the host cell's outer membrane as the envelope. HIV-1 entry is a complex interaction of host cell CD4 receptor and chemokine co-receptors (CXCR4 and CCR5) with the HIV env protein (trimer of gp120 non-covalently bound to gp41) in a process that comprises attachment to the host cell, binding of CD4 receptor , co-receptor binding, cell fusion, and deposition of viral genetic material (Wilen, Tilton, & Doms, 2012). Targeting HIV-1 entry into the host cell presents opportunities for therapeutic intervention as treatment and prevention strategy of the HIV infection (Haqqani & Tilton, 2013; Henrich & Kuritzkes, 2013). The current ART targets various steps in the viral life cycle, however, only Enfuvirtide (fusion inhibitor) and Maraviroc (CCR5 antagonist) have been approved for use clinically in the HIV treatment, by the US Food and Drug Administration (FDA) as targets of the viral entry (entry inhibitors) (Henrich & Kuritzkes, 2013). Some limitations are associated with the clinical use of these entry inhibitor drugs for the treatment of HIV infections. Treatment with maraviroc is associated with the emergence of CXCR4 tropic viruses (Fätkenheuer et al., 2008; Gulick et al., 2008), enfuvirtide is a large polypeptide administered subcutaneously which is associated with painful injection sites and therefore has limited the clinical use of the drug (Lazzarin et al., 2003). There is the need for research focused on development HIV-1 entry inhibitors to target various steps of the HIV-1 entry into the host cell.

HIV-1 Broadly Neutralizing antibodies (bNAbs) are monoclonal antibodies that solely target the HIV-1 Env protein; they possess exceptional potency and breadth against variant strains of HIV-1.

bNAbs have been isolated from about 20-30% of individuals who are chronically infected with the virus (Binley et al., 2004) out of which 1% of the infected persons are termed the "elite neutralizers" (Simek et al., 2009). These bNabs have been shown to completely prevent Simian-Human Immunodeficiency Virus infections in other primates (Hessell et al., 2009), suppress viremia in HIV-1 infected individuals (Caskey et al., 2016), and effectively control HIV-1 infection and suppress viremia in humanized mice even after discontinuing therapy for about sixty days owed to the longer half-life of the antibodies compared to ARVs (Halper-Stromberg et al., 2014; Horwitz et al., 2013; F Klein et al., 2012; Florian Klein et al., 2012). The remarkable breadth and potency of the bNabs are attributed to their ability to interact to conserved regions on the HIV Env protein (Wibmer, Moore, & Morris, 2015; Wu et al., 2010). Based on their epitopes of interaction on the HIV-1 Env protein, bNAbs is grouped into five classes: CD4 binding site(CD4bs), gp120 and gp41 interface, high mannose patch, the membrane proximal region (MPER), and trimer apex of HIV Env (McCoy, 2018). CD4 binding site (CD4bs) class bNAbs exhibit high potency and breadth to variant HIV strains, this is mainly because CD4bs is one the most functionally conserved sites of the HIV-1 Env protein. The CD4bs is required for initial CD4 binding and successful infection of host cell by HIV (Scheid et al., 2011). VRC01 is an example of CD4bs bNAbs with neutralization breadth of about 80-90% HIV strains and high potency of IC_{50} of 0.33µg/ml using HIV group M envelope pseudotype virus (Wu et al., 2011). VRC01 shares 98% similarity with CD4 with respect to their binding site on HIV-1 gp120 (T. Zhou et al., 2010), however, they differ in CD4 preference for gp120 in an unbound state, while VRC01 has an affinity for gp120 in both CD4 bound and unbound state. Other similarities of CD4 and VRC01 include the hydrogen bonding interaction between $Arg59_{CD4}$ and $Gly54_{VRC01}$ with $Asp368_{gp120}$. Additionally, there is a significant correlation between VRC01 and CD4 amino acids residues of interaction in gp120 (T. Zhou et al., 2010).

VRC01 bNAbs have demonstrated efficacy in the prevention of HIV in humanized mice, prolonged the time of HIV rebound during treatment interruption (K. J. Bar et al., 2016) and it is currently in clinical trials for prevention of HIV transmissions in human (Mayer et al. , 2017a) (;).

The use of antibodies as therapeutic agents has been FDA approved for cancer treatment, prevention and treatment of some viral infections, they also possess the advantages of safety and specificity over chemical therapeutics (Salazar, Zhang, Fu, & An, 2017; Scott, Wolchok, & Old, 2012). There is currently no HIV antibody approved for clinical use; despite promising results as a potential therapeutic agent, this is due to various challenges associated with the development of antibodies as therapeutics. These challenges include; laborious and time-consuming antibody production techniques, high cost of production, the stability of the antibody, and risk of treatment failure due to host to host variation (Awi & Teow, 2018). In order to overcome these challenges, small molecule mimetics of large biological molecules can be developed as therapeutic agents against HIV infection. Peptidomimetics are compounds that functionally and structurally mimic biological molecules like proteins and peptides, but with improved properties in terms of selectivity, potency, oral bioavailability, and reduced side effect (Vagner, Qu, & Hruby, 2008). These compounds are designed to mimic protein-protein interaction between a biological receptor and its ligand. The concept of peptidomimetics is not new in drug discovery and development, and have been used successfully in the development of FDA approved peptide inhibitors such as ACE inhibitors, Thrombin inhibitors, and HIV-1 protease inhibitors (Kikelj, 2003; Ripka & Rich, 1998). Various strategies have been employed in developing peptidomimetics, and in current times computational approaches like molecular modelling, molecular docking, molecular dynamics, virtual high throughput screening, quantitative structural activity relation (QSAR) etc., have gained popularity in peptidomimetics drug design (O. N. Akram et al., 2014; Doro et al.,

2015; Duprez et al., 2015; Frecer, Berti, Benedetti, & Miertus, 2008). The shift in dynamics towards computational drug design is due to the advantages it offers over the traditional high throughput screening (HTS) and combinatory medicinal chemistry. Computational drug discovery increases the rate of identifying novel drug-like compound at a lowered cost than conventional HTS, elucidate the molecular mechanism for therapeutic activity of drug compound, guide lead compound optimization by predicting the most biologically active and pharmacologically effective derivative, and overall lessen the time and cost of early drug discovery (Sliwoski, Kothiwale, Meiler, & Lowe, 2014a). Current improved technologies in HIV pseudotype production and computational drug discovery have led to the development of small compound mimetics of CD4 receptor, chemokine co-receptors inhibitors as HIV entry inhibitors (A M Andrianov, Kashyn, & Tuzikov, 2013; Alexander M. Andrianov, Kashyn, & Tuzikov, 2014; Courter et al., 2014).

This study seeks to use a computational approach to identify compounds derived from natural products that mimic broadly neutralizing antibody VRC01 in interaction with the conserved amino acid residues of CD4-bs and assess the inhibitory activity of these peptidomimetics compound on HIV-1 infection of host cell using pseudotype technology.

1.1. RATIONALE

Due to the high incidence of HIV infection and the unavailability of a therapeutic intervention that will completely eliminate the infection, there is the need to exploit potential compounds for treatment and as prophylaxis. BNAbs have proven to be very potent for use as a therapeutic intervention for HIV infection, but the isolation of the antibodies is associated with high cost, and the large size of the macromolecule poses challenges of oral delivery as therapeutics. Therefore, identifying compounds that will mimic bNAbs may offer a cost-effective and efficient therapeutic agent that can be utilized as pharmacophores in bNAbs-based HIV-1 entry inhibitor drug development.

1.2. HYPOTHESIS

Compounds derived from natural products that mimics HIV-1 broadly neutralizing antibody, by interacting with the conserved amino acid residues of HIV-1 gp120 will inhibit the HIV infection of target cells.

1.3. AIM

To identify mimetics of HIV-1 broadly neutralizing antibody VRC01 from a natural product-derived compound library that can inhibit HIV infection of target cells

1.4. SPECIFIC OBJECTIVES

The specific objectives are:

i. Identify compounds derived from natural products that mimic VRC01 via high-throughput virtual screening (vHTS).
ii. Cell-based neutralization assay to quantify the infectivity inhibition concentration of the selected compounds obtained from vHTS.

CHAPTER TWO

2.0. LITERATURE REVIEW

2.1. HUMAN IMMUNODEFICIENCY VIRUS (HIV)

2.1.1. Virology

Human Immunodeficiency Virus (HIV) belongs to the genus Lentivirus and family Retroviridae. HIV is a single-stranded, enveloped, +sense RNA virus. The viral genome contains two identical single-stranded RNA, each sized approximately 9.8kb. The genome is encased in a cone-like capsid to form the nucleocapsid. The viral genome has nine ORFs, the major ones: pol, gag, and env that encodes for essential enzymes; structural proteins Tat and glycoprotein Rev which encode for regulatory proteins; and Vpu, Vpr, Vif, and Nef which codes for the accessory proteins necessary for viral replication. Long terminal repeats (LTRs), required for viral integration and replication, surrounds the viral genome (Sundquist & Kräusslich, 2012; B. G. Turner & Summers, 1999).

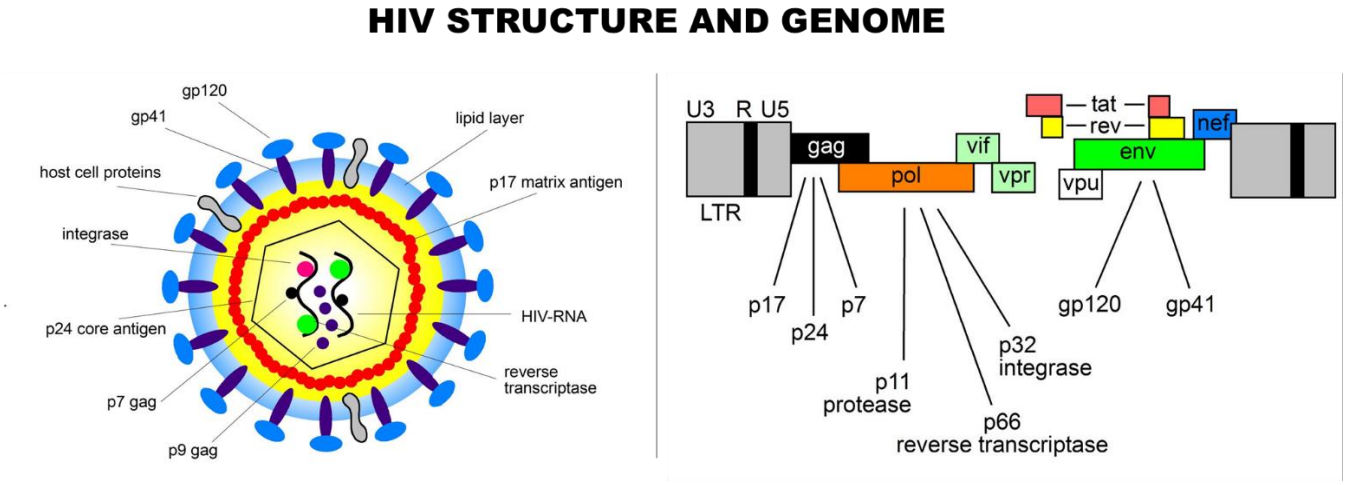

Figure 1. *The structure and genome organization of the nine protein-coding genes of HIV* (Altfeld, *et al*. 2011. HIV 2011. https://www.hivbook.com/tag/structure-of-hiv-1/)

Based on the genetic makeup of HIV, two types of HIV are known: HIV-1 and HIV-2. HIV-1 is characterized by high virulence, infectivity, and ease of transmission, and is responsible for global HIV pandemic. There are four major types (M, N, O and, P), Group M is the primary cause of global HIV infections and has been further classified into nine subtypes or clades (A-D, F-H, J, and K) and other circulating recombinant strains (CRFs). HIV-2, on the other hand, is less virulent compared to HIV-1 and its occurrence is mostly restricted to West Africa, HIV-2 has 5 major groups (A, B, C, D and, E), where group A and B are the significant and well-studied group (Taylor, Sobieszczyk, McCutchan, & Hammer, 2008).

HIV can infect various host immune cells, such as $CD4^+$ T-lymphocyte cells, microglial cells, and macrophages. HIV infection of host cells begins with cell entry, which is mediated by the interaction between the envelope protein of the virus with CD4 receptors and chemokine (CCR5 and CXCR4) co-receptors from the host cell. The receptor and co-receptor interaction are followed by viral and target cell membrane fusion and deposition of viral genetic material into the host cell. Once inside the host cell, the viral RNA genome is converted to cDNA through reverse transcription by reverse transcriptase in the virus, and then the viral cDNA is integrated into the host genome by the viral enzyme called integrase. The host genome carrying the viral genome (provirus) can either go through the latent viral cycle, where it is dormant or the actively replicative phase (lytic cycle), where the host cell machinery is hijacked for viral replication. In the active replicative cycle, the provirus is transcribed into RNA and subsequently translated into viral proteins, which are cleaved and processed by the viral enzyme protease. The processed proteins are packaged with the addition of full-length untranslated viral RNA into new viral particles, which buds of the host cell, taking the outer membrane of the host cell as envelope (Campbell & Hope, 2008; U.S. Department of Health and Human Services, 2016).

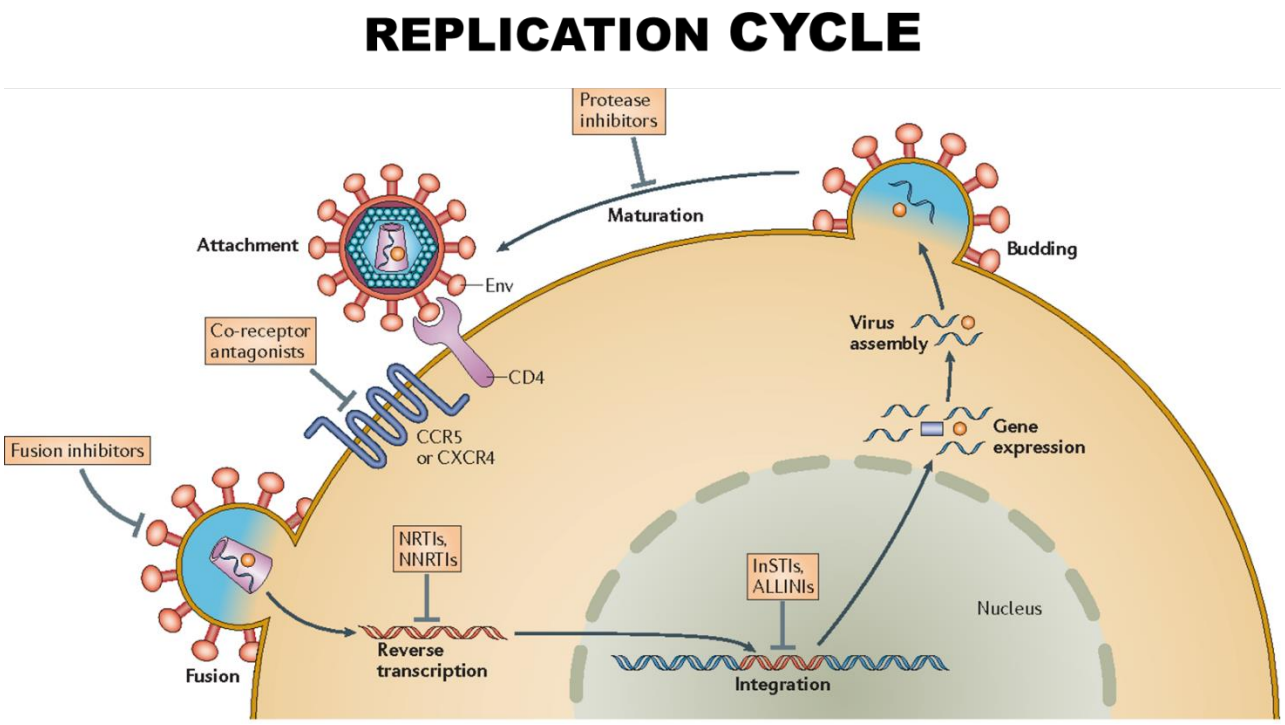

Figure 2. The life cycle of HIV. *Starting from attachment to the host cell, deposition of the viral genome, reverse transcription, integration, replication, packaging, assembly, and budding off as the new viral particles (Freed, 2015).*

2.1.2. Pathogenesis

HIV causes HIV infection, and in advanced stage leads to acquired immunodeficiency syndrome (AIDS). AIDS is characterized by a dilapidating host immune system that allows the thriving of life-threatening opportunistic infections. In the early stage of HIV infection, viral replication is very high, and may or may not present with clinical symptoms. Mild flu-like symptoms, rashes, muscle pain, and fever that usually last for a few weeks is typical of acute infection stage. HIV antibodies become detectable in the serum of infected person around 6–18 weeks after infection (Stine., 2000). The incubation period of HIV infection is long and highly variable among individuals (5-11 years), and it is asymptomatic which correlates to low viral

replication combined with a periodic increase in viremia and a slight decrease in CD4 cells number. Without intervention, most infected persons progress to AIDS, which is the last stage characterized by highly deficient immunity and an influx of opportunistic infections and eventual death. However, treatment with antiretroviral therapy (ART) increases the survival chance of HIV infected individual allowing for long healthy life. Aside from the two extremities (with ART and without ART intervention), There are individuals with a characteristically long asymptomatic period, even without ART intervention. These individuals are grouped into three main classes: Long term non-progressors (LTNP), Viraemic controllers, and 'Elite controllers.' LTNP are HIV infected ART naïve individuals with stable CD4 count about 500cells/ml, and minimal viral replication copy, the status of LTNP can be lost due to decline in the CD4 level and increase viremia, which may take longer time than other HIV infected individual but happens eventually (Madec et al., 2009). Elite controllers are ART-naive HIV infected patients with viremia (below 1000 copies/ml), quantified at least 3 times for 12 months, while Viraemic controllers are distinguished from the 'Elite controllers' by the level of the HIV RNA viral load which is in the range of 1000–2000 copies/ml (Okulicz & Lambotte, 2011).

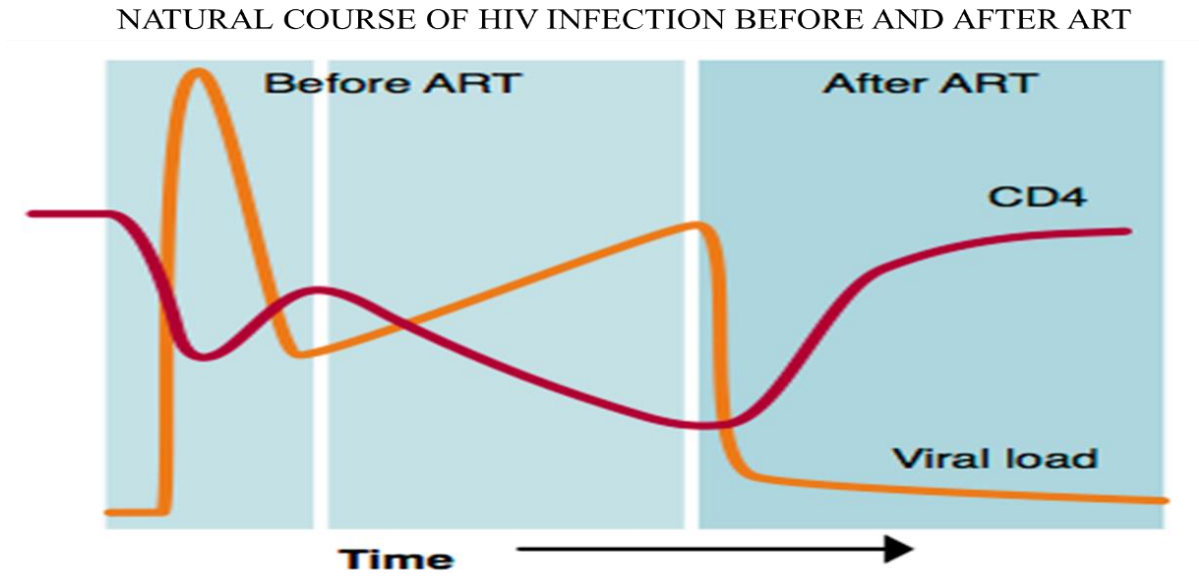

Figure 3. The natural history of HIV infection before and after ART. Before *ART, there is a decline in the CD4 levels with increased plasma viral load, however with ART, the viral is reduced to the minimal levels in the plasma, and the CD4 levels are increased* (Vergis & Mellors, 2000).

2.1.3. Transmission, Treatment, and Control

HIV infection is through contact with body fluids containing HIV infected cells and/or infectious virion. HIV is present in virtually all the body fluids of an infected person; however, the transmission usually occurs through blood, breastmilk, vagina, semen, and rectal fluids (Maartens, Celum, & Lewin, 2014). The most common paths of HIV infection are penetrative sexual intercourse, blood transfusion, breastfeeding, injective drug use, vertical transmission from mother to child (Shaw & Hunter, 2012). There is currently no therapeutic cure; however, early and chronic stages of HIV infection are managed with antiretroviral drug (ARVs). Antiretroviral therapy (ART) is a lifelong therapy, which does not completely eradicate the virus from the infected individual but suppresses viral replication to undetectable levels in the plasma, allowing the CD4 cells to rebound. The main aim of the ART is to prolong a healthy life of the HIV infected person through the

suppression of viral replication, which slows down the disease progression and prevent opportunistic infections that lead to clinical diseases. Successful ART treatment is defined as maintaining a plasma viral load of <1000 copies/ml after six months on ART (World Health Organisation, 2016). Discontinuing ART can result in the rebound of plasma viral load and the decline of CD4 levels, it also increases the risk of acquiring drug resistance. ART is also used for pre and post-exposure prophylaxis (PrEP and PEP), as a prevention tool for most at risk population like couples in serodiscordant relationship, maternal to child transmission (MTCT) and victims of sexual assaults (Centers for Disease Control and Prevention, 2014; Maartens et al., 2014). Antiretrovirals suppress viral replication because they are designed to target different steps in the viral replication cycle. Since the introduction of Zidovudine (AZT) about 3 decades ago, there are currently more than 2 dozen FDA approved ARVs, each fallen under the six classes of ARVs [Chemokine receptor antagonist, Fusion inhibitors, Nucleoside/nucleotide analogue reverse transcriptase inhibitors (NRTIs), Nonnucleoside analogue reverse transcriptase inhibitors (NNRTIs), Protease inhibitors (PIs), and Integrase inhibitors] (Dickinson, Khoo, & Back, 2010).

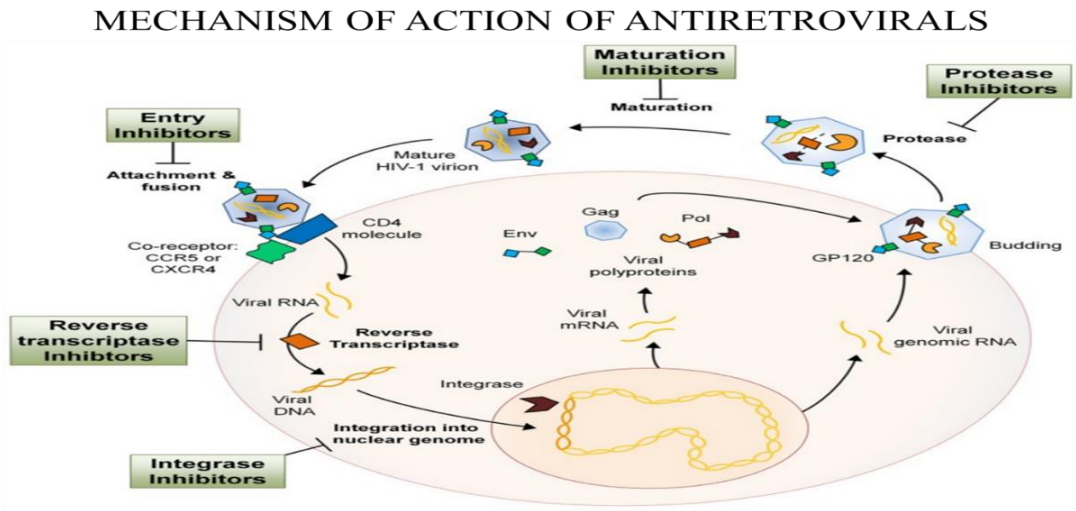

Figure 4*. Classes of antiretrovirals, their targets on the HIV life cycle, and mechanism of action* (Smith, de Boer, Brul, Budovskaya, & van der Spek, 2013).

Various intervention strategies have been employed for HIV epidemic control; the aim of this epidemic control is to prevent onward transmission of HIV while maintaining healthy living for people living with HIV. Among the various strategies includes:

1) Eliminating mother to child vertical transmission through a comprehensive Prevention of Mother to Child Transmission (PMTCT) (WHO, 2010)

2) Expanding HIV prevention through the combination of behavioural, medical, social, and structured HIV prevention intervention strategy tailored to reduce new infections like the use of pre and post-exposure prophylaxis (Baeten et al., 2012), use of male and female condoms, male circumcision, etc.

3) Scaling up HIV testing and counselling to the whole population well-structured treatment strategy (Suthar et al., 2013),

4) Prevention by treatment, i.e., using antiretroviral drugs to suppress viral replication in infected persons such that they cannot transmit HIV (Nichols, Boucher, & van de Vijver, 2011). All these strategies are not used in isolation but effective when used together (UNAIDS, 2014).

2.1.4. Antiretroviral Drug Resistance

The use of ARVs for treatment and prevention of HIV infections have had a remarkable impact on the epidemic control of HIV and increasing the life expectancy of individuals living with HIV. Despite the significant effort in scaling-up ART globally there are still gaps in quality ART delivery service, including poor treatment retention (Nachega, Mills, & Schechter, 2010), non-compliance to the ARVs, unavailability of ARVs, and suboptimal treatment monitoring (Obiako & Muktar, 2010). HIV Drug Resistance (HIVDR) has been described as the ability of HIV to replicate and

infect cells in the presence of ARVs (S Bertagnolio, Beanland, Jordan, Doherty, & Hirnschall, 2017).

HIVDR is due to mutations in the genetic material of the virus that diminishes the ability of a class of ARV or a combination of ARVs to inhibit viral replication; these mutations could be caused by the error-prone HIV reverse transcriptase, high replication rate, selective drug pressure, and suboptimal drug in the blood. HIVDR have grave consequences on the epidemic control of HIV like ART treatment failure and increased infection and re-infection with a drug-resistant virus, increasing the incidence of HIV infection, morbidity, and mortality (S Bertagnolio et al., 2017). WHO has projected the percentage contribution of HIVDR on AIDS-related death, new infections and increased cost of ART in sub-Saharan Africa as 16%, 8.7%, and 7.7% respectively from the year 2016 – 2030 (Phillips et al., 2017).

HIVDR is broadly categorized into three (Silvia Bertagnolio, Beanland, Jordan, Doherty, & Hirnschall, 2017):

1. Acquired drug resistance (ADR), described as the resistance that develops in HIV infected person receiving ART, caused by spontaneous mutation arising from rapid viral replication
2. Transmitted drug resistance (TDR), this is HIVDR found in HIV infected persons with no exposure to antiretroviral drugs (ARV naïve), the resistance virus is usually transmitted to a person and not developed like the ADR
3. Pre-treatment drug resistance (PDR), this resistance is prevalent in individuals with previous exposure to ARVs either as prophylaxis or treatment interruptions. PDR can be acquired during exposure to ARVs or transmitted at the point of infection.

2.2. HIV BROADLY NEUTRALIZING ANTIBODIES

HIV-1 neutralizing antibodies were first considered as a possible therapeutic agent people with HIV infections. Early approaches in the 1980s used serum from HIV infected patients with high titre of antibodies that recognize the HIV capsid (Jackson et al., 1988), by 1990 HIV-1 envelope protein was established as the sole target of the neutralizing antibodies and not the capsid (Karpas et al., 1990). In the early 2000s, the first generation of monoclonal neutralizing antibodies (NAbs) that targets various epitopes on the HIV-1 envelope protein were isolated, characterized and pursued for immunotherapy (Jaworski, Vendrell, & Chiavenna, 2017). The first set of NAbs isolated that target the HIV envelope protein include 4E10 and 2F5 (binds to epitopes on the gp14 ectodomain) and 2G12 (binds to N-linked glycan of gp120). These antibodies were well tolerated and safe. However, they only show modest suppression of viremia and resistance were seen for the 2G12 antibody (Jaworski et al., 2017). The significant challenges of the NAbs are the HIV envelope protein, which is heavily glycosylated and have variable loops; this variation causes problems with recognition of the epitopes and subsequent immune escape (Stephenson & Barouch, 2016). The emergence of resistance, few numbers, narrow spectrum HIV target, and low potency limited the practical use of these NAbs. In recent years, with cutting edge technology in HIV research, pseudotype virus production, B-cell technology, and high throughput neutralization assay, etc., there has been a dramatic change in the field of HIV-1 neutralizing antibodies. A subset of HIV-1 infected people called “elite neutralizer*s” have been identified; the individuals can generate high titers of highly potent and broadly active neutralizing antibodies termed broadly neutralizing antibodies (bNAbs). This new generation bNAbs have shown high efficacy in reducing viremia in both human and animal model, and they are being explored for their use in HIV prevention, treatment and possibly eradication (Altfeld et al., 2015; McCoy & Burton, 2017).

2.2.1. Targets for HIV-1 Broadly Neutralizing Antibodies (bNAbs)

HIV-1 envelope protein that mediates host cell entry is the only target of broadly neutralizing antibodies. The envelope protein (glycoprotein), collectively termed as gp160, consist of a trimer of extracellular receptor binding gp120 bound noncovalently to three transmembrane protein gp41. The HIV-1 gp120 is covered with a glycan shield and protected by regions: V1, V2, V3, V4, and V5 loops, and alpha helix, and β14 sheet which are hypervariable. The gp41 protein however, has less glycosylation, is conserved, and is shielded from solvent (Shen, Raska, Bimczok, Novak, & Smith, 2014; Wilen et al., 2012). The HIV-1 envelope protein shows the most genetic variation between subtypes due to pressure from the host immune system, these variations are due to mutations and glycan shifts that occur mostly in the variable region of the glycoprotein. Due to these genetic variabilities, the first isolated neutralizing antibodies (NAbs) are strain specific and have a narrow spectrum. Elite neutralizers, which are HIV infected individuals that have developed antibodies that are highly potent across a broad range of HIV strains called broadly neutralizing antibodies (bNAbs) (Hraber et al., 2014). B-cell technology advancements have led to the isolation of bNAbs and characterization of their epitopes of interaction on the HIV envelope protein (Walker, Huber, Doores, Falkowska, Pejchal, Julien, Wang, Ramos, Chan-Hui, Moyle, Mitcham, Hammond, Olsen, Phung, Fling, Wong, Phogat, Wrin, Simek, Koff, et al., 2011), five defined sites of interaction of bNAbs have been identified on the HIV Env: CD4 binding sites, V2 site, gp120-41 interface, membrane proximal external region (MPER), and N332 supersite.

2.2.2. The V2 site

The V2 site is formed by the joining of amino acid sequence from the V1 domain, V2 domain, and V3 loop of HIV Env conserved region. It is found at the apex of the gp120 trimer, and it is shielded by tightly packed glycan at N160 and N156 position, and the V1 and V2 hypervariable loops (J. H.

Lee et al., 2016). Antibodies that interact with the V2 site have a remarkably long loop three heavy chain Complementarity Determining Region (CDR-H3) that is anionic (Nicole A. Doria-Rose et al., 2014). PG9 and CAP256-VRC26 are antibodies that target the V2 sites, PG9 interact with glycan N160 from two different promoters while CAP256-VRC26 is not glycan N160 dependent (Nicole A. Doria-Rose et al., 2014; J.-P. Julien et al., 2013; Loving, Sjoberg, Wu, Binley, & Garoff, 2013). Despite the differences in their binding, both antibodies have a short stretch of seven cationic amino acids at the 165-171 position, as their primary peptide epitope. The breadth of these antibodies is most likely due to the conserved nature of the peptide epitope and the glycans (N. A. Doria-Rose et al., 2012).

2.2.3. The N332 supersite

The N332 supersite has several overlapping epitopes that are dependent on glycan, the most well characterized of these epitopes is the V3 epitope, which is structurally close to the V2 site (Kong et al., 2013). V3 antibodies show similarity to V2 antibodies, as they interact with a short peptide epitope of eight amino residue between position 323 -330 using their long CDR-H3 (Pejchal et al., 2011). Most V3 antibodies are glycan-dependent, PGT128 and PGT121 interact N332 and N301 glycans, PGT121 somatic variants also interact with V1 (N137) and V2 (N156) glycans (J. P. Julien et al., 2013; Walker, Huber, Doores, Falkowska, Pejchal, Julien, Wang, Ramos, Chan-Hui, Moyle, Mitcham, Hammond, Olsen, Phung, Fling, Wong, Phogat, Wrin, Simek, Koff, et al., 2011). Somatic variation in the antibodies that leads to recognition of variant V3 sites immunotypes has been identified. Antibodies PGT130 and PGT128 are V3 antibodies isolated from the same individual, while PGT128 interacts with N332 glycan, PGT130 prefers N334 glycan which is mutually exclusive to the N332 glycan. The co-evolution of these two antibodies in a single individual

indicates the effect of virus variation in the maturation of bNAbs (Doores et al., 2015; Moore, Williamson, & Morris, 2015).

The second epitope of the supersite distinct from V3 site is defined by the antibody PGT135. PGT135 interacts with the basal V4 loop amino acids, and unlike PGT128 of the V3 site, it binds mainly to the non-polar side of N332 glycan, N295, N392, and N386 glycans (Kong et al., 2013)

The third defined epitope of the supersite overlaps with the epitope of PGT135 without contact with the V4 peptide. An antibody that interacts with this epitope id 2G12, 2G12 uses a rare swap of the variable domain of its heavy chain to form a paratope that can bind to the terminal sugars of N295, N332, N339 and N392 glycans located at the gp120's silent face. Although 2G12 interacts with similar glycan as PGT135, it does not penetrate the glycan shield (Calarese et al., 2003; Scanlan et al., 2002).

2.2.4. The CD4 binding site

CD4 binding site antibodies (CD4bs) makes little or no contact with glycans on the HIV Env. The most extensively characterized mode of interaction of the CD4bs antibodies is that VH1-46 or VH1-2 derived antibody, e.g., 8ANC131 and VRC01. These bNAbs can mimic CD4 binding to gp120, e.g., Arg71 of the heavy antibody chain interact with highly conserved Asp368 of gp120 CD4 binding loop, which is similar to the interaction of Arg59 of CD4 and Asp368 of gp120 (Scheid et al., 2011; T. Zhou et al., 2013). The VH1-2 derived antibodies possess an untypical short CDR-L3, which helps prevent interaction with the N276 glycan in the gp120 loop D (McGuire et al., 2013). The second subsite for CD4bs is defined by the VH3-30, typified by HJ16 bNAbs. HJ16, unlike VH1-2 antibodies, has no interaction with Asp36, but neutralization effect is entirely dependent on the N276 glycan (Balla-Jhagjhoorsingh et al., 2013). The VH3-30 derived antibodies possess long

CDR-H3 loops used for interaction with the g120. However, this interaction is hindered by the large glycan shield and the gp120 trimer quaternary nature (Corti et al., 2010).

2.2.5. The gp120–gp41 Interface

8ANC195 bNAb has been shown to bind to an epitope of the gp120–gp41 interface. 8ANC195 interaction is N234 and N276 glycan-dependent and uses the insertion of four amino acid residues to push its heavy chain in-between the N234 and N276 glycan making contact with Arg456 at the tip of gp120. The CDR-H3 of 8ANC195 comprises of 22 amino acids. However, it is not used for the penetration of the glycan shield. The long CDR-H3 forms part of a wide paratope by folding towards the light chain, the paratope formed is then used to make contact with the gp41 interacting region (7-stranded β-sandwich) of gp120 (Scharf et al., 2014), making 8ANC195 the first bNAbs identified to target epitopes in the gp120–gp41 interface.

Antibodies 35O22 and PGT151 also target the gp120–gp41 interface; however, they do not bind to the monomeric form of gp120. 35O22 uses its FWR3 eight amino acid insertion to interact with an epitope near N234 glycan and adjacent to the 8ANC195 epitope, this interaction has close contact with the seven-stranded β-sandwich (Pancera et al., 2014). PGT151 epitope is close to the cavity between the protomers of gp160, sandwiched in-between the 35O22 and 8ANC195 epitopes. PGT151 requires a specifically cleaved trimer and a maximum of two antigen-binding fragments (Fabs) on each trimer. This binding mechanism suggests the alteration of a third binding site allosterically after the binding first two Fabs and allows the stabilization of natively cleaved Env trimer from the cell membrane by PGT151 (Blattner et al., 2014).

Neutralization of both 35O22 and PGT151 are highly dependent on glycans in their respective epitopes, 35O22 requires N88, N230, and N241 glycans in the gp120, while PGT151 favors N611 and N637 glycans at gp140 (Falkowska et al., 2014; J. Huang et al., 2014)

2.2.6. The Membrane Proximal External Region (MPER)

The gp41 MPER epitopes are contained exclusively in an α-helical stretch of linear amino acids that connects the ectodomain and transmembrane of gp41. The MPER is divided into C-terminal, and N-terminal helix wound around the position 674 twists, and it is used in defining various epitopes of the MPER. Antibodies 10E8 and 4E10 interact with a C-terminal helix epitope, 2F5 binds to an epitope of the N-terminal helix, and Z13e1 binds to an epitope in-between the N- and C- terminal helices. The MPER C-terminal is buried partially in the viral membrane, due to its hydrophobic nature. The MPER C-terminal is highly conserved due to their critical role in viral fusion with the host cell membrane, making the C-terminal antibodies (4E10 and 10E8) have the highest breadth of the MPER bNAbs (J. Huang et al., 2012). MPER bNAbs exhibit high levels of autoreactivity attributed to their interaction with the vital Env protein with their long CDR-H3 loops. It is worthy to note that before viral membrane fusion, the exact conformation and location of the MPER have not been adequately characterized (Montero, van Houten, Wang, & Scott, 2008).

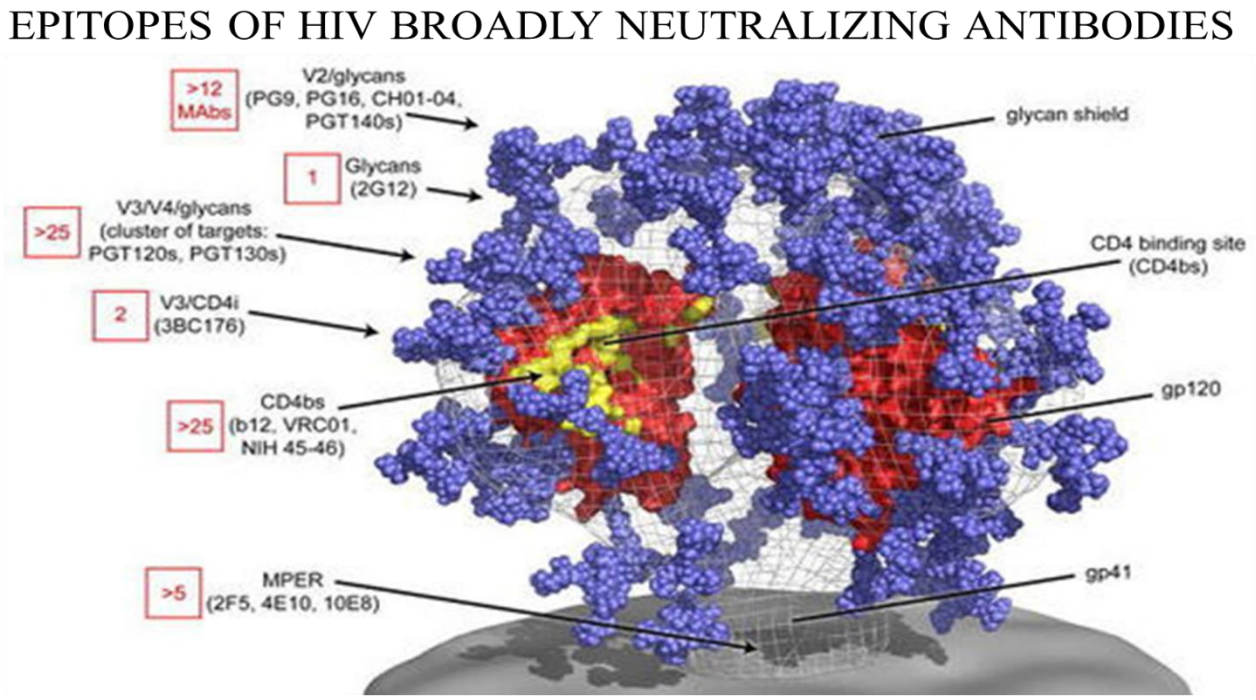

Figure 5. *Characterized targets and epitopes of HIV-1 broadly neutralizing antibodies on the HIV Env protein (Burton et al., 2012).*

2.3. PEPTIDOMIMETICS

Peptidomimetic can be defined as a compound that mimics natural peptide with structural and functional similarity to the native peptide. They are designed to interact with receptors of a native peptide with equal or higher affinity than the peptide to produce an agonistic or antagonistic effect. In medicinal and organic chemistry, the concept of peptidomimetics in drug development is relatively new and has shown immense promises designing new drug candidate. Peptidomimetics are designed to be more selective, biologically active and orally bioavailable than the native peptide, resulting in an efficacious drug candidate with reduced side effects (Pelay-Gimeno, Glas, Koch, & Grossmann, 2015; Vagner et al., 2008). The basic knowledge of the compound conformation is space, electronic features and interactions between the native peptide its active site on the receptor are required for the development of peptidomimetics (Vagner et al., 2008). The development of biologically active peptidomimetics requires: **i)** Substitution of the native peptide backbone with a non-peptide structure that preserves or enhances the biological activity of the native peptide and conservation of the biologically active side chains that make up the pharmacophore. **ii)** Designing a compound with similar pharmacophore as the native peptide by using knowledge of the 3D-structure of the native peptide in their bioactive conformation or by using the structural activity relationship (SAR) of the native peptide. **iii)** Introduction of various modifications such as addition of constraint, modification of chain length, replacement of cyclopeptide bond with covalent bond, etc. to the primary mimetics to enhance their bioactivity (Farhadi & Hashemian, 2018; Marshall, 1993; Vabenø, Haug, & Rosenkilde, 2015)**.**

2.3.1. Classes of Peptidomimetics

Peptidomimetics are classified into three groups based on their functional and structural properties (Ripka & Rich, 1998)

2.3.1.1. Structural mimetics (Type I) – Type 1 mimetics are a structural analog of the native peptide; they show similarity to the topography of the native substrate while possessing all the pharmacophore fingerprint responsible for the functional interaction with a receptor of the native peptide in a correct spatial orientation (Avan, Dennis Hall, & Katritzky, 2014).

2..3.1.2. Functional mimetics (Type II) - This type of mimetics has mainly functional similarity to the native peptide with little or no seeming structural similarity. The similarity is modeled based on the interaction of the native peptide and its receptor (Omar N. Akram et al., 2014)**.**

2.3.1.3. Functional-structural mimetics (Type III) - This class of mimetics consists of a scaffold without structural similarity to the native protein but possesses all the critical functional groups responsible for biological interactions arranged in a correct spatial orientation (Reese, Shanahan, Proulx, & Menegatti, 2020)**.**

2.3.2. Successful Examples of Peptidomimetic Drugs

The application of peptidomimetics in drug discovery has yielded fruitful results, especially in the development of protease inhibitors. Proteases are a crucial therapeutic target in numerous physio-pathologies; they play a crucial role in neuromodulators and peptide hormones through proteolytic regulation of peptide precursors. Common examples of peptidomimetic-based protease inhibitors Include thrombin inhibitors, human immunodeficiency virus (HIV) protease inhibitors, and angiotensin-converting enzyme (ACE) inhibitors.

2.3.3. HIV Protease Inhibitor (PI)

The HIV protease is a member of the hydrolase's superfamily and the aspartic family of protease that cleaves the peptide bond present in the protein. It is in charge for the processing of the gag-pol polyprotein precursor in the viral maturation stage. HIV protease is an essential biological target for therapeutic agents against HIV infection due to its essential role in viral replication and maturation. Protease inhibitors are active therapeutic agents against HIV infection as they act to hinder viral replication and maturation required for active viral infection. As an aspartic protease, HIV protease contains two aspartic acid residues in their active catalytic site, that is responsible for coordinating water molecule by through hydrogen-bonds (Eder, Hommel, Cumin, Martoglio, & Gerhartz, 2007; Seelmeier, Schmidt, Turk, & von der Helm, 1988). The HIV protease is a dimer, with an identical monomeric unit consisting of 99 amino acids. Each monomer contributes a single aspartic acid to the active site during the process of dimerization. HIV protease is divided into the core, the 'flap,' and the terminal domain. The 'core' domain also has a ß- sheet structure, it contains highly conserved Asp25-Thr26-Gly27 tripeptide motif found at the interface in both monomers, and it plays a vital role in the stability of the active catalytic site and the monomers. The 'flap' region is a flexible domain located above the active site formed by two ß-sheets in antiparallel orientation, which allows the peptide substrates/inhibitors to enter the catalytic site and the release of the peptide after cleavage. The terminal domain consisting of the C-and N- terminals are also responsible for stabilization of the two monomers and the formation of the homodimer (Dunn, Goodenow, Gustchina, & Wlodawer, 2002; Fairlie et al., 2000)**.**

Pepstatin is a natural peptide inhibitor of HIV protease but has limitation in therapeutic use due to the characteristic properties of quick excretion from the bile, lipodystrophy side effect, and low oral availability. Additionally, the emergence HIV resistant strain reinforces the need to develop new

generation protease inhibitors (Mahmoud, Hrapovic, & Luong, 2008; Seelmeier et al., 1988; Wensing, van Maarseveen, & Nijhuis, 2010). First generation protease inhibitors were developed by utilizing the knowledge of the enzyme's 3-dimensional structure and their interaction with Pepstatin. Subsequent replacement of the features of pepstatin peptide improved the pharmacological properties and provided a platform to develop novel effective protease inhibitors. The cyclic scaffold was introduced in the new peptidomimetics design to increase rigidity and reduce flexibility noticed in the native peptide. A central cyclic scaffold that interacts with the active site of the enzyme was used to replace the dipeptide isosteres; this scaffold possesses a functional group that can interact with the flap region and the active site of the protease enzyme (Abdel-Rahman, Al-karamany, El-Koussi, Youssef, & Kiso, 2002).

There are two main classes of peptidomimetic HIV-protease inhibitors; i) First-generation inhibitors which include: Indinavir (IDV), Ritonavir (RTV), Nelfinavir (NFV), Amprenavir (APV), and Saquinavir (SQV). ii) Second-generation inhibitors example: Lopinavir (LPV), Atazanavir (ATV), Fosamprenavir (FPV), and Tipranavir (TPV) iii) Third generation inhibitors example: Darunavir (DRV).

First-generation inhibitors show similarities to the substrates by mimicking the intermediate tetrahedral transition-state formed when the catalyzed peptide bond is cleaved**.** Saquinavir (SQV), a first-generation PI mimetic, was the first FDA approved HIV PI designed to mimic the hydroxyethyl amine isostere. SQV had an inhibition constant of 0.12nM. The SQV peptidomimetic consists of a central hydroxyethyl amino moiety that is flanked on both sides by Phe and Asn isosteres sidechain and decahydroisoquinoline that mimics Pro. The choice of the side chain mimetics is because of the specific recognition of Pro residue and Phe-Asn dipeptide by the protease. The first-generation PI peptidomimetics had several limitations that affected the clinical

use such as high toxicity, low pharmacokinetics that increases daily drug burden, and the emergence of a mutant viral strain that s resistant to the existing PIs. Efforts to develop PIs with better therapeutic features like increased potency, high resistant profile, and better pharmacokinetics profile led to the development of second-generation peptidomimetics PIs.

Second-generation PIs, typified by Tipranavir (TPV), do not possess structural similarities to the native peptide substrate. TPV is a potent FDA approved HIV protease inhibitor, which, when compared to most other PIs, possesses a superior resistant profile. The resistant profile of TPV is attributed to its ability to interact with protease uniquely. TPV was discovered from a high-throughput screening in which 4-hydroxy-5,6-dihydro-2-pyrones and 4-hydroxybenzopyran-2-ones with micromolar inhibition towards HIV-1 protease was selected and optimized in the hit to lead the process. Characteristically TPV possesses a central scaffold that interacts with a hydrogen-bonds network of conserved residue found at the protease backbone, instead of the hydroxyethyl amino group used by other PIs to interact with the active site. This unique conserved interaction of TPV with protease is the reason for the superior resistant profile and increased inhibition towards mutant resistant virus (Ali et al., 2010; Drag & Salvesen, 2010; Weber & Agniswamy, 2009).

2.4. COMPUTER-AIDED DRUG DISCOVERY

Drug discovery and development process are considered expensive, tedious, and time-consuming, with the high risk involved. The typical cost and time of discovery and development of a single drug compound is about 0.8-1 billion US dollar and 14 years, respectively (Mullard, 2014). High throughput screening (HTS) and combinatorial chemistry technologies have enabled the reduction in time of drug discovery process by expediting the screening and synthesizing time for large chemical libraries (Paslay, Morin, & Harrison, 2010). There has been increased investment in the development of new drug due to increasing unmet clinical needs. However, the yield of marketable drugs does not correlate with the number of drug compounds discovered; this can be attributed to the high rate of failure and inefficiency of the drug discovery process (Mullard, 2014). Tremendous research efforts are put to develop drug discovery approaches with reduced cost and shortened time (Shekhar, 2008). Computer-aided drug design (CADD) has emerged as an effective and efficient approach to minimize cost and shorten drug discovery time. CADD is particularly useful in early drug discovery to screen large compound libraries and identify lead compounds with high efficiency and significantly reduced cost, workload, and time. In early drug discovery, CADD has several advantages over the traditional methods of drug discovery (combinatory chemistry and HTS). CADD increases the rate of identifying novel hit compounds due to its targeted approach, it also helps to elucidate the molecular mechanism of a drug compound and predict derivatives with higher therapeutic activity at a reduced cost and time (Jorgensen, 2004; Shekhar, 2008; Xiang, Cao, Fan, Chen, & Mo, 2012). In drug discovery and development, CADD is useful for the following purposes: Predict sets of the active drug compound to be validated experimentally from large compound libraries, Provide a guide for the optimization of the pharmacological properties of lead compounds, and *In silico de novo* design of novel drug compounds. CADD approaches can be

broadly categorized into ligand-based, structure-based drug design. The sequence-based approach or functional genomics which involves the use of some bioinformatic tools for de-novo identification of biological target and ligands are currently being employed in drug discovery (Acharya, Coop, E. Polli, & D. MacKerell, 2011; Chen et al., 2012; Wang et al., 2011).

2.4.1. Structure-based

The structure-based approach depends on the knowledge of the structure and the structural properties of the biological target to generate an active compound that can be developed into drugs. The structure-based virtual screening program uses the knowledge of the atomic structure of the target, the active/binding site and several conformations of the ligands and target to generate different target-ligand complexes and estimate the binding energies and binding affinities of the ligands to the target (Ferreira, Dos Santos, Oliva, & Andricopulo, 2015). Different docking programs utilize different approaches to evaluate ligand-target interaction. Most of these programs assume a rigid receptor (target), while the ligands assume several conformational poses (flexible ligands); this approach is known as semi-flexible docking. Other programs use induced fit docking (IFD), which assumes flexibility for both the target and ligands (Sherman, Beard, & Farid, 2006; Xu & Lill, 2013). After docking ligands to the active site of the target, the scoring function of the docking program identifies the best binding conformation of the ligand and target and assign a score which is ranked in descending order and represent the free binding energy ΔG of the ligand-target interaction (equation 1). The binding affinities of the ligands are inversely related to the binding energies with the equation (S.-Y. Huang, Grinter, & Zou, 2010)

$$\Delta G = RTInKi$$ ----------**(Equation 1)**

ΔG is defined as the free binding energy, while R, T, and Ki are gas constant, temperature (Kelvin), and inhibition constant respectively.

2.4.2. Ligand-Based

The ligand-based approach is used when the structure of the target is unknown, therefore, it depends on the knowledge of a known ligand of the target to generate active compounds that are structurally similar to the known ligand (Leelananda & Lindert, 2016). The fundamental principle of the ligand-based CADD is that ligands with similar structural and pharmacophore fingerprint may exhibit similar activity towards the target (Kapetanovic, 2008; Leelananda & Lindert, 2016). Structural similarity search, Quantitative structure-activity relationship (QSAR) and pharmacophore fingerprint are the methods used in ligand-based CADD. Structural similarity search uses several metrics, of which the Tanimoto score is the most common, to calculate the similarity between the chemical structure of the reference compound and other compounds in a compound database (Willett, 2006). Pharmacophore fingerprinting uses the knowledge of the ligand structure to identify the pattern of interaction between the reference ligand and the target, then uses this to generate active compounds with similar interaction pattern (Yang, 2010). QSAR method relates the chemical structure of a compound to its biological activity, i.e., compounds with similar structure will have similar biological activity (Cherkasov et al., 2014; Davis, 2017). These methods are not used independently; instead, they are used together to generate compounds that are similar to the reference ligands with optimal interaction with the target protein (Ekins, Mestres, & Testa, 2007; Kitchen, Decornez, Furr, & Bajorath, 2004).

2.4.3. Techniques used in Computer-Aided Drug Discovery (CADD)

2.4.3.1. Virtual High Throughput Screening (vHTS)

Virtual high throughput screening is a computational equivalent of the conventional HTS, where chemical compound libraries are screened against a biological target to identify lead compounds (Rester, 2008). Virtual screening uses computational tools to score, rank and filter large chemical libraries to accurately identify compound structures that can be validated downstream as lead compound; it is quicker, cheaper and more efficient than the conventional HTS (McGregor, Luo, & Jiang, 2006).

2.4.3.2. Molecular Docking

Molecular docking is used to analyse the interaction between a protein (target) and a ligand (small molecule), it analyses and identifies the best ligand conformation and orientation in a protein-ligand interaction. It is also used to determine the active site of a protein and the type of interaction (bond type and residues involved) that exist between a protein and a ligand (Meng, Zhang, Mezei, & Cui, 2011).

2.4.3.4. Molecular Dynamic (MD) Simulation

MD Simulation is used to examine the structure and dynamic behaviour of biological molecules together with their complexes. MD simulation uses computational techniques to elucidate time-dependent patterns, structure, and conformations of biological molecules in a molecular system; it can also provide information on the molecular level, the interactions of macromolecules at a cellular level in a living system (Durrant & McCammon, 2011). MD simulation has application in protein structural biology, molecular recognition of biological molecules, and ion transportation in a biological system (Liu et al., 2018).

2.5. *In Vitro* Validation of 'hit' Compounds from CADD

CADD is a very useful ammunition in the 'hit' discovery process of drug discovery and development pipeline (Sliwoski *et al*., 2014b). A 'hit' compound is referred to as a compound identified, which possesses the desired activity towards the biological target. In the 'hit' discovery process, virtual high throughput screening (vHTS) are employed to screen compound libraries in order to identify these 'hit' compounds (McInnes, 2007). Compound libraries are generated using prior knowledge of the protein structure of the biological target and/or the chemotype of known active compounds against the target. CADD tools like molecular modelling, molecular docking, pharmacophore modelling etc are useful in the 'hit' discovery process (Keseru & Makara, 2006). Following the identification of a 'hit' compound, series of experimental assays are carried out to validate the activity of the 'hit' compounds against the biological target (Hughes *et al*., 2011). Several assays are available for compound screening, these can be either biochemical or cell-based assay (Janzen, 2014). The choice of assay depends on the nature of the biological target, properties of the compounds, size of the screening library, cost, laboratory equipment, researcher's experience (Hughes *et al*., 2011). Typically, cell-based assays are favoured for drug targets like ion channels, membrane receptors, and nuclear receptors (Michelini *et al*., 2010), conversely, biochemical assays can be used for both enzymes and receptors targets (Hughes *et al*., 2011).

In the discovery of new antiviral compounds, several assays are available for quantifying the antiviral activity of a compound *in vitro*. The classic assays test the ability of the test antiviral compounds to decrease viral yield, inactivate cell-free or recombinant viral protein, reduce transcription of viral RNA (Postnikova et al., 2018a). High throughput antiviral screening methods have also been developed to measure endpoints such as viral protein or reporter gene expression, cytopathic effect, which serves as proxy for viral replication (Towner *et al*., 2005). Cell-based

assay for screening potential antiviral compounds has gained popularity in recent times, because of its ability to provide the means for intracellular screening of compounds with potent viral inhibition properties and desired pharmacological properties (Basu *et al*., 2011; Elshabrawy *et al*., 2014; Panchal *et al*., 2012). In cell-based assays, live viruses are used in cell culture to determine the optimum inhibition concentration for antiviral activity of the compounds, however, highly infectious virus particles require biosafety level-4 laboratory (BSL-4) to perform assay (Postnikova *et al*., 2018b; Salata *et al*., 2019). Surrogate models such as pseudotype virus and virus-like particles are being developed for BSL-2 laboratories to facilitate the identification of promising antiviral compounds (Postnikova *et al*., 2018b; Salata et al., 2019). Pseudotype virus technology have been useful in the screening and identification of potential compounds with antiviral activities against several virus, especially in low-level bio containment (Barrientos *et al*., 2004; Garcia *et al*., 2009; Talekar *et al*., 2012; Wolf *et al*., 2010).

2.6. Production of Pseudotype Virus

pseudotype virus is defined as a hybrid cell-free virus particle comprising of a ‘core’ nucleocapsid protein, which encases the viral genome, and a lipid envelope membrane, which encapsulate the ‘core.’ The pseudotype virus ‘envelope’ is derived from the host cell as the ‘core’ exit the cell, and they can contain proteins from other viruses. Pseudotype virus can also be engineered to carry foreign genes, which is transferred into a susceptible host cell by an interaction between the virus envelope protein and host cell receptors, resulting into entry into the cell and ultimate expression of the foreign gene (Temperton, Wright, & Scott, 2015).

Retroviruses are broadly used as pseudotype virus cores, due to their innate ability to reverse transcribe single-stranded RNA genome into a double-stranded deoxyribonucleic acid (dsDNA) and integrate the dsDNA into the host cell genome for replication and expression. In retrovirus

pseudotypes, an easily quantifiable reporter gene is usually expressed, and the expression of the reporter gene is directly correlated to the efficiency of the interaction between the viral envelope protein and the target cell receptor (Temperton & Wright, 2009). This interaction is utilized in determining the dose-dependent response of antibody or antiviral agents that can inhibit viral entry and replication. Current protocols for making pseudotype virus have been optimized to minimize the production of viral particles that can replicate. These protocols require transient transfection of the separate components of the virus elements into a packaging cell line in order to produce pseudotype particles incapable of replication (Pear, Nolan, Scott, & Baltimore, 1993). Despite this, titres of replication-competent viral particles were still detected, therefore a three plasmid system where the pseudotype elements (the 'core', which has the retrovirus gag/pol and accessory gene, the virus envelope protein 'env', and a reporter gene) were inserted in three different plasmids, and then transfected into a packaging cell line, was adopted (Soneoka et al., 1995). The expression of the genes simultaneous allows for the assembly and packaging of new viral particles that can 'transduce' target cells and integrate a quantifiable reporter gene but are unable to replicate in the cell.

2.6.1. Methods of Generating Pseudotype Virus

Retrovirus pseudotypes are produced by co-transfection three plasmids comprising of 'core' retrovirus genes, cloned viral envelope protein of interest, and a reporter/transfer gene into stable transfectable cell line such as HEK (Human Embryo Kidney) 293T Cell.

1. Gene of the envelope protein of the virus of interest is obtained through custom gene synthesis or PCR (polymerase chain reaction) amplification of the corresponding viral cDNA. The envelope gene is then cloned into an expression plasmid under a constitutive promoter using appropriate restriction enzymes.

2. The ‘core’ plasmid comprises of retroviral gag-pol genes. The gag/pol genes codes for structural proteins, reverse transcriptase, protease, and integrase. These proteins and enzymes are responsible for the reverse transcription of viral RNA to DNA and also the integration of the reporter/transfer gene into the genome of the host cell.

3. The reporter/transfer plasmid. This plasmid contains a quantifiable gene that is integrated into the host cell genome with the help of the genes in the ‘core’ plasmid and is expressed using several cis- transcriptional elements. The upstream of the reporter gene contains a viral packaging signal, which ensures that the viral RNA is incorporated into the ‘core’ during the generation of the pseudotype particle. After transfection, the host cell machinery transcribes and translates the transfected genes, then incorporates an RNA dimer present in the region between the LTR (Long Terminal Repeats) on the reporter gene using the packaging signal. Other nucleic acids are prevented from being incorporated into the matured pseudotype particles because only the reporter gene is engineered to have the packaging signal. The viral nucleocapsid, containing the envelope protein, is inserted into the host cell plasma membrane via an N-terminus domain of the Gag gene. The pseudotype particles buds from the cell, encased in the viral envelope obtained from the host cell membrane. The pseudotype particles are then released by the host cell into the growth medium and collected as the supernatant. The concentration of the pseudotype particles is measured by titrating the supernatant onto a target cell, which the pseudotyped particles attach to via receptor-envelope protein interaction. The genome of the pseudotype virus, bearing the quantifiable reporter gene, is integrated into the target cell genome where it is expressed. The number of viable pseudotype particle correlates to the level of the reporter gene expressed. Propagation of the pseudotype in the target cells does not occur, because only the reporter gene is expressed in the target cells. This inability to propagate in target cells makes pseudotype virus safer to work within

low-level biosafety lab than wildtype virus particles. Common reporter gene used for pseudotyping include: GFP (Gren fluorescent protein) which quantified with flow cytometry or fluorescent microscopy, luciferase quantified using a luminometer, and Beta-galactosidase (β-gal) quantified using colorimetric methods.

The pseudotype virus titres calculated depends highly on the type of target cell and the receptor density on the target cell. Other methods for quantifying pseudotype particles include measurement of the retroviral core Gag, core p24 or envelope protein using ELISA, determination of viral genome copy number using qRT-PCR to determine the number of genome copies, measurement of reverse transcription activity, etc.

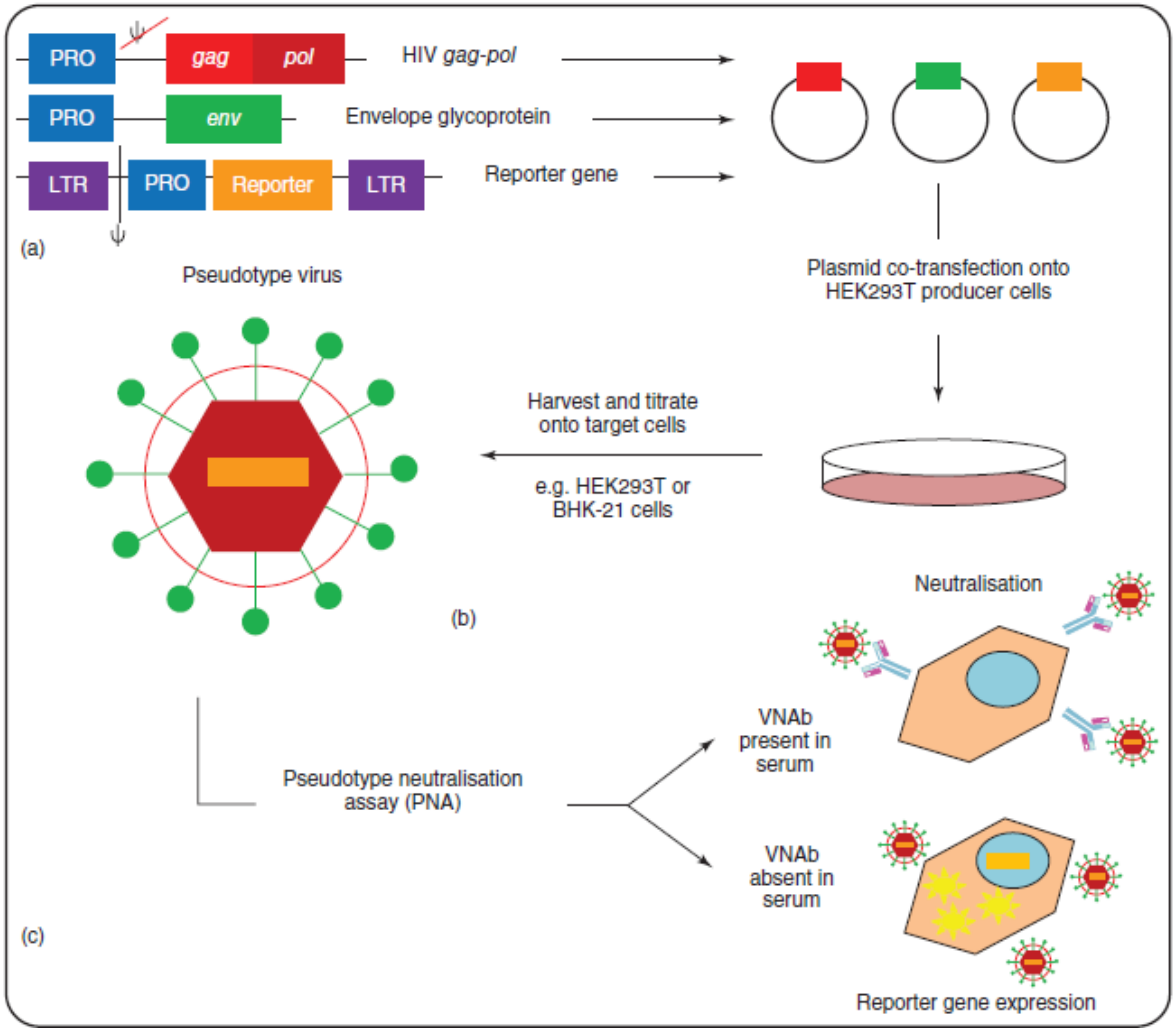

Figure 6. *Schematic of the production of pseudotype using the triple-plasmid co-transfection system and downstream neutralization using the pseudotype and use to measure antibody neutralization (Temperton et al., 2015).*

2.6.2. Application of Pseudotype virus

Pseudotypes have been used as essential research tools because they possess distinct advantages over wildtype viruses: Pseudotype particles are employed in gene therapy research, due to their ability to bind, enter, and integrate transfer gene into a target cell via a receptor-mediated mechanism. Pseudotype particles can be engineered to target a specific type of cell. Example, pseudotype particles having VSV (vesicular stomatitis virus)-glycoprotein can bind to a wide range of host (Burns, Friedmann, Driever, Burrascano, & Yee, 1993), while pseudotypes that have the hepatitis B virus envelope leads to hepatotropism (Sung & Lai, 2002).

Pseudotypes are used in studying virus-cell interaction, elucidating the mechanism of virus entry into the host cell, and identification of virus receptors on the host cell. In studying the interaction between host cell receptors and virus envelope protein, pseudotypes offer the advantage of having only the envelope protein of interest on the surface without the interference of other proteins, unlike the wildtype virus (Funke et al., 2008; Khetawat & Broder, 2010; Saeed, Kolokoltsov, & Davey, 2006).

Pseudotypes can be used as tools in the assessment of novel antiviral agents and antibody neutralization assay (Kim, Lee, Han, & Cho, 2001; Y. Lu & Jiang, 2013; Temperton et al., 2005; Y. Zhou et al., 2011).

Since pseudotypes cannot propagate in host cells and therefore not infectious, they are a safer substitute of highly pathogenic wildtype virus. They require lower biosafety level containment. They are also relatively stable, at 37∘C, they have a half-life of several days and several weeks at room temperature (Mather, Wright, Scott, & Temperton, 2014).

CHAPTER THREE

3.0. MATERIALS AND METHODS

3.1. MATERIALS

3.1.1. Reagents

Complete Cell culture medium was prepared using Dulbecco's Modified Eagle Medium (DMEM) supplemented with L-Glutamine, Streptomycin, Penicilli, and Heat Inactivated Fetal Bovine Serum (FBS), all from Thermo Fisher. 10X Trypsin-EDTA (0.5 %), Phosphate Buffered Saline (PBS), Dimethyl sulfoxide (DMSO) were purchased from Sigma Aldrich.

3.1.2. Plasmid

Plasmids: p8.91, pCSFLW, and pCAGGS-HXB2 were donated by Dr. Edward Wright from the University of Sussex. Plasmid p8.91, described in PNAS Naldidni et al., 1996, expressing HIV gag-pol, tat, and rev. Plasmid pCSFLW is a lentiviral vector expressing firefly luciferase. Plasmid pCAGGS-HXB2—Env is a mammalian expression vector expressing HIV-1 envelope protein (gp160) Clade B clone 2.

3.1.3. Cell lines

TZM-bl cell lines are HeLa cells with HIV-1-tat directed luciferase reporter gene, engineered to express CD4 receptors and coreceptors. HEK 293T/17 is an adherent human kidney cells lines that are highly transfectable capable of producing retroviruses in high titre. Both TZM-bl and HEK 293T/17 cell lines were donated by Dr. Edward Wright from the University of Sussex.

3.2. METHODS

3.2.1. *IN SILICO* HIGH THROUGHPUT SCREENING OF NATURAL COMPOUND MIMETICS OF VRC01

3.2.1.1. Protein structure Extraction

The 3D structure of crystallized antigen-binding fragment (Fab) of broadly neutralizing antibody VRC01 in complex with core gp120 of HIV-1 clade A/E recombinant 93TH057 (PDB ID: 3NGB), with resolution of 2.68 Å was downloaded from Protein Data Bank (PDB). The core gp120 trimer consisting of outer and inner domain with truncated N- and C-termini as well as V1/V2 and V3 variable loops, were extracted from the complex as protein chains G, A, and D using PYMOL 1.74 (Yuan, Chan, & Hu, 2017).

3.2.1.2. Determination of gp120 core residues of interaction with VRC01

VRC01 is a CD4 binding site (CD4bs) broadly neutralizing antibody (bNAb) which makes contact with 98% of gp120 site of vulnerability (T. Zhou et al., 2010). The gp120 vulnerability site is the highly conserved CD4 receptor contact site on gp120 outer domain. The gp120 amino acid residues that interact VRC01 and CD4 were obtained elsewhere (T. Zhou et al., 2010).

3.2.1.3. Molecular Dynamics (MD) Simulation

MD simulations of the HIV-1 gp120 core (PDB ID: 3NGB) were carried out to determine the conformation, stability and dynamics of the structure. A 10 ns MD simulation was performed using GROMACS 5.1.4 (Abraham et al., 2015). Chemistry at HARvard Macromolecular Mechanics (CHARMM27) force field was adopted to prepare the topology input file for the protein. The protein was solvated by SPCE water molecules and immersed in a 1 nm thick cubic periodic water box. Before the simulation, a short minimization of 500 steps using the steepest descent method

was carried out to remove possible distortion in the protein structure caused by the addition of water to the system. 8 Cl- ions were added to neutralize the system. The system was equilibrated at a temperature of 300 K and normal pressure for 50 ps to restrain the heavy atoms of the proteins to their starting position to allow water molecule to saturate the system. The final production simulation was performed for 10 ns under the similar conditions as the equilibration steps. The root-mean-square displacement (RMSD) of the minimized protein heavy atom with respect to the resolved X-ray structure was calculated and plotted using GRACE 5.1.4 (P. Turner, 2005). The final minimized GROMACS protein file (gro file) was visualized with Visual Molecular Dynamics (VMD) 1.9.3 version and saved as frames in pdb format for further analysis (Humphrey, Dalke, & Schulten, 1996).

3.2.1.4. Receptor Preparation

The minimized HIV-1 gp120 was prepared for molecular docking using AutoDockTools version 4.2.6 (Morris G.M. & Dallakyan S., 2013). Water molecules were removed from the structure. Polar hydrogen atoms were added, and non-polar hydrogens were merged with a parent carbon atom. Gasteiger partial charges of the atoms were calculated and added. The protein file was then converted to AutoDock compatible format (pdbqt). The energy grid box was set around the conserved residues of HIV-1 gp120 with a dimension of 42 Å x 50 Å x 56 Å, and coordinates of X= 52.318 Å, Y= 26.081 Å, and Z=46.493 Å for the receptor macromolecules.

3.2.1.5. Ligand Compound Library Generation

Libraries of natural compounds were obtained from three commercially available natural product-derived compound databases consisting of AnalytiCon Discovery, specs and InterBioScreen (IBS). Structures of compounds retrieved from these databases were downloaded as a single structure-data file (SDF) format.

3.2.1.6. Ligands Preparation

SDF format files of the ligand libraries were split into individual compounds using a split utility module in Open Babel 2.3.1 (O'Boyle et al., 2011) accessible via the PyRx 0.8 (Dallakyan & Olson, 2015). The compounds were optimized and converted to AutoDock compatible (PDBQT) format. A total of 27,824 ligands were minimized for molecular docking.

3.2.1.7. High-throughput Virtual Screening

High-throughput virtual screening of the compound libraries was performed on a Linux Operating System High-Performance Computing System (Zuputo) hosted by West African Centre for Cell Biology of Infectious Pathogen (WACCBIP). AutoDock Vina 1.1.1, a molecular docking tool was used for the virtual screening of compound libraries. AutoDock Vina utilizes rigid receptor and flexible ligand docking mode and empirical scoring function to rank protein-ligand complexes (S.-Y. Huang, 2017). The previously prepared HIV-1 gp120 protein (receptor) PDBQT file with defined grid box dimensions (42 Å x 50 Å x 56 Å, coordinates of: x= 52.318 Å, y= 26.081 Å, z=46.493 Å) and exhaustiveness of 9 along with all optimized ligands were used for docking. A custom bash script was prepared for the docking procedures. All virtual screening results were aggregated and written to a single log file. The log file contained binding energies for each of the docked complex.

3.2.1.8. Virtual screening Result Analysis

AutoDock Vina scores the binding affinities of the ligand to the receptor using empirical data obtained from the summation of energies contributed by the receptor and ligand interactions, which is calculated as the total atom pair distance-dependent interactions of the protein and ligand (Trott & Olson, 2010). The binding energy values are inversely related to the binding affinity, i.e., the lower the binding energy value, the higher the binding affinity. The single log file containing the

binding energies in (KJ/mol) of all processed ligands was extracted into comma-separated value (CSV) file format and was analyzed using Microsoft Excel 2016. The docked poses of each ligand were visualized using PYMOL. The poses with the best fit in the binding site with the lowest binding energies were selected for further analysis.

3.2.1.9. Protein-Ligand Interaction Profiling

The protein-ligand complex interaction profiles were determined using LIGPLOT version 1.4.5 (Laskowski & Swindells, 2011). LIGPLOT analyses the molecular interaction between proteins and ligands and generate 2-D schematic representations of the interactions in terms of bond types. The bond types include hydrogen and hydrophobic interactions, as well as bond lengths and interacting residues. Hydrogen bond interactions are represented by broken green lines of distinct length, while arcs with spikes pointing towards the ligands represent the hydrophobic interactions.

3.2.1.10. HIV-1 HXB2 Envelope Protein

Human Immunodeficiency Virus Clade B clone 2 (HIV HXB2) was used as a reference HIV strain. HXB2 envelope protein was used in the production of HIV-1 pseudotype virus utilized in the cell-based viral infectivity inhibition assay.

3.2.1.11. Determination of HIV-1 HXB2 Envelope Protein Structure

The nucleic acid sequence of HXB2 envelope protein (gp160) that was cloned into PCAGGGS plasmid was retrieved from the HIV sequence database. The nucleic acid sequence was converted to an amino acid sequence using the ExPasy Translate tool, which translates nucleic acid sequences into an amino acid sequence. The HXB2 gp160 amino acid sequence was retrieved for the ExPasy Translate tool server as a FASTA file and used as a query for BLASTP via ExPasy platform. BLASTP is used to query protein sequence database to identify similar sequences. The protein

sequence with the highest similarity score to our query protein sequence was retrieved from UniProt Knowledgebase (UniProtKB). UniProtKB is a comprehensive protein database that contains annotations and functional information of the proteins. A structure similarity search was performed using the UniProt ID of the protein sequence to retrieve the 3D protein structure (PDB ID: 3J70) from Protein Data Bank.

3.2.1.12. Protein Structure Extraction and Energy Minimization of HXB2 gp120

The 3D structure of HXB2 gp160 with the entire variable regions in complex with CD4 and antibody 17b was retrieved from Protein Data Bank (PDB ID: 3J70) with a resolution of 2.0 Å (Rasheed, Bettadapura, & Bajaj, 2015). The gp120 trimer was extracted from the protein complex using PYMOL 1.74 (Yuan, Chan, & Hu, 2017) as protein chains D, P and U. The energy of the extracted gp120 protein was then minimized using Swiss-Pdb Viewer 4.2 with default settings. Swiss-pdb Viewer (Kaplan & Littlejohn, 2001) utilizes Groningen Molecular Simulation computer program package (GROMOS 43B1) force field to minimize the energy of the protein and repair distorted geometries of the protein structure. The minimized protein was extracted and saved as a pdb file.

3.2.1.13. Receptor Preparation

In preparation for molecular docking, the minimized HIV-1 HXB2 gp120 was optimized using AutoDockTools version 4.2.6 (Morris G.M. & Dallakyan S., 2013). Water molecules were removed from the structure to prevent interference with the docking process. Polar hydrogens were added, and non-polar hydrogens were merged with a parent carbon atom. Gasteiger partial charges of the atoms were calculated and added. The protein file was then converted to AutoDock compatible format (pdbqt). The energy grid box was set around the conserved residues of HIV-1 gp120 at dimensions (54 Å x 40 Å x 44 Å) with coordinates of X= 249.640 Å, Y= 230.870 Å, and Z=198.249

Å. After optimization, the protein was used a receptor for molecular docking as described in *(3.2.1.7)*. The resultant complex was analyzed as described in *(3.2.1.8)*, and the protein-ligand interaction profiled as described in *(3.2.1.9)*.

3.2.1.14. Physicochemical and Pharmacokinetics and Drug-likeness Properties Prediction

SwissADME (Daina, Michielin, & Zoete, 2017) was used to predict the relevant physicochemical, pharmacokinetics and drug-likeness properties of the shortlisted ligands (Daina et al., 2017). The Simplified Molecular Input Line Entry Specification (SMILES) formats of the query ligand files were used to generate parameters such as physicochemical properties, lipophilicity (trans-membrane movement), absorption, distribution, metabolism and excretion (ADME) profiles. The others include gastrointestinal absorption, blood brain barrier permeability, P-glycoprotein substrate, cytochrome enzyme inhibition, water solubility and drug-likeness (Lipinski's rule of 5).

3.2.1.16. Toxicity Profile Prediction

The toxicity profiles of selected compounds were predicted using ProTox-II (Drwal, Banerjee, Dunkel, Wettig, & Preissner, 2014). ProTox-II utilizes compound pharmacophore fingerprint, structural similarity and machine learning models designed from both *in vitro and in vivo* assay data to predict immunotoxicity, hepatotoxicity, cytotoxicity, mutagenicity and carcinogenicity. The toxicity profiles of the compounds have probability range of 0 - 1 (0 = not likely, 1 = very likely), predicted lethal dose (LD_{50}), and toxicity class which ranges from 1 -6 (1 = highly toxic/fatal, 6 = least toxic).

3.2.2. CELL-BASED VIRAL INFECTIVITY INHIBITION ASSAY

3.2.2.1. Transformation of Competent Bacteria Cells

Three plasmids: p8.91 containing HIV gag, pol and tat structural proteins, pCSFLW containing firefly luciferase gene, and pCAGGS-HXB2 which contains HIV envelope protein were transformed in competent top10 bacteria cells. 50µl of competent bacteria cell was pipetted into a 1.5ml prechilled Eppendorf tubes (one tube for each plasmid), then 5 µl oaf 10ng/µl of re-suspended plasmid DNA was added into the 1.5ml tube containing competent bacteria cells. The tube was gently flicked to mix and incubated on ice for 30mins after which it was transferred to a water bath at 42°C for 30 secs for heat shock. The tube mixture was then quickly placed back into ice after the heat shock. 120µl of SOC media was pipetted into the mix and incubated for 1 hour at 37°C with shaking at 180 rpm. 50µl of the transformation mix was transferred into a Petri dish containing 25ml of solidified agar and 20µl of ampicillin antibiotics. The mixture was evenly distributed across the agar plate using a sterilized spreader and incubated at 37°C overnight. After overnight incubation, a single colony of the transformed bacteria was grown overnight at 37°C in 3ml of Luria Broth (LB) media containing 25µl of Ampicillin antibiotics. Two control plates were set up; positive control plate contained competent bacteria cells grown on an agar plate with no antibiotics, while negative control plates contained competent bacteria cell +grown in agar plate with no antibiotics (test for contamination).

3.2.2.2. Plasmid Extraction and Quantification

Plasmids: p8.91, pCSFLW, and pCAGGS-HXB2, contained in transformed bacteria culture, grown overnight in LB media, were extracted as directed by the manufacturer, using Sigma Aldrich GenElute™ HP Five–Minute Plasmid Miniprep Kit. Plasmid DNA present in the eluate was quantified using ThermoFisher Scientific NanoDrop™ One/One^{C} Microvolume UV-Vis

Spectrophotometer, the concentration of the DNA was recorded in ng/µl, while the purity of the plasmid DNA was read as the absorbance at 260/280 nm. Plasmid DNA was stored at –20 °C.

3.2.2.3. Plasmid Restriction Digestion

Three plasmids: p8.91, pCSFLW, and pCAGGS-HXB2 were used for the experiments. In a 1.5ml tube placed on ice, the following reaction components were added sequentially to the tube: 10x buffer, distilled water, plasmid DNA, and restriction enzyme(s). The quantity of each of the reaction component added for each plasmid is listed in the table 1 below. The restriction digests mix were gently pipetted up and down to mix, after which they were transferred to a water bath for 1-hour incubation at 37°C. After the incubation, the restriction digest result was visualized on 1.5% agarose gel.

Table 1. List of the reaction components used for the restriction digest of respective plasmid

Plasmids	**p8.91**	**pCSFLW**	**Pcaggs**
Reaction Component			
10X Buffer	2µl	2µl	2µl
Water	x µl	x µl	x µl
Plasmid DNA	y µl (3µg/ µl)	y µl (3µg/ µl)	Y µl (3µg/ µl)
BglIII	2µl	N/A	N/A
BamH1	N/A	2 µl	N/A
Not1	N/A	2 µl	N/A
KpnI	N/A	N/A	2 µl
XhoI	N/A	N/A	2 µl
Total	**20 µl**	**20 µl**	**20 µl**

3.2.2.4. Agarose Gel Electrophoresis

The 1.5% agarose gel was prepared by dissolving 1.5 grams of agarose powder in 100ml of TAE (Tris-Acetate-EDTA) buffer, and the mixture was heated to dissolve the powdered agarose. The heated agarose was left to cool down and then poured into a pre-set gel cast, where it is left to solidify and used for further analysis.

3.2.2.5. Thawing cryopreserved cells.

The cryovial containing the frozen HEK 293T/17 and TZM-bl cells were removed from liquid nitrogen storage and immediately place it into a 37°C water bath. The frozen cells were quickly thawed by gently swirling the vial in the 37°C water bath for <60 seconds until thawed. The thawed cells were resuspended in 1 ml of warm media (DMEM-10% FCS + 50unit/ml pen + 50ug/ml strep). The resuspended cell was then transferred into a sterile centrifuge tube containing 6ml of media and centrifuged for 5 min at 2,000 rpm at room temperature to remove DMSO. The supernatant was decanted, and the cells were re-suspended in 1 ml of media and transferred into a 10cm culture dish containing 10 ml of media and incubated in a sterile tissue culture $C0_2$ incubator at 37°C.

3.2.2.6. Cell Passaging

The media from the primary culture above was removed from the culture plate using sterile serological pipet. The adhering cell monolayer was washed with Phosphate-buffered saline (PBS) twice after which the PBS was discarded. 1.5 ml of 1X Trypsin/EDTA solution at 37°C was added to the culture plate to cover adhering cell layer and placed in the incubator for 2 minutes at 37°C to separate cell monolayer. The cells were dislodged from the bottom of the culture plate by gently tapping off the plate on the countertop and then viewed using an inverted microscope to determine if the cells are sufficiently detached from the surface of the cell culture plate. The detached cells

were resuspended in 8.5 ml of 37°C DMEM-10 media. 2 ml of the cell suspension was aliquoted into 10cm cell culture plates containing 8 ml of media plus serum to inhibit further trypsin activity and incubated in a sterile tissue culture CO_2 incubator at 37°C.

3.2.2.7. Cell Seeding

The media from primary cell culture was discarded, and the cell monolayer was washed twice with PBS. The PBS was discarded, and 1.5ml of 1X Trypsin-EDTA was added directly onto cell monolayer and incubated for 5 minutes 37°C. The cells were monitored for detachment using an inverted microscope. Once detached, 8.5 ml of DMEM-10 media was added to resuspend cells. 2 ml of the re-suspended cells were seeded into 10 ml of new culture plates for transfection assay.

3.2.2.8. Transfection with Polyethyleneimine (PEI)

DAY 1

$5x10^6$ cells/per ml of HEK293T-17 cells were seeded overnight in 6-well plate dish containing complete media (DMEM-10% FCS + 50unit/ml pen + 50µg/ml strep) and incubated at 37°C and 5% CO_2 until 60-80% confluence is achieved.

DAY 2

The overnight media was replaced with 1.5ml complete media and in sterile 2ml Eppendorf tube placed in a laminar flow hood plasmid DNA mix was prepared by adding: 1µg of env plasmid (pCAGGSHXB2), 1µg of gag-pol plasmid (p8.91) and 1.5µg of the luciferase reporter plasmid (pCSFLW) to 100µl of OptiMEM serum-free media In another separate Eppendorf tube transfection reagent was prepared by adding 20ul of 1mg/ml PEI to 100 µl of OptiMEM serum-free media. Both tubes were left 5 minutes, then mixed by adding the transfection reagent mix to the plasmid. The tube containing transfection -plasmid DNA mix was gently flicked to thoroughly mix and then incubated for 20 minutes at room temperature. After incubation, the mixture was added in

a dropwise manner into a cell culture plate; the plate was gently swirled around to distribute. The plate was incubated overnight at 37ºC and 5% CO_2.

DAY 3

The culture media was changed and replaced with fresh 1.5ml of fresh complete media.

DAY 4+5

Culture supernatant was filtered using a 0.45µm Millipore filter, aliquoted into 1.5 ml Eppendorf tubes, and stored at -20°C to harvest pseudotype at 48- and 72-hours post transfection.

3.2.2.9. Pseudotype Virus Titration Determination of Tissue Culture Infectivity Dose (TCID50)

100ul of media was placed into all wells in a 96 well plate, 100 ul of harvested pseudotype virus was added to the first wells and thoroughly mixed by pipetting up and down. The mixture from the first well was serially diluted (dilution factor = 2) across the other well and incubated for 1-hour at 37ºC (5% CO_2). Cells (TZM-bl) were prepared by discarding the media from the primary cell culture and was washed twice with PBS. The PBS was discarded, and 1.5ml of 1X Trypsin-EDTA was added directly onto cell monolayer and incubated for 5 minutes at 37°C. The cells were monitored for detachment using an inverted microscope. Once detached, 8.5 ml of DMEM-10 media was added to resuspend cells. The resuspended are transferred into a 15ml falcon tube, and an aliquot of 10µl was used to for cell counting using a haemocytometer. The cells are diluted appropriately to give approximately 2*10^5 cells/ml. 100µl (approximately 2x10^4 cells) of prepared cells were added to each well and incubated for 48 hours at 37ºC (5% CO2). The media was gently discarded from the wells, after 48 hours of incubation. 50µl of a 50:50 mix of media and Bright Glo substrate was added to the well and incubated for 5 minutes with occasional gentle tapping of the plate. The Luminescence of each well was quantified using the Glomax plate reader at a 0.3 shake rate. TCID50 was calculated with TCID50 MACRO.

3.2.2.10. Cell Viability Assay

TZM-bl cells were prepared, as stated above (3.2.9). 100µl (approximately 2x10^4 cells) of prepared cells were seeded overnight in a 96-well plate and incubated for 48 hours at 37°C (5% CO2). The cells were treated with 10µl of the serially diluted test compound (starting concentration = 100µg/ml, dilution factor = 2), and incubated for 48 hours at 37oC (5% CO2). Control well include positive control (Cells treated with Ursolic acid, a known cytotoxic compound), negative control (Cells with no compound treatment), colour control (compounds and media only), and blank (media only). 10µl of Alamar blue was added to the plates and incubated overnight. The absorbance was read at 570nm – 595nm. The assay was set up in triplicates, and the mean value was calculated for analysis.

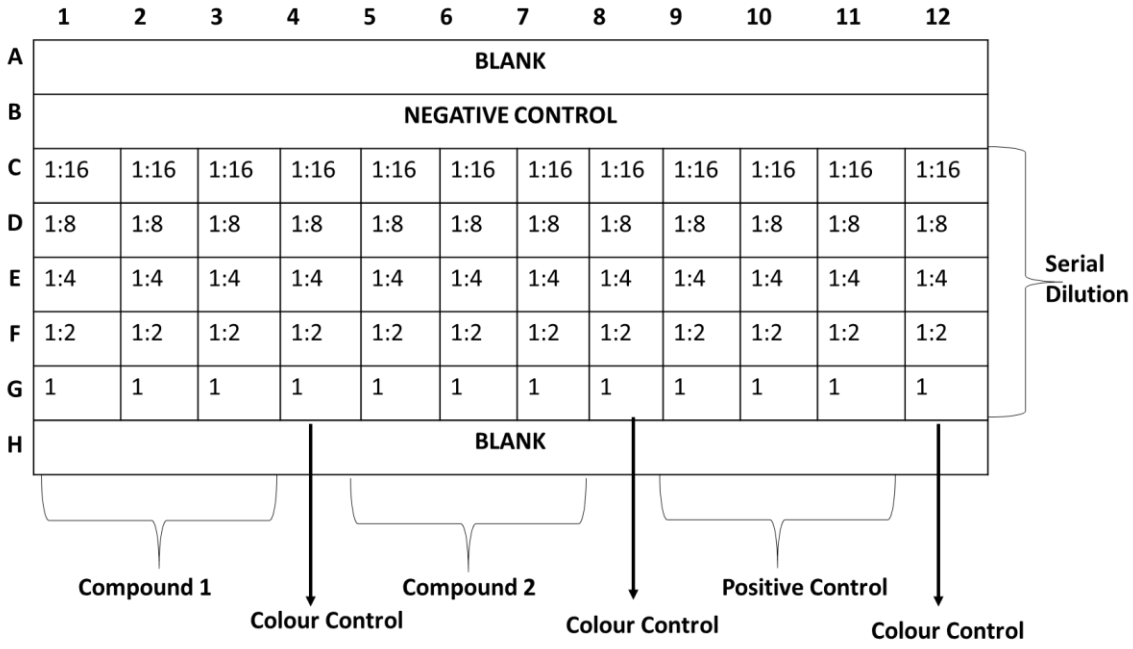

Figure 7. *A typical 96-well plate layout for Alamar blue cell viability assay.*

3.2.2.11. Viral Infectivity Inhibition Assay

50µl of the growth media was added to all the wells in a 96-well plate with the exception of the control wells. 25µl of the 1000µg/ml of compound solution in 10% DMSO was added to the growth media in column 1 and was serially diluted (1, 1:2, 1:4, 1:8, 1:16) to column 6. Similarly, compounds were serially diluted from column 7 to 12. In the control wells, 100µl, 150µl, and 50µl of growth media were added. The control wells are included:

- Row $F_{7\text{-}12}$ 1 – Cell only control
- Row $G_{7\text{-}12}$ – Pseudotype virus only
- Row $H_{7\text{-}12}$ – Cell and Pseudotype virus control

100µl of diluted pseudotype virus was added to all wells except cell only control. The plate was incubated for 1h at 37oC (5% CO_2). After incubation, 100µl TZM-bl cells ($2x10^4$ cells) was added to each well except the virus only control wells, bringing the total volume in each well to 250µl. The plate was centrifuged at 500rpm for 5s and incubated for 48 hours at 37°C (5% CO_2). After 48 hours, the media was removed, 50µl of a 50:50 mix of new media and Promega Bright Glo substrate was added, and the plate luminescence was read using Glomax plate reader.

	1	2	3	4	5	6	7	8	9	10	11	12	
Compound 1 – A	1:2	1:4	1:8	1:16	1:32	1:64	1:2	1:4	1:8	1:16	1:32	1:64	Compound 5
B	1:2	1:4	1:8	1:16	1:32	1:64	1:2	1:4	1:8	1:16	1:32	1:64	
Compound 2 – C	1:2	1:4	1:8	1:16	1:32	1:64	1:2	1:4	1:8	1:16	1:32	1:64	Compound 6
D	1:2	1:4	1:8	1:16	1:32	1:64	1:2	1:4	1:8	1:16	1:32	1:64	
Compound 3 – E	1:2	1:4	1:8	1:16	1:32	1:64	BLANK						
F	1:2	1:4	1:8	1:16	1:32	1:64	CELLS ONLY						
Compound 4 – G	1:2	1:4	1:8	1:16	1:32	1:64	PSEUDOTYPES ONLY						
H	1:2	1:4	1:8	1:16	1:32	1:64	CELLS + PSEUDOTYPES ONLY						

Figure 8*. Viral infectivity inhibition assay plate layout.*

CHAPTER FOUR

4.0. RESULTS

4.1. *IN SILICO* HIGH THROUGHPUT SCREENING OF NATURAL COMPOUND MIMETICS OF VRC01

4.1.1. Protein structure Extraction

The crystal structure of the protein (PDB ID: 3NGB) with a resolution of 2.68 Å was obtained from the Protein Data Bank (PDB). 3NGB is a complex of the crystallized antigen-binding fragment (Fab) of broadly neutralizing antibody VRC01 and core gp120 of HIV-1 clade A/E recombinant 93TH057. The protein consist of twelve chains comprising G, A, D, I, H, B, E, J, L, C, F and K. Chains G, A, D and I are HIV-1 envelope glycoprotein, chains H, E, J, and B are the heavy chains of the VRC01 Fab, while chains L, C, F and K are the light chains of VRC01 Fab. The core gp120 trimer (chains G, A and D), consisting of outer and inner domain with truncated N- and C-termini and V1/V2 and V3 variable loops (T. Zhou et al., 2010).

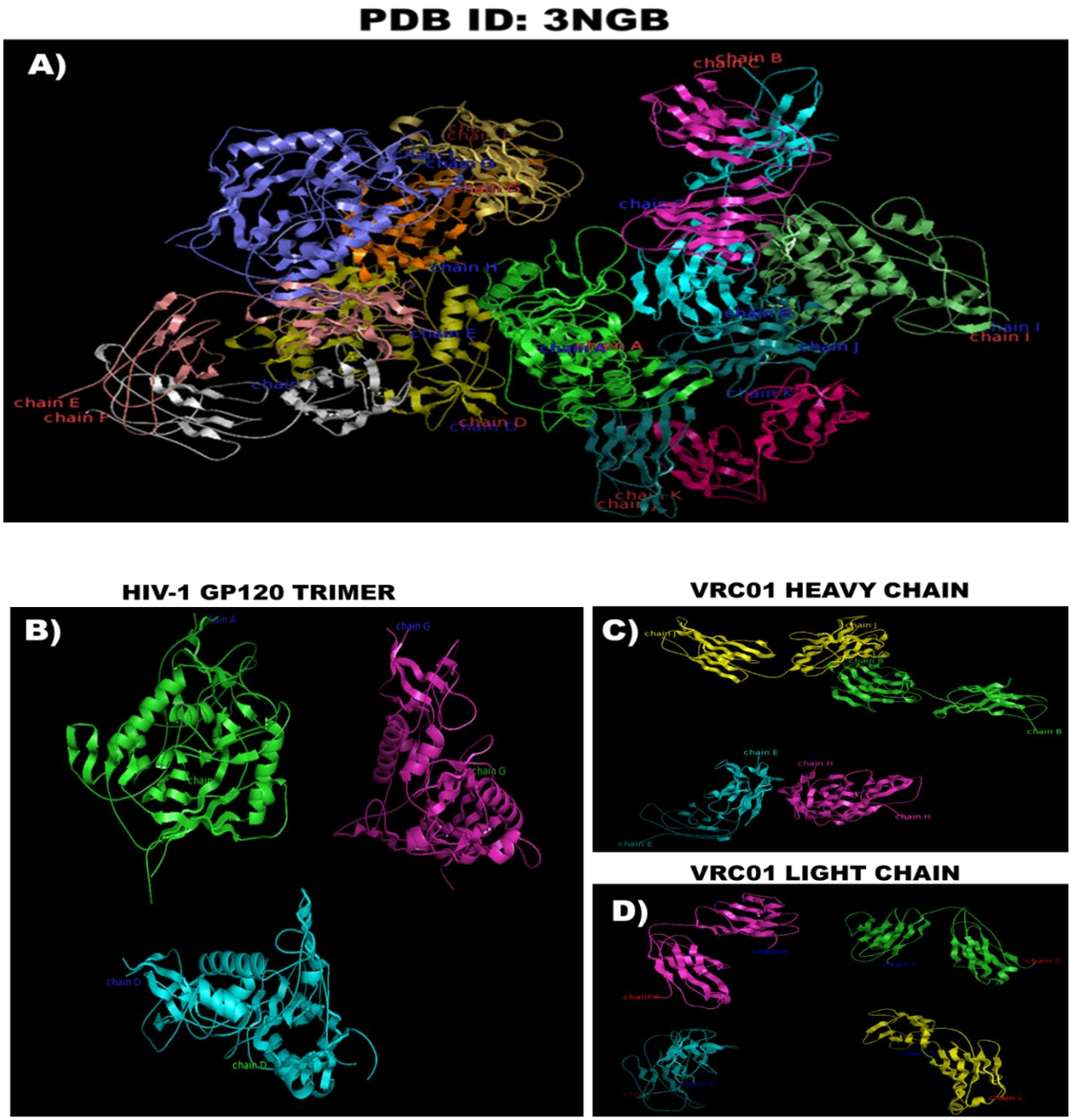

Figure 9. Protein structure with PDB ID: 3NGB. ***(A)*** *3-D structure of VRC01 broadly neutralizing antibody Fab in complex with HIV gp120 at 2.68 Å. The protein structure consists of 12 chains G, A, D, I, H, B, E, J, L, C, , and K.* ***(B)*** *and HIV-1 gp120 trimer chains G, D, and A.* ***(C)*** *Heavy chain of VRC01 Fab chains H, E, B, and J.* ***(D)*** *Light chain of VRC01 Fab (chains L, C, F, and K)* (Bonsignori et al., 2018).

4.1.2. Determination of gp120 core residues of interaction with VRC01

The site of vulnerability on the gp120 site is the highly conserved contact site for CD4 receptor on the gp120 outer domain. VRC01 makes contact gp120 with amino acid residues in the positions 275–283, 364 – 371, 421-437 and 455-478, which represent 98% of CD4 binding site on the HIV-1 gp120.

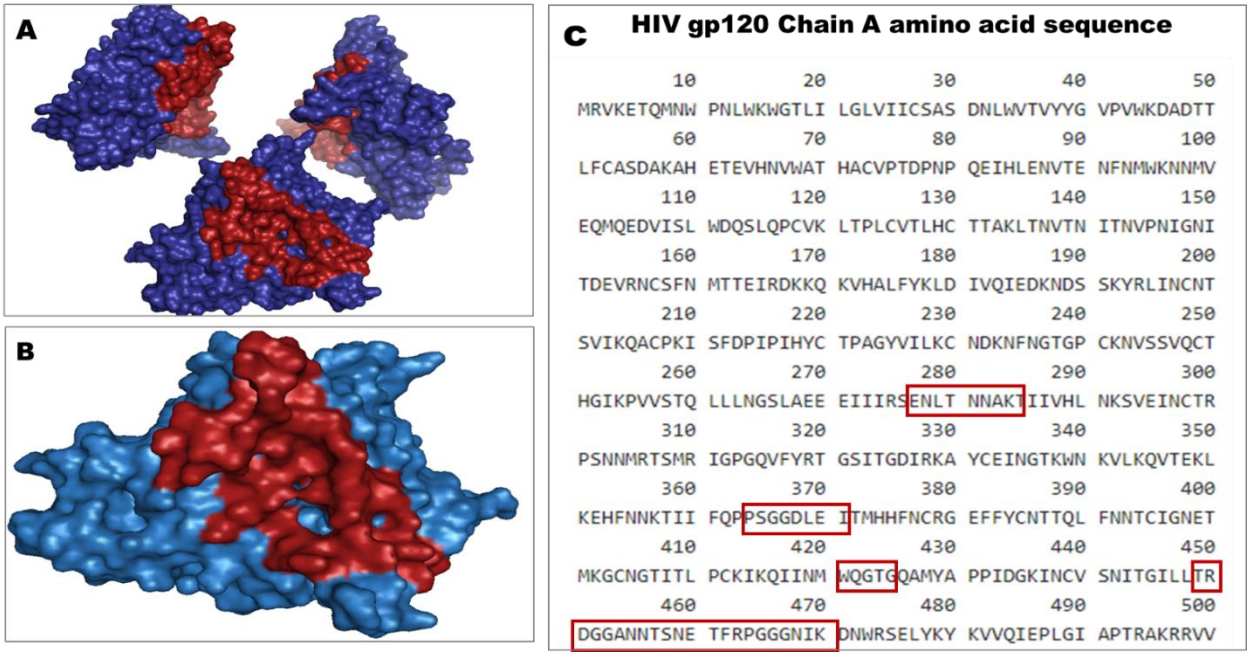

Figure 10. HIV-1 gp120 site of vulnerability for VRC01. (A) *gp120 trimer with the site of vulnerability (red),* ***(B)*** *gp120 monomer (chain A) with the site of vulnerability (red), and* ***(C)*** *gp120 amino acid sequence (chain A) with residues of interaction with VRCO1 (red boxes).*

4.1.3. Molecular Dynamic (MD) Simulation

The results obtained from the MD simulation of the receptor indicated that the Root Mean Square deviation (RMSD) of the protein backbone steadily increased from 0.075 nm at 0 ns to 0.175 nm at 1 ns. There was constant fluctuation of the RMSD between 0.15 nm (lowest point) and slightly above 0.225 nm (highest point) within the period of 1 ns and 9 ns. The system stabilized after 9 ns between

about 0.175 nm and 0.2 nm till the end of the simulations. The low root means square deviation after 9 ns is indicative of less fluctuations and more stable protein structure (Kufareva & Abagyan, 2012).

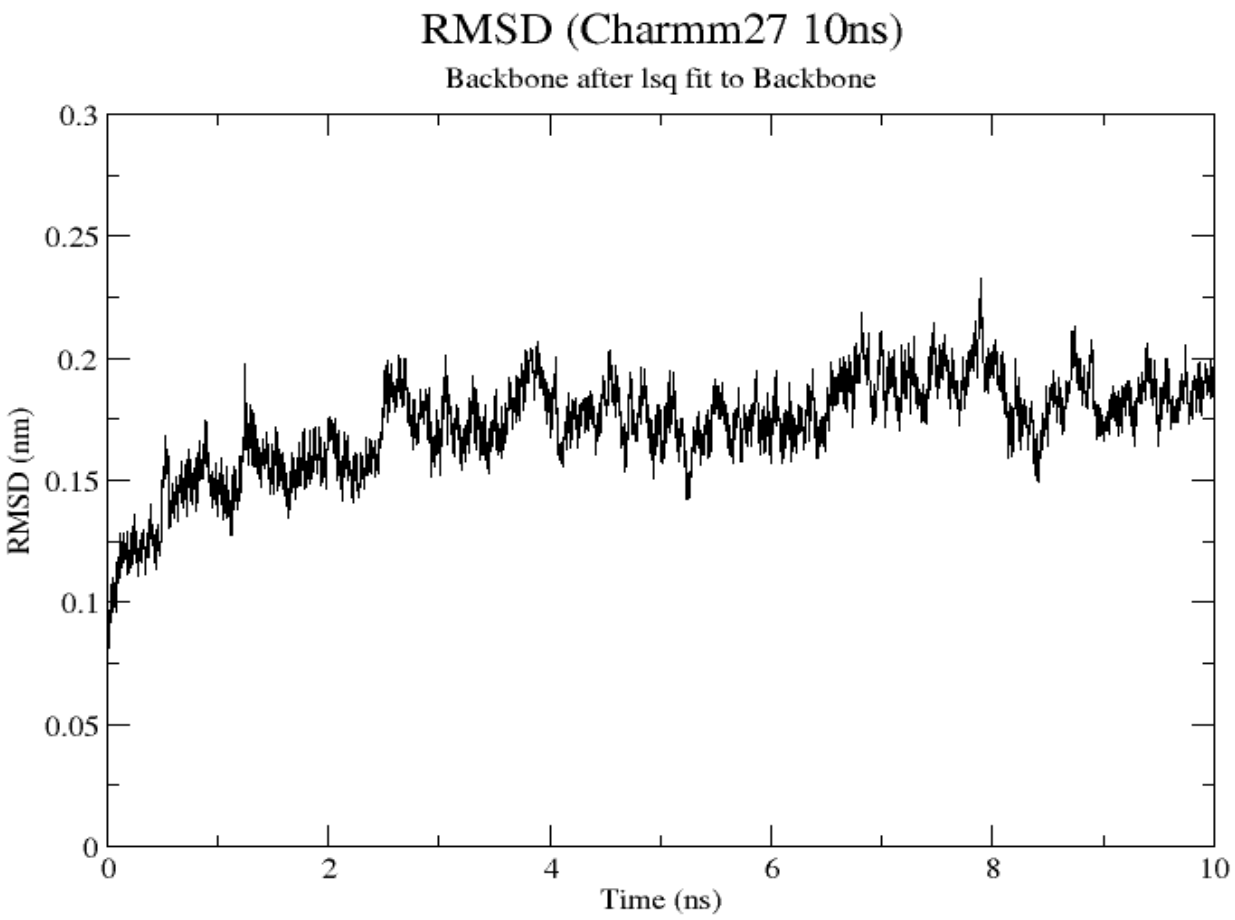

Figure 11. ***Root Mean Square Deviation (RMSD) of the MD simulation of HIV-1 gp120 monomer using GROMACS.*** *A plot of RMSD in nanometres (nm) against time in nanoseconds (ns). The RMSD increased from 0 ns to 1 ns and fluctuated till 9 ns after which it stabilized till the end of the simulation.*

4.1.4. Ligand Generation and Preparations

Six purchasable natural product-derived compounds libraries were downloaded from three natural compound companies. A total of 27,824 distinct ligands were generated from these compound libraries (Table 2). The ligands were minimized and optimized using the default setting in OpenBabel via PyRx.

Table 2. Summary of natural product compound libraries used for virtual screening.

S/N	Company	Library	Number of distinct compounds
1	AnalytiCon Discovery	Fragment from nature (FRGx)	247
2		Macrocyclic semi-synthetic compounds (MACROx)	2,040
3		Purified Natural Product Screening Compounds (MEGx)	3,781
4	SPECS	Pre-plated 20k diverse compound library	20,636
5		Pre-plated Natural product library	373
6	InterBioScreen (IBS)	IBS 2017_sep_Natual compound Libraries	747
		Total	**27,824**

4.1.5. Molecular Docking

A total of 27,824 ligands generated from six natural product libraries were used for molecular docking using AutoDock Vina (Table 2). The AutoDock molecular docking program assumes a rigid receptor and a conformationally flexible ligand. Different conformational poses of the ligands were docked into a rigid receptor (HIV gp120) and scored according to the binding energies of the receptor-ligand complexes. The best ligand poses with the lowest binding energies were selected and visualised in PyMOL. NP-005114, NP-007382 and NP-008927 were docked firmly in the receptor (Figure 12). Compounds NP-005114, NP-007382 and NP-008927 IUPAC name and structure is summarized in table 3. The molecular docking poses of the selected 10 hit compounds are shown in Appendix I.

Table 3. IUPAC name and Structure of Ligand NP-005114, NP-007382, and NP-008297

Compound 1D	IUPAC Name	Structure
NP-005114	1,3,6-Tris-O-(3,4,5-trihydroxybenzoyl)-β-D-glucopyranose	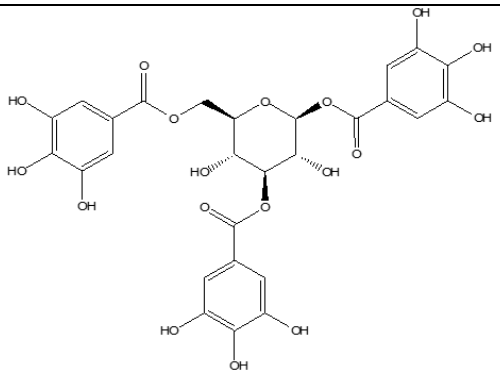
NP-007382	((3R)-4-{6-[(1R,3R,5S,8S,10R,12R,14R)-5,14-dimethyl-6-oxo-2,4,9,13-tetraoxatricyclo[8.4.0.0³,⁸]tetradec-12-yl]-1,5-dihydroxy-9,10-dioxoanthracen-2-yl}-3-hydroxy-3-methylbutanoate);	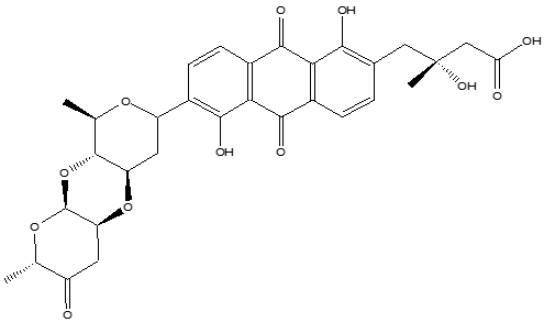
NP-008927	(2R,3S,4S,5R,6S)-6-[(2S,3R,4R,5R,6S)-2-[5,7-dihydroxy-2- (4-hydroxyphenyl)-4-oxochromen-3-yl]oxy-4,5-dihydroxy-6-methyloxan-3-yl]oxy-3,4,5-trihydroxyoxan-2-yl]methyl(E)- 3-(4-hydroxyphenyl)prop-2-enoate)	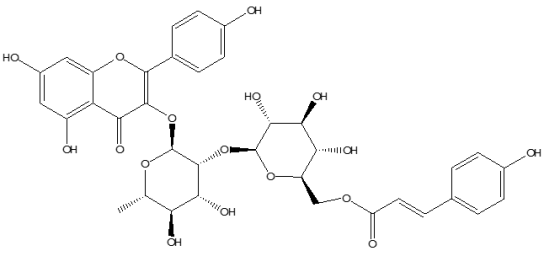

Table 4. Summary of 10 selected hit compounds with binding energies and molecular formula

Compound Names	Formula	Binding Energies (kcal/mol)
NP-008297	C36H28O17	-10.3
NP-004255	C27H22O18	-9.6
NP-000088	C28H30O15	-9.7
NP-007422	C40H62O15	-9.3
NP-005114	C27H30O18	-9.1
NP-007382	C31H32O12	-9.6
NP-000954	C47H74O16	-9.5
NP-005003	C36H38N8O9	-9.3
NP-001800	C41H52N8O9	-9.2
FRG-00075	C13H16F3N3O2	-7.4

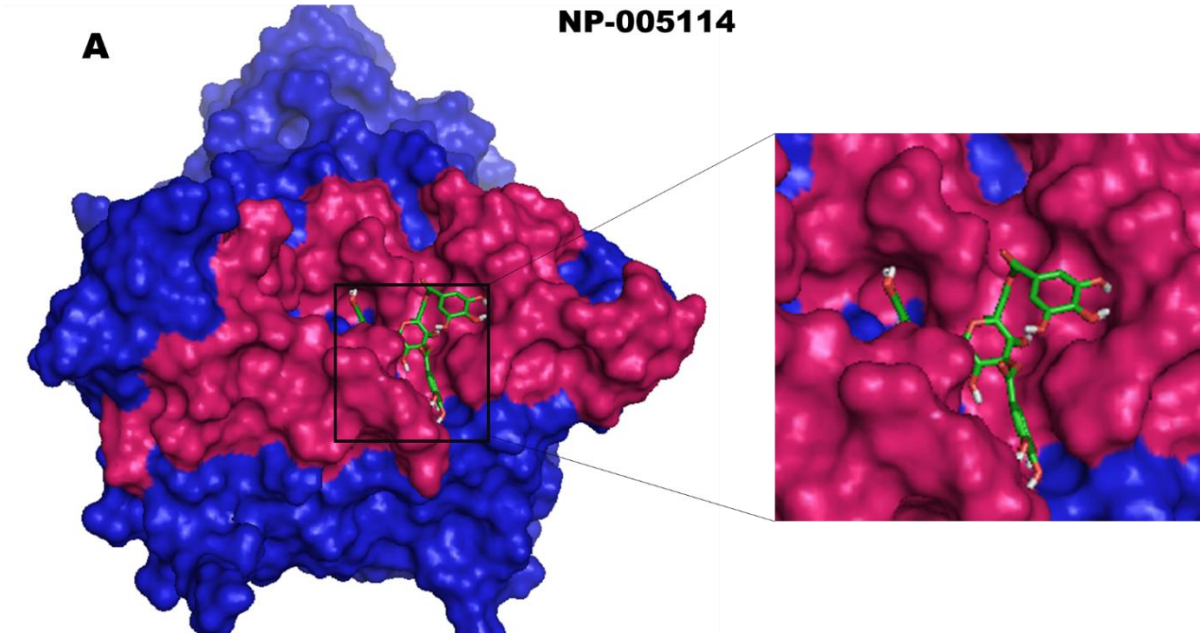

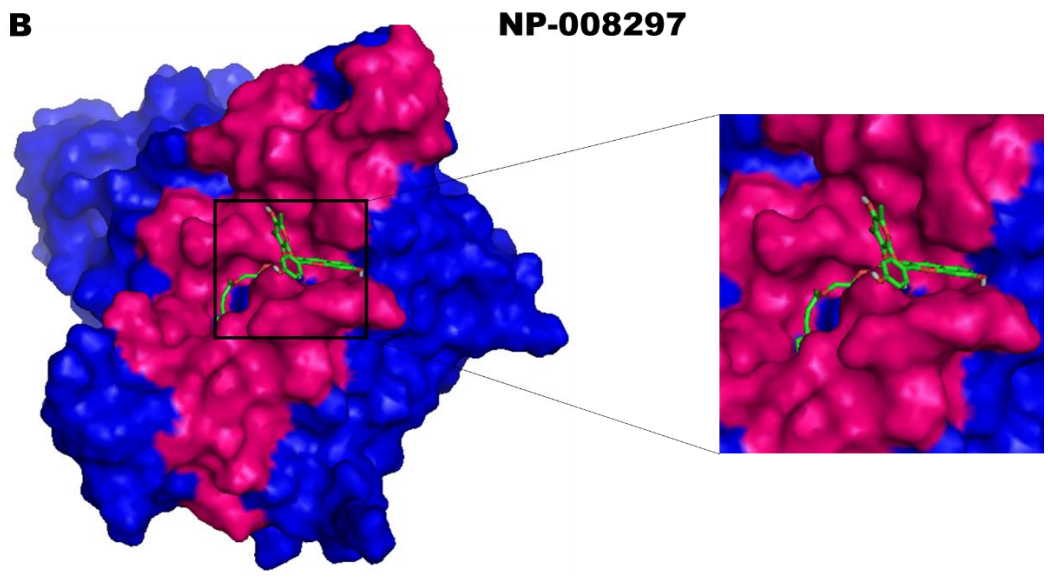

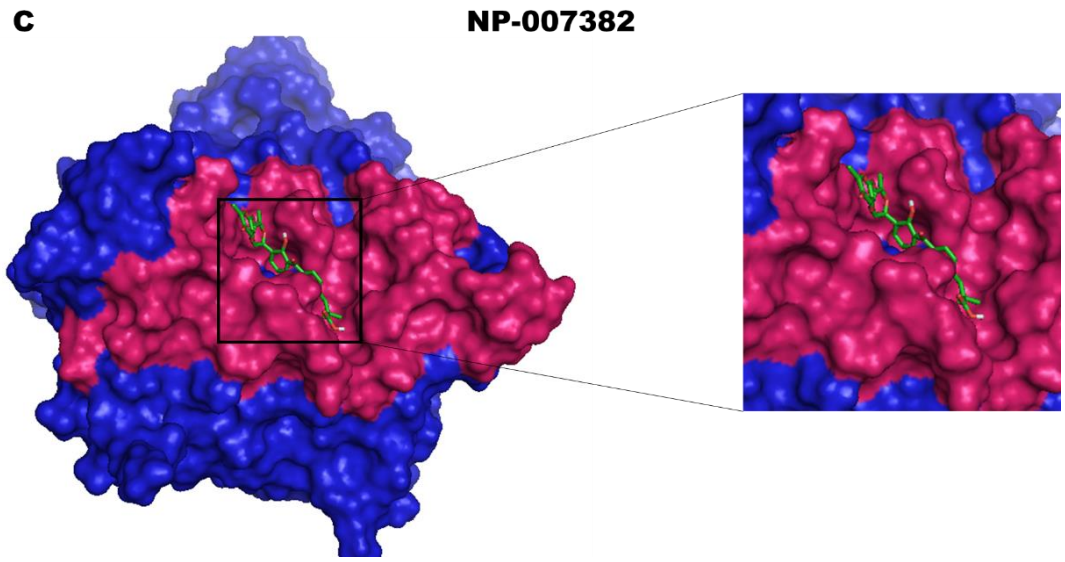

Figure 12. Molecular docking of the receptor (HIV gp120) and Ligands (compounds derived from the natural product). *A) Compound NP-005114 (coloured green) docked into CD4-bs (coloured pink) of HIV-gp120 (coloured blue). B) Compound NP-008927 (coloured green) docked into CD4-bs (pink) of HIV-gp120 (coloured blue). C) Compound NP-007382 (coloured green) docked into CD4-bs (coloured pink) of HIV-gp120 (blue).*

4.1.6. Protein-ligand Interaction Profiling

LIGPLOT was used to elucidate the amino acid residues in the binding site of the receptor (HIV gp120) that interact with the ligands (Laskowski & Swindells, 2011), and 2-D schematic diagrams that shows the protein-ligand interactions were obtained. The green dotted lines represent hydrogen bonds while the red arcs with spikes represent hydrophobic interactions. Amino acid (aa) residues of the receptor are shown as orange lines with black and red dots, while the ligands are shown as purple lines with black and red dots. Ligand NP-005114 had hydrogen bond interactions with eight amino acid residues and hydrophobic interaction with eleven amino acids residues in the CD4-bs of HIV gp120. Ligand NP-008927 had ten hydrogen bond interactions with amino acids residues and hydrophobic interactions with eleven amino acid residues in the CD4-bs of HIV gp120. Ligand NP-

007382 formed hydrogen bond interactions with five and seven hydrophobic interactions with amino acid residues in the CD4-bs. The binding energies and interacting amino acid residues are summarized in (Table 4)

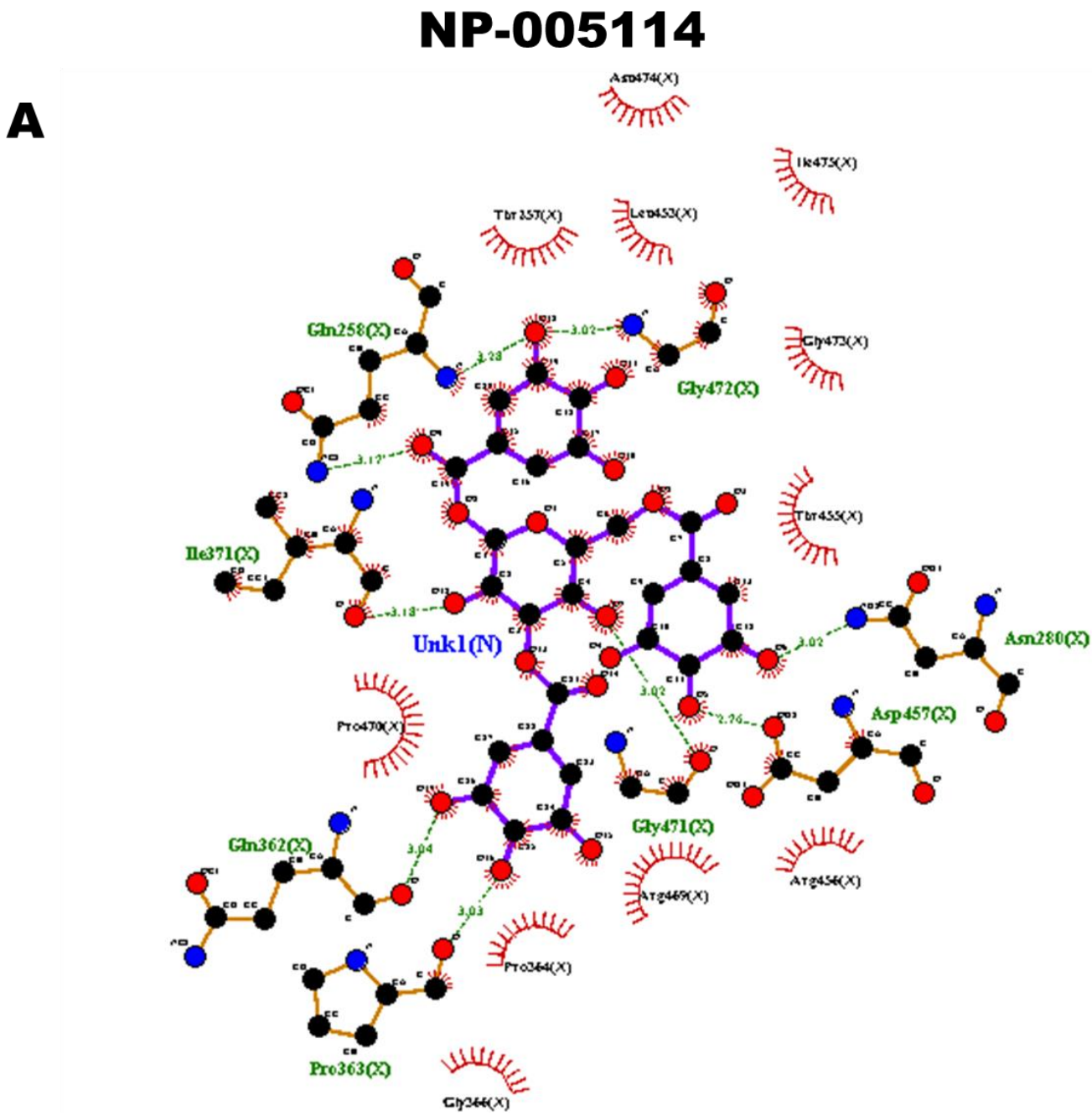

B

NP-008927

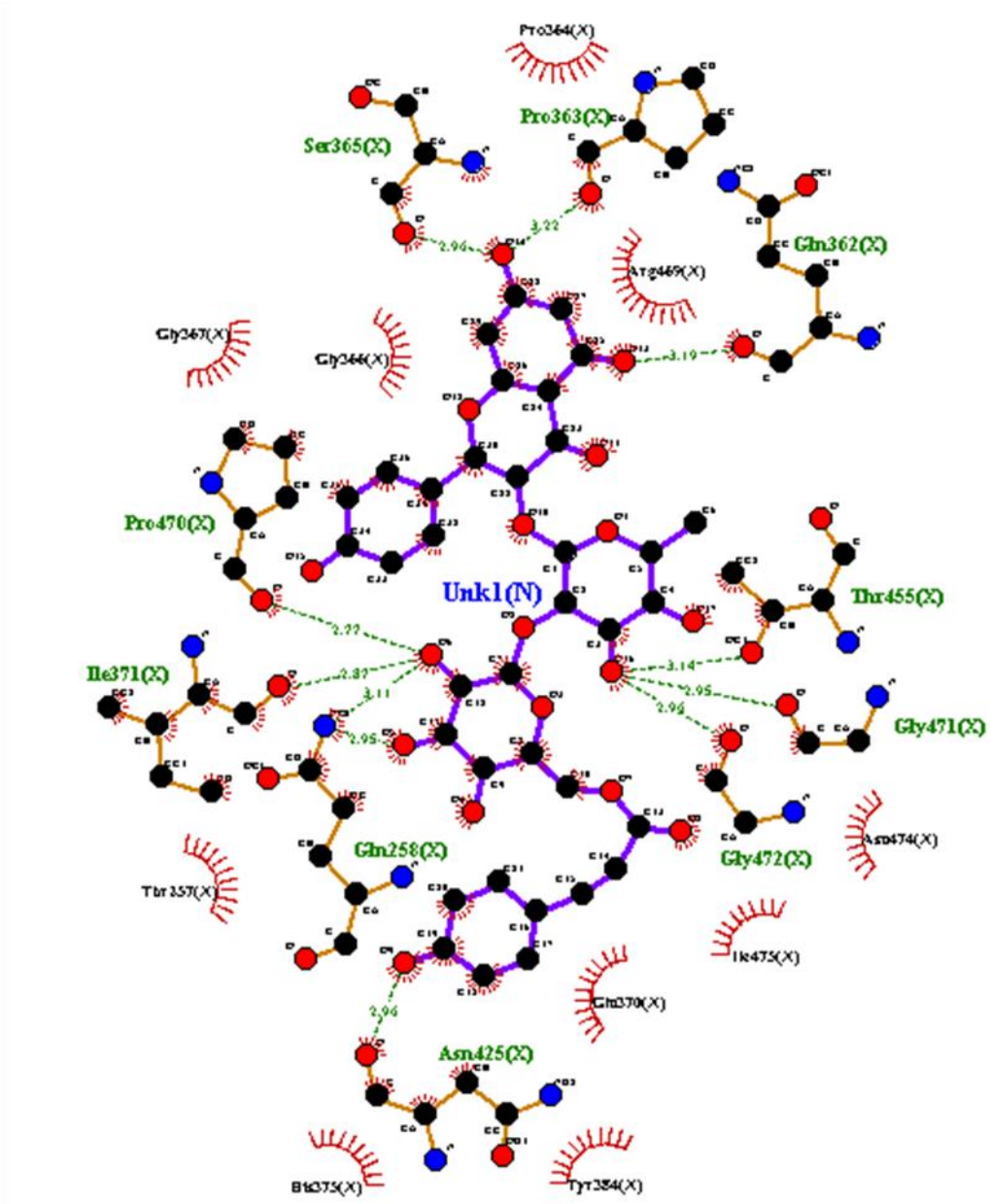

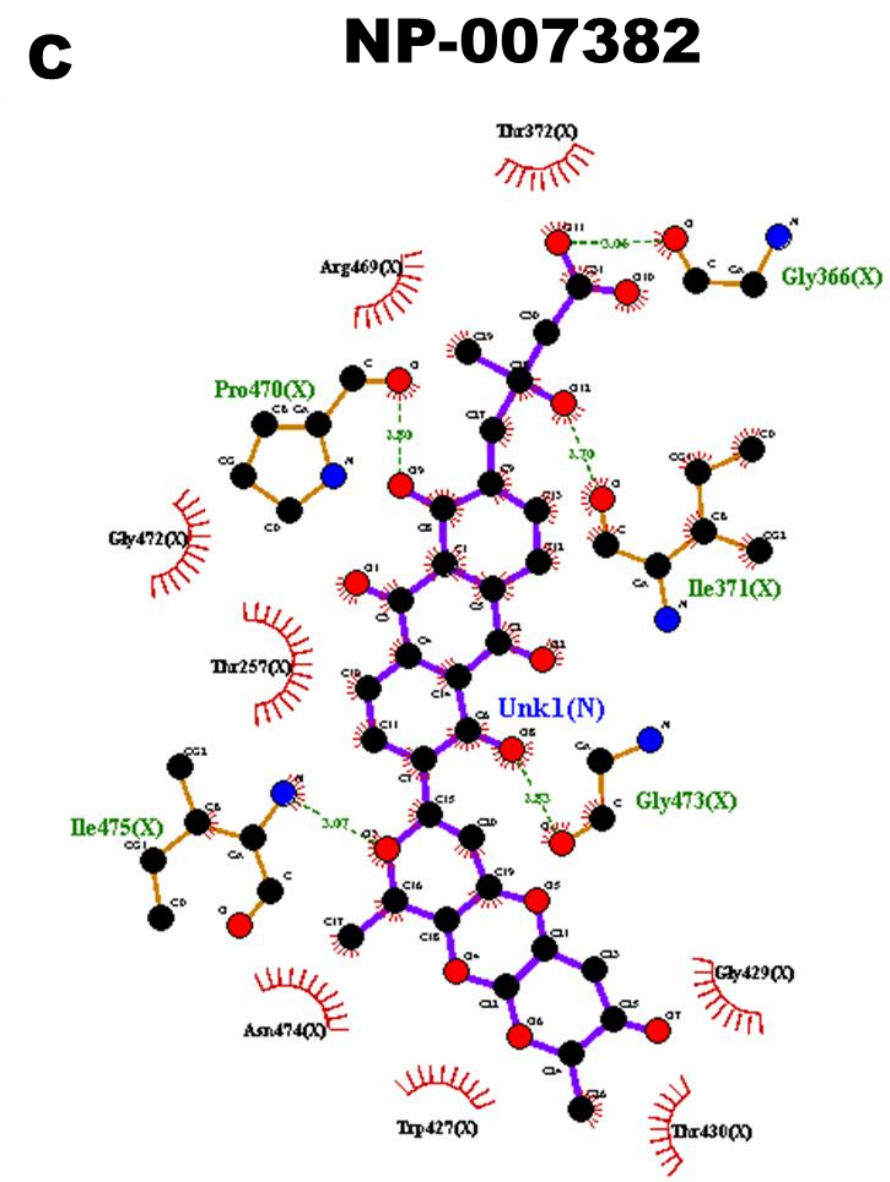

Figure 13. Protein-ligand interaction profiles. *The interactions of the selected ligands with the HIV gp120 were determined with LIGPLOT. The green dotted lines represent hydrogen bond interactions, while red arcs with spikes represent hydrophobic interactions. Residues of the receptor are shown as orange lines with black and red dots, while the ligands are shown as purple lines with black and red dots.* ***A)*** *Ligand NP-005114 had 8 hydrogen bonds and 11 hydrophobic with residues in the CD4-bs of HIV gp120.* ***B)*** *Ligand NP-008927 had 10 hydrogen bond 10 hydrophobic interactions with residues in the CD4-bs of HIV gp120. C) Ligand NP-007382 had 5 hydrogen bonds and 7 hydrophobic interactions with residues in the CD4-bs of HIV gp120.*

4.1.7. High Through-put Virtual Screening (vHTS) and Analysis.

The top 100 ligands from each of the six libraries (total 600) ranked according to their binding energies were analysed for binding interactions with HIV-1 gp120. Out of a total of 470 ligands with high binding affinity analysed from the selected 600 ligands, 386 ligands had hydrogen bonds interactions with HIV-gp120, while 84 ligands had no hydrogen bond interactions with HIV gp120. Of the 386 ligands with hydrogen bond interactions with gp120, 263 ligands had hydrogen bond interactions with less than four conserved amino acid residues within the site of vulnerability, while 41 had hydrogen bond interactions with 4 or more amino acid residues in the site of vulnerability on the HIV-1 gp120. The best 10 compounds selected for *in vitro* downstream evaluations was based on their binding energies and the number of interacting amino acid residues with the HIV-1 gp120 CD4 binding site (Figure 14). The binding energies of the best 10 compounds ranged from -10.3 to -6.4 kcal/mol (Table 4). The lower the value of the binding energy, the higher the binding affinity with HIV-1 gp120.

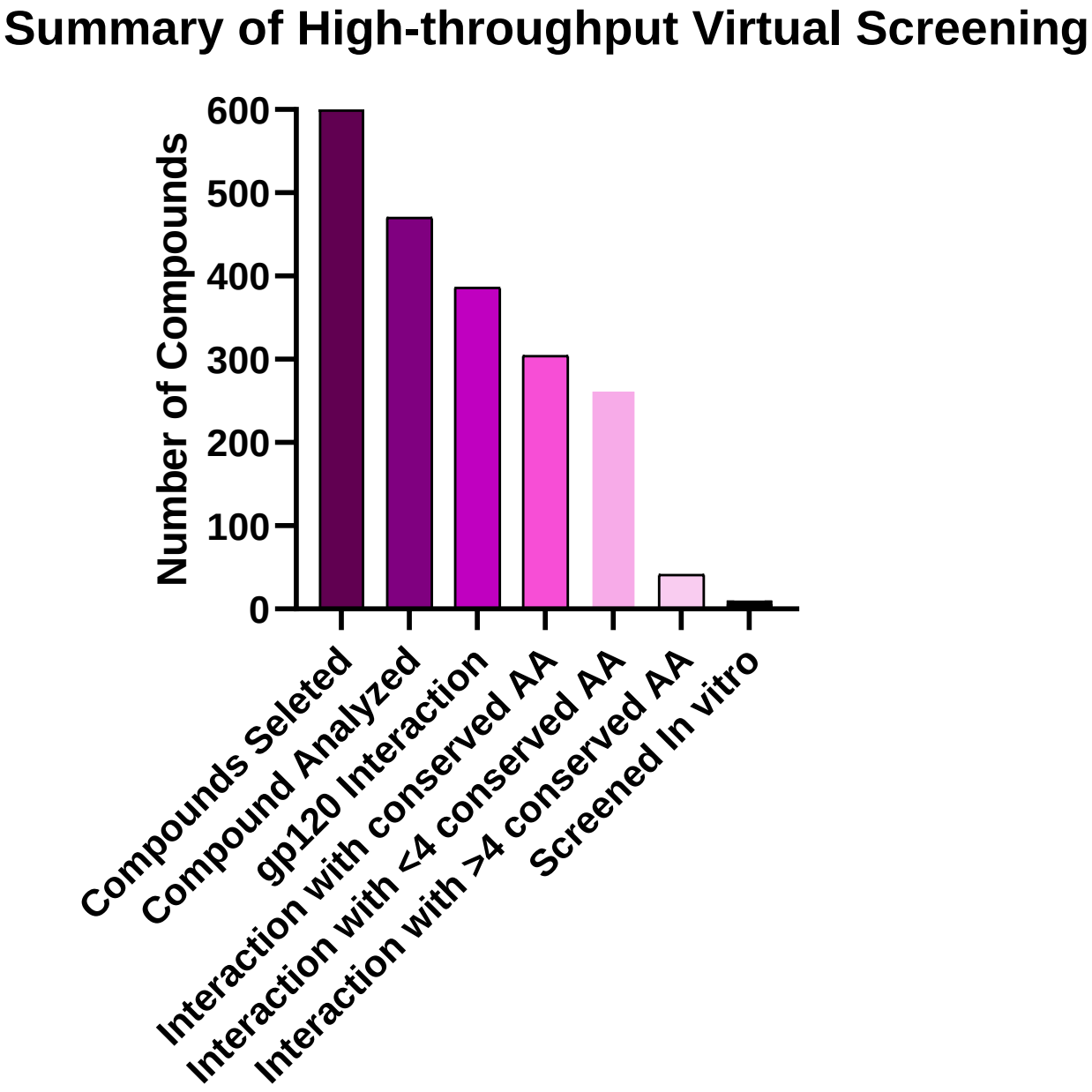

Figure 14. Summary of virtual high throughput screening. *The best 600 ligands were selected from the ligand library based on binding energies and 470 ligands of the selected ligands were analysed. A total of 304 ligands had hydrogen bond interactions with the CD4-Binding site (CD4-bs) amino acid residues. 41 had hydrogen bond interactions with 4 or more amino acid residues in the CD4-bs. The best 10 compounds were selected from the 41 for in vitro analysis.*

4.1.8. Determination of HIV HXB2 Envelope Protein Structure

Human Immunodeficiency Virus Clade B clone 2 (HIV HXB2) is a reference HIV strain. HXB2 envelope protein was used in the production of HIV -1 pseudotype virus that was used in the cell-based viral infectivity inhibition assay. The cDNA sequence of the HXB2 envelope protein (gp160) was retrieved from the HIV sequence database (Figure 15 A) and converted into an amino acid sequence using the ExPasy Translate tool (Artimo et al., 2012). The HXB2 gp160 amino acid sequence used to query the ExPasy server platform. The protein sequence (UniProtKB ID: P04578) with the highest similarity score to our query protein sequence was retrieved from UniProtKB (Figure 15 B). The 3D structure of the protein (PDB ID: 3J70), with 100% structural similarity to P04578 was retrieved from Protein Data Bank. The structure consists of HIV HXB2 gp160 chains D, P, U, E, Q and V) in complex with CD4 (chains C, O, and T) and 17b antibody chains A, M, R, B, N and S) (Figure 15 C). The HIV HXB2 gp120 trimer (chains D, P, and U) was extracted from 3j70 using PyMOL (Figure 15 D)

A

	10	20	30	40	50
1					
2	MRVKEKYQHL	WRWGWRWGTM	LLGMLMICSA	TEKLWVTVYY	GVPVWKEATT
3	60	70	80	90	100
4	TLFCASDAKA	YDTEVHNVWA	THACVPTDPN	PQEVVLVNVT	ENFNMWKNDM
5	110	120	130	140	150
6	VEQMHEDIIS	LWDQSLKPCV	KLTPLCVSLK	CTDLKNDTNT	NSSSGRMIME
7	160	170	180	190	200
8	KGEIKNCSFN	ISTSIRGKVQ	KEYAFFYKLD	IIPIDNDTTS	YKLTSCNTSV
9	210	220	230	240	250
10	ITQACPKVSF	EPIPIHYCAP	AGFAILKCNN	KTFNGTGPCT	NVSTVQCTHG
11	260	270	280	290	300
12	IRPVVSTQLL	LNGSLAEEEV	VIRSVNFTDN	AKTIIVQLNT	SVEINCTRPN
13	310	320	330	340	350
14	NNTRKRIRIQ	RGPGRAFVTI	GKIGNMRQAH	CNISRAKWNN	TLKQIASKLR
15	360	370	380	390	400
16	EQFGNNKTII	FKQSSGGDPE	IVTHSFNCGG	EFFYCNSTQL	FNSTWFNSTW
17	410	420	430	440	450
18	STEGSNNTEG	SDTITLPCRI	KQIINMWQKV	GKAMYAPPIS	GQIRCSSNIT
19	460	470	480	490	500
20	GLLLTRDGGN	SNNESEIFRP	GGGDMRDNWR	SELYKYKVVK	IEPLGVAPTK
21	510	520	530	540	550
22	AKRRVVQREK	RAVGIGALFL	GFLGAAGSTM	GAASMTLTVQ	ARQLLSGIVQ
23	560	570	580	590	600
24	QQNNLLRAIE	AQQHLLQLTV	WGIKQLQARI	LAVERYLKDQ	QLLGIWGCSG
25	610	620	630	640	650
26	KLICTTAVPW	NASWSNKSLE	QIWNHTTWME	WDREINNYTS	LIHSLIEESQ
27	660	670	680	690	700
28	NQQEKNEQEL	LELDKWASLW	NWFNITNWLW	YIKLFIMIVG	GLVGLRIVFA
29	710	720	730	740	750
30	VLSIVNRVRQ	GYSPLSFQTH	LPTPRGPDRP	EGIEEEGGER	DRDRSIRLVN
31	GSLALIWDDL	RSLCLFSYHR	LRDLLLIVTR	IVELLGRRGW	EALKYWWNLL
32	810	820	830	840	850
33	QYWSQELKNS	AVSLLNATAI	AVAEGTDRVI	EVVQGACRAI	RHIPRRIRQG

B

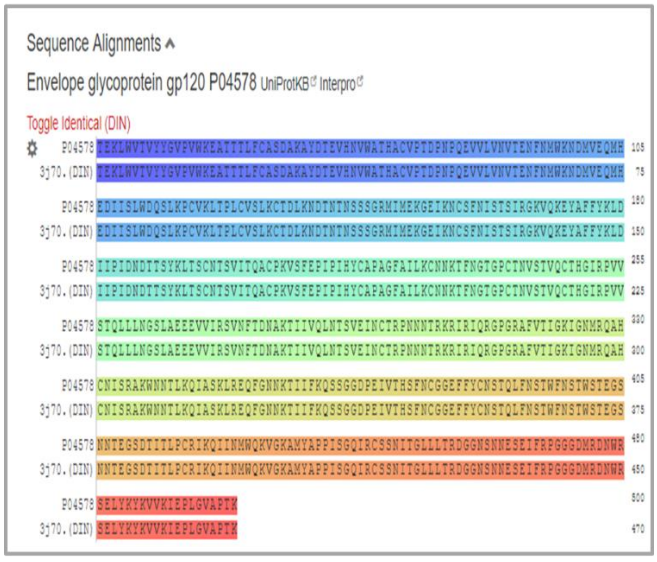

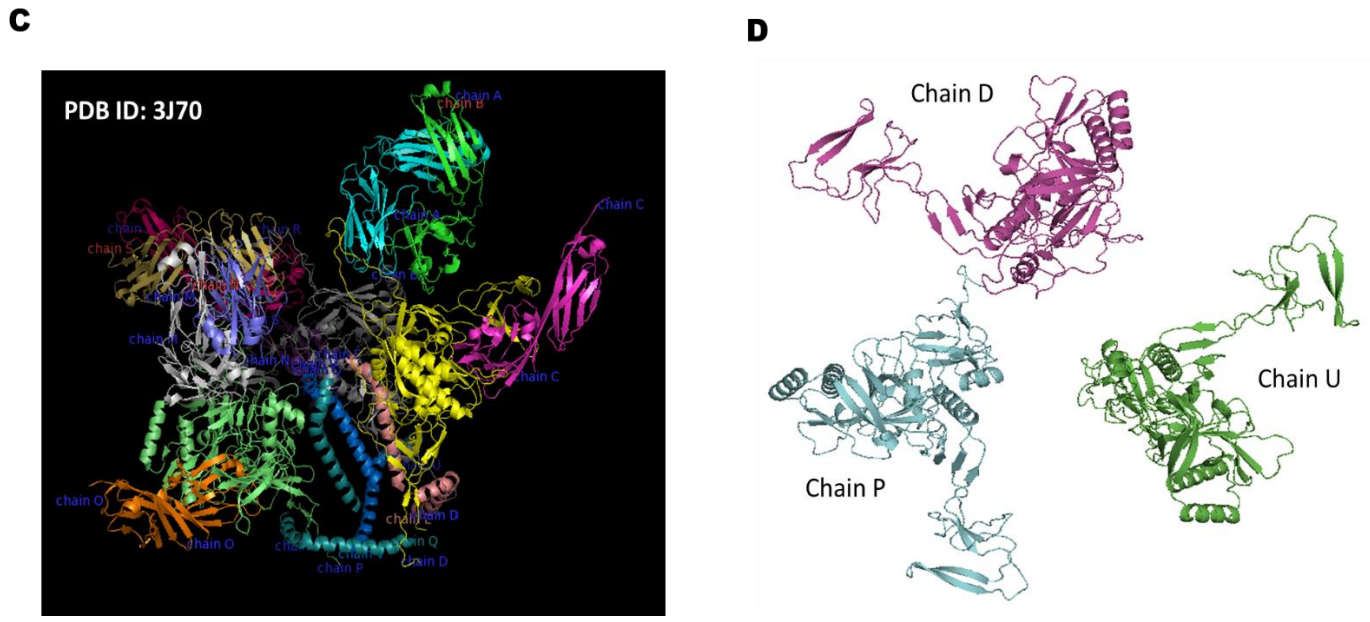

Figure 15. Determination of the 3-D structure of HIV HXB2. A) *The amino acid sequence of the HXB2 envelope protein retrieved from the HIV database.* ***B)*** *BlastP similarity search result of HXB2 Env amino acid sequence (sequence alignment).* ***C)*** *3-D structure of 3J70, which consist of HXB2 gp160 in complex with CD4 and 17b antibody.* ***D****) HXB2 gp120 extracted from 3J70 using PyMOL.*

4.1.9. Virtual Screening and Analysis of HIV HXB2 Envelope Protein

The ten selected compounds were used for virtual screening on HXB2 envelope protein. The compounds were docked against the HXB2 gp120 monomer. The compounds interacted with the conserved CD4-bs on HXB2 gp120 (Figure 16). NP-005114 had hydrogen bond interactions with eleven amino acids and hydrophobic interactions with four amino acids on the CD4-bs. There were four and ten hydrogen and hydrophobic interactions, respectively, between NP-008297 and the amino

acids in the gp120 CD4-bs. Compound NP-007382 had five hydrogen bond interactions and twelve hydrophobic interactions with the amino acids of CD4-bs.

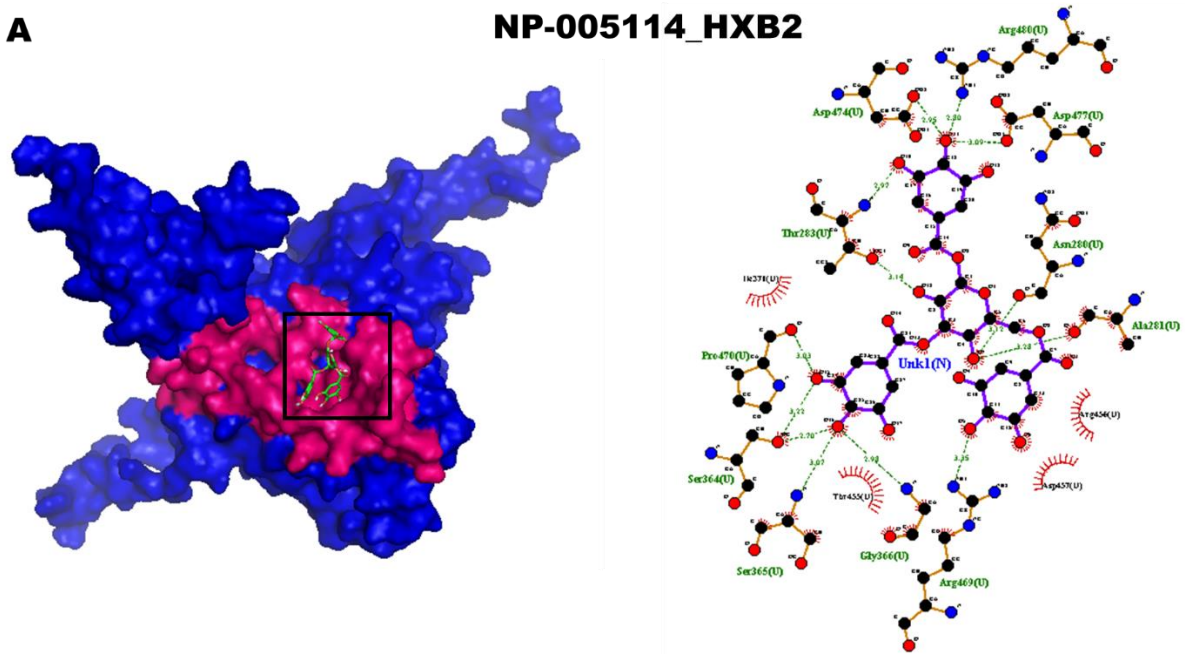

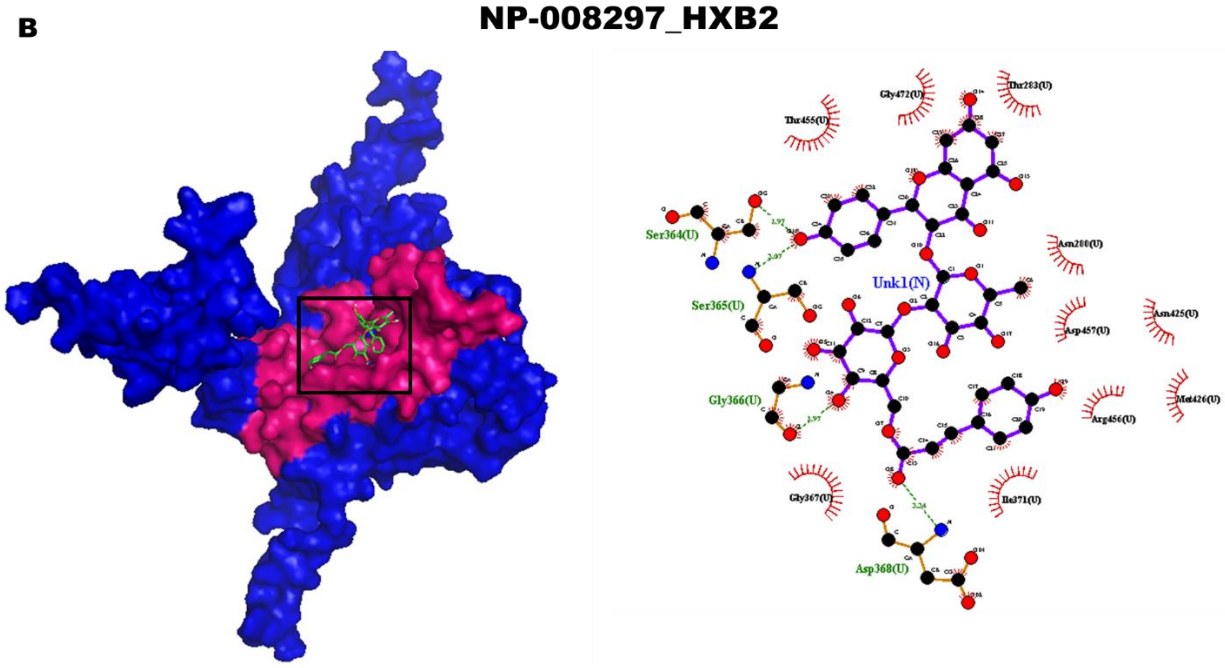

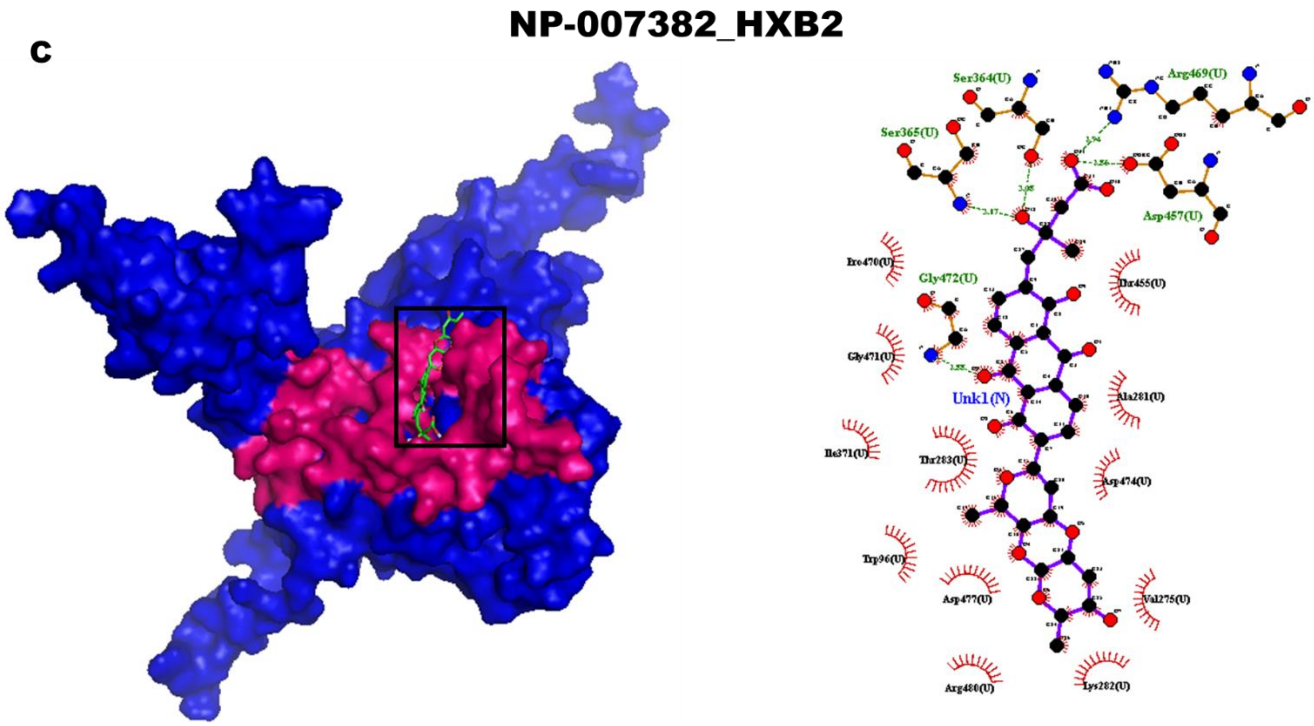

Figure 16. Virtual Screening and Protein-Ligand Interaction Profile of the Selected Compounds and HXB2 gp120. A) *NP-005114 had hydrogen bond interactions with eleven amino acids and hydrophobic interactions with four amino acids on the CD4-bs.* ***B)*** *NP-008297 had four and ten hydrogen and hydrophobic interactions with the amino acids in the gp120 CD4-bs.* ***C)*** *NP-007382 had five hydrogen bond interactions and twelve hydrophobic interactions with the amino acids of CD4-bs.*

Table 5. Binding Energies and Interacting Amino Acid Residues of Recombinant Clades A/E and B

	Recombinant clade A/E		Clade B	
Compounds	**Binding Energy (kcal/mol)**	**Amino Acid Residues**	**Binding Energy (kcal/mol)**	**Amino Acid Residues**
NP-008297	-10.3	Glu370, Gln258, Pro470, Ile371, Pro363, Ser365, Glu362, Gly471, Thr455, Gly472, and Asn425	-7.9	Asp368, Ser365, Ser364, Gly366, Asn425, and Met426
NP-000088	-9.7	Glu370, His375, Gln258, Gly472, Gln363, and Ser365	-7.1	Gly473, Thr283, Ser364, and Ser365
NP-007382	-9.6	Pro470, Gly366, Ile371, Gly473, and Ile475	-7.2	Asp457, Arg469, Ser364, Ser365, and Gly472
NP-000954	-9.5	Pro470, Arg469, Ile371, Met373, Gln258, and Gly472	-4.8	Arg456, Asp457, Pro470, Ser364, Ser365, Met426, and Trp427
NP-005003	-9.3	Asp457, Asn280, Pro470, and Arg468	-7.3	Thr283 Ala281
NP-007422	-9.3	Gln258, Ile371, Thr257, Met373, Glu370, Asn425, Asp280, and Asp457	-6.7	Asp474, Arg476, Trp427, Gly473, Asn425, Asp368, and Glu370
NP-001800	-9.2	Glu370, Trp427, Gly429, Gln105, and Asn474	-7.8	Ser365 and Gln363
NP-005114	-9.1	Gln258, Ile371, Gln362, Pro363, Gly471, Asp457, Asn280, and Gly472	-8.2	Arg476, Gly472, Pro470, Gly366, Ser364, Glu370, Asn425, Trp427, and Met426
NP-004255	-9	Trp427, Gly429, Ile371, Gln258, Pro470, and Gly472	-7.3	Arg47, Asp474, Thr455, and Pro470
FRG-00075	-7.4	Glu370, Ile371, Ser365, Arg469, and Gly472	-6.8	Gly431 and Ser375

4.1.10. Origin and Sources of the Selected Compounds

Out of the ten selected natural product-derived compounds, six were obtained from plants, three from microorganisms and one was a synthetic fragment of the natural compound (Table 6).

Table 6. The Origin and Sources of the Selected Compounds

Compound Structure	Organism	Name
NP-000088	Plant	*Mentha piperita*
NP-000954	Plant	*Ononis spinosa*
NP-004255	Plant	*Terminalia chebula*
NP-005003	Microorganism	*Aspergillus*
NP-005114	Plant	*Terminalia chebula*
NP-007382	Microorganism	*Bacteria*
NP-007422	Plant	*Withania somnifera*
NP-008297	Plant	*Ginkgo biloba*
NP-001800	Microorganism	*Fungi*
FRG-00075	Fragment	

4.1.11. Pharmacological Profiling of 10 Selected Compounds

The pharmacological and physicochemical properties of the 10 selected compounds were obtained from SwissADME (Tables 7 and 8). The compounds have high molecular weights between 335.72 and 895.09 Dalton. Rotatable bonds are predictors of ligand conformational flexibility and small compound bioavailability (Veber et al., 2002). Rotatable bond less than or equal to seven are considered ideal in drug discovery, and eight of the compounds fell within this range. The pharmacological properties indices such as lipophilicity, solubility, gastrointestinal (GI) absorption, brain-blood barrier (BBB) permeant, P-glycoprotein (P-gp) substrate and Cytochrome 450 inhibitor were used to predict the absorption, distribution, metabolism, and excretion (ADME) profiles of the compounds which describe the pharmacokinetic properties. Lipophilicity value for the selected compounds were between -0.98 and 1.91. The ideal lipophilicity value lies between 1 and 3 (Arnott, Kumar, & Planey, 2013); only 4 of the selected compounds fell within this range. Eight of the compounds were predicted to be soluble in water (Table 8). The summation of all the polar atoms of a molecule is defined by the topological polar surface area (TPSA) (Fernandes & Gattass, 2009). The TPSA value is a metric used to define cell permeability by a drug. The ideal TPSA usually falls within 140 to 90 Å, above 140 Å indicates poor permeability into cell (Pajouhesh & Lenz, 2005), and below 90 indicates penetration into the blood-brain-barrier (BBB)(Hitchcock & Pennington, 2006). None of the compounds fell within this range. However, 9 of the compounds had low GI absorption. None of the compounds selected was BBB permeant. Nine compounds were substrates of P-gp transporter. None of the selected compounds were inhibitors of CYP 450 enzyme (Table 7).

Table 7. Physicochemical Properties of 10 Selected Compounds

Compound Name	MW (Dalton)	#Rotatable bonds	#H-bond acceptors	#H-bond donors
NP-008297	740.66	9	16	9
NP-004255	634.45	2	15	11
NP-000088	610.56	7	15	8
NP-007422	782.91	9	14	9
NP-005114	636.46	5	15	11
NP-007382	596.57	5	12	4
NP-000954	895.08	7	16	9
NP-005003	723.78	5	9	9
NP-001800	800.90	7	9	9
FRG-00075	335.72	2	4	2

Table 8. Adsorption, Distribution, Metabolism, and Excretion Properties of 10 Selected Compounds

Compound Name	TPSA	Lipophilicity	Water Solubility	GI Absorption	BBB Permeant	Pgp Substrate	CYP inhibitor
NP-008297	275.5	1.79	Soluble	Low	No	Yes	No
NP-004255	310.66	-0.87	Soluble	Low	No	Yes	No
NP-000088	234.29	-0.43	Soluble	Low	No	Yes	No
NP-007422	245.29	0.07	Soluble	Low	No	Yes	No
NP-005114	310.66	-3.12	Soluble	Low	No	No	No
NP-007382	186.12	1.91	Soluble	Low	No	Yes	No
NP-000954	254.52	1.82	Insoluble	Low	No	Yes	No
NP-005003	251.16	-0.98	Soluble	Low	No	Yes	No
NP-001800	251.16	0.61	Insoluble	Low	No	Yes	No
FRG-00075	71.18	1.3	Soluble	High	No	Yes	No

4.1.12. Toxicity Profiling of the Selected Compounds

The result of the toxicity profile of the selected compounds predicted using Pro-Tox II were summarized in Table 9 (Drwal et al., 2014). ProTox-II generate the toxicity profiles of small compound molecules by measuring parameters such as immunotoxicity, hepatotoxicity, cytotoxicity, mutagenicity, carcinogenicity and toxicity class (Drwal et al., 2014). Toxicity class ranges from 1 -6 (1 = highly toxic/fatal, 6 = least toxic) with probability range of 0 - 1 (0 = not likely, 1 = very likely). Nine of the compounds belonged to the less toxic drug class associated with high LD_{50} with the exception of NP-007422, which belongs to the toxicity class 2 (Table 9). None of the compounds were hepatoxic and mutagenic. Also, nine of the compounds were inactive for carcinogenicity and cytotoxicity, whilst eight were predicted as immunotoxin.

Table 9. Toxicity Profiles of 10 Selected Compounds Predicted using ProTox-II

Compound Name	Toxicity Class	Hepatoxicity	Carcinogenicity	Immunotoxicity	Mutagenicity	Cytotoxicity	LD_{50} (mg/kg)
NP-008297	4	Inactive	Inactive	Active	Inactive	Inactive	1000
NP-004255	5	Inactive	Inactive	Active	Inactive	Inactive	2260
NP-000088	6	Inactive	Inactive	Active	Inactive	Inactive	5530
NP-007422	2	Inactive	Inactive	Active	Inactive	Active	7
NP-005114	6	Inactive	Inactive	Inactive	Inactive	Inactive	8000
NP-007382	4	Inactive	Inactive	Active	Inactive	Inactive	2000
NP-000954	4	Inactive	Inactive	Active	Inactive	Inactive	2500
NP-005003	4	Inactive	Inactive	Active	Inactive	Inactive	500
NP-001800	4	Inactive	Inactive	Active	Inactive	Inactive	1000
FRG-00075	4	Inactive	Active	Inactive	Inactive	Inactive	1000

4.2. CELL-BASED VIRAL INFECTIVITY INHIBITION ASSAY

4.2.1. Transformation of Competent Bacteria Cells

To obtain a high quantity of plasmids required to produce HIV pseudotype virus, top10 competent bacteria cells were transformed with a plasmid containing HIV gag-pol gene (p8.91), HIV HXB2 gp160 (pCAGGGS HXB2, and luciferase gene (pCSFLW) under ampicillin selection marker using the heat shock method. Positively transformed colonies were observed for cells transformed with plasmids p8.91, pCSFLW, and pCAGGGS-HXB2 (Figure 17 A-C). Positive control consisting of top10 cells grown in the absence of ampicillin selection marker showed colonies of top10 cells (Figure 17 D). Negative control consisting of top10 cells grown in the presence of ampicillin selection marker showed no growth of colonies (Figure 17 E).

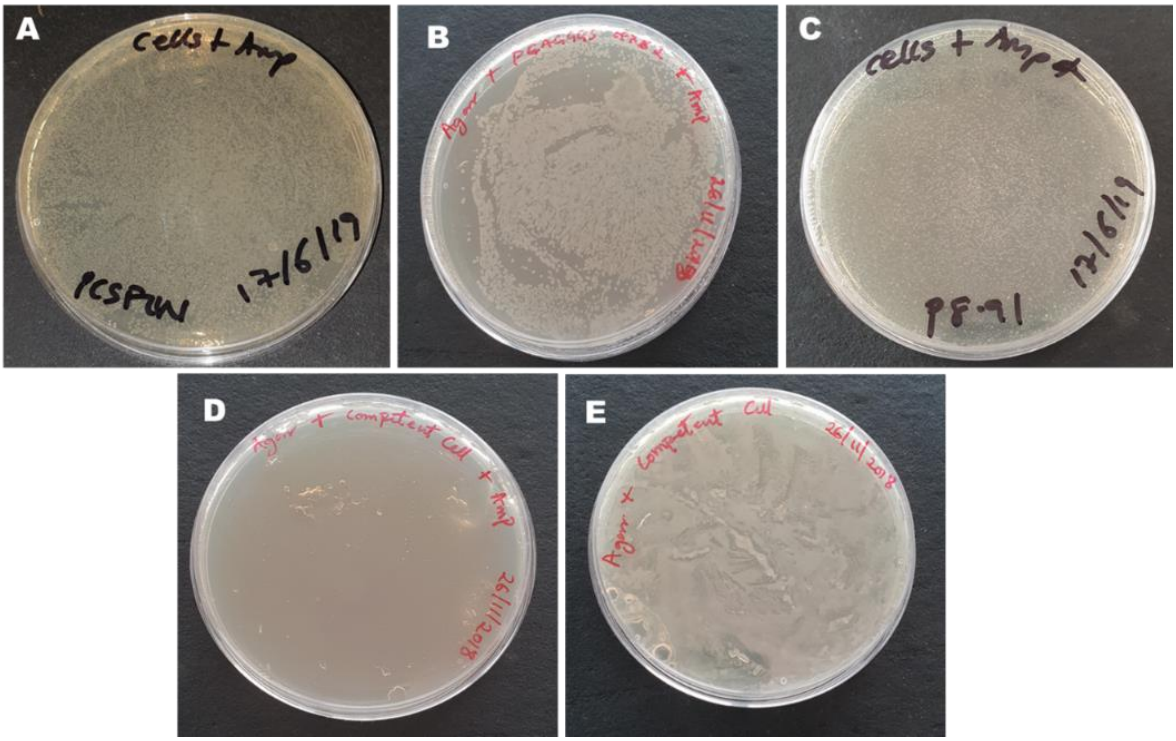

Figure 17. Transformation of Top10 competent bacteria cells. *Top10 competent bacterial cells transformed using the heat shock method. A-C) Colonies of cell transformed with plasmids PCSFLW, HXB2, and P8.91 respectively. D) Negative control consisting of competent cells grown in the presence of ampicillin selection marker. E) Positive control consisting of competent cells grown in the absence of ampicillin selection marker.*

4.2.2. Restriction Digest

Restriction digest was done to confirm the plasmids extracted from the transformed competent cells. Plasmids were extracted from single colonies of positively transformed cells

(Fig. 17 A-C) and digested with appropriate restriction enzymes. a p8.91 plasmid containing HIV-1 gag-pol gene, which was digested with restriction enzyme BglIII showed expected band size at 3.9kb, and 8. 2kb. pCSFLW plasmid containing luciferase reporter gene, which was digested with BamH1 and Not1 showed band sizes at 1.7kb and 8.9kb as expected. Expected band sizes of 4.7kb and 2.6kb were observed for pCAGGGS HXB2 plasmid digested with Kpnl +Xhol.

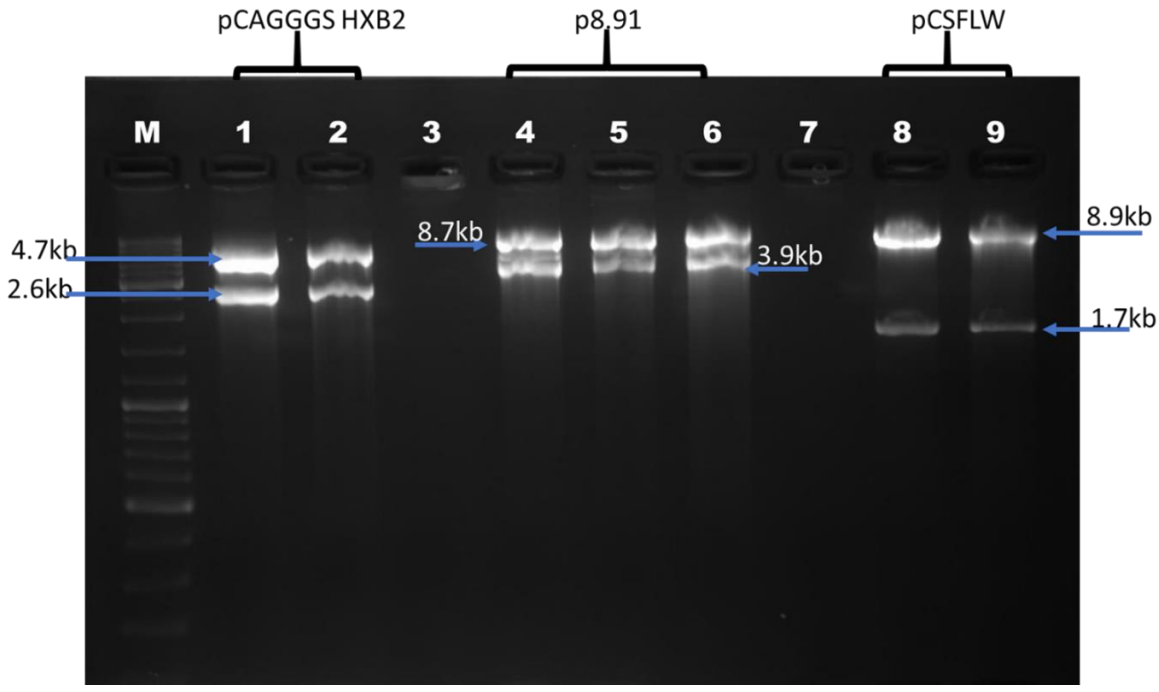

Figure 18. Restriction digest of extracted plasmids. *(Lane 1 and 2) pCAGGGS HXB2 plasmid expected band sizes of 4.7kb and 2.6kb. (Lane 4, 5 and 6) p8.91 plasmid expected band size at 3.9kb and 8.2kb. (lane 8 and 9) pCSFLW plasmid expected band size 1.7kb and 8.9kb. M is a molecular maker.*

4.2.3. Pseudotype Virus (PV) Titration and Determination of 50% Tissue Culture Infectivity Dose ($TCID_{50}$)

Pseudotype virus titration was used to determine the amount of viable pseudotype that was produced. A viable pseudotype virus was defined as pseudotype virus that can transduce/infect a target cell, integrate the luciferase reporter gene, leading to the expression of the reporter gene. The quantity of light produced by the luciferase enzyme (relative light unit RLU), measured with a luminometer directly correlates with the amount of viable pseudotype virus. $TCID_{50}$ was defined as the amount of pseudotype virus that was able to transduce/infect 50% of target cells (TZM-bl cells). A positive transduction/infection was defined as one with 2.5 times the RLU of the cell only control well. $TCID_{50}$ calculated in $TCID_{50}$ MACRO sheet, using the Spearman and Karber methods was 5657 $TCID_{50}$/ml. The cut-off for the luminescent was set at 10,000RLU. The recommended volume of pseudotype virus that will produce 10,000RLU was calculated as 105µl.

4.2.4. Cell Viability Assay

To determine the cytotoxic effect of the selected compounds on the target cells, TZM-bl cells, Alamar blue cell viability assay was carried out. TZM-bl cells were treated with the selected compounds in serial dilution. The assay was carried out in triplicate and the mean value was used to calculate the cell viability. Cell viability was calculated relative to the absorbance of the negative control wells (TZM-bl cells only), which were set as 100% of absorbance. Compounds FGR-0075, NP00603, NP00088, NP001800, NP005114, and, NP-007422 had no cytotoxic effect on the TZM-bl cells (Figure 19) at tested concentration. Compound NP008297 had minimal effect on the TZM-bl cells, NP00738 has cytotoxic *effect* from 25µg/ml, while NP-000954 and NP004255 ha cytotoxic effect from 12.5µg/ml. Ursolic acid, a known cytotoxic compound, was used as the positive control.

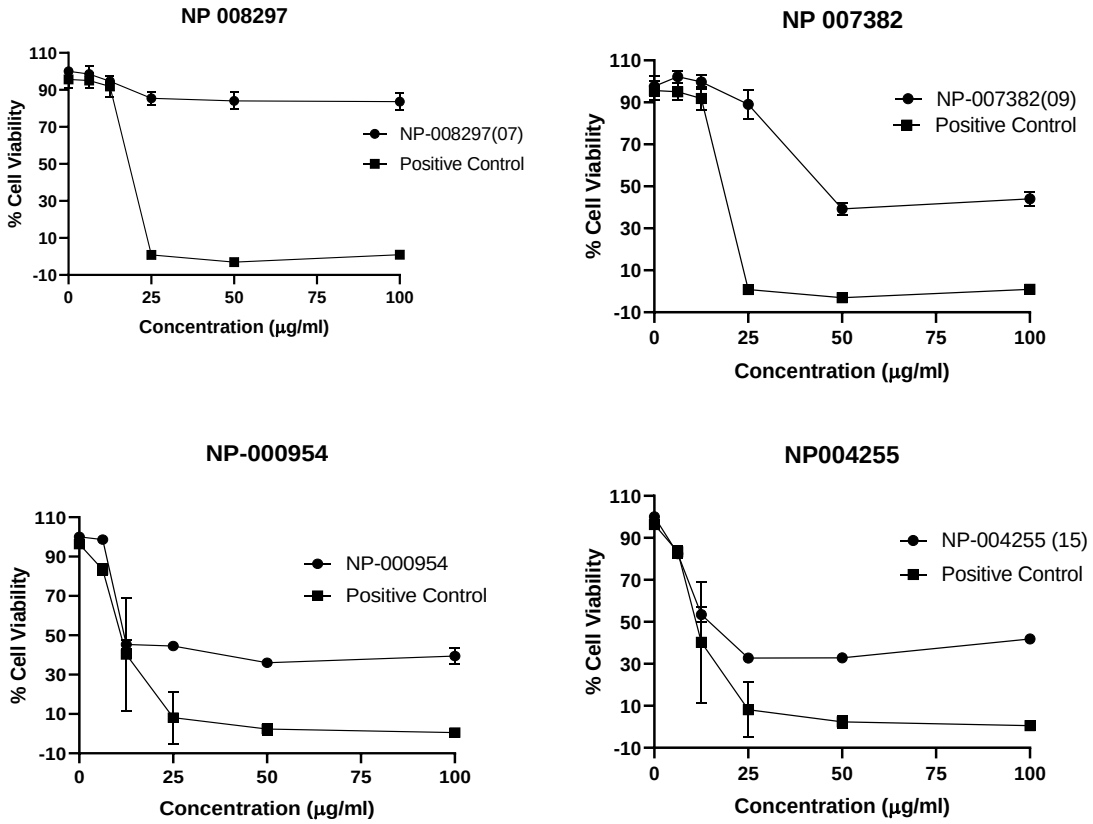

Figure 19. Alamar blue cell viability assay*. Compound NP008297 (top left) has minimal effect on the TZM-bl cell line, NP00738 (top right) has cytotoxic effect from 25µg/ml, while AD194735-10 and NP004255 (lower panel) has cytotoxic effect at 12.5µg/ml*

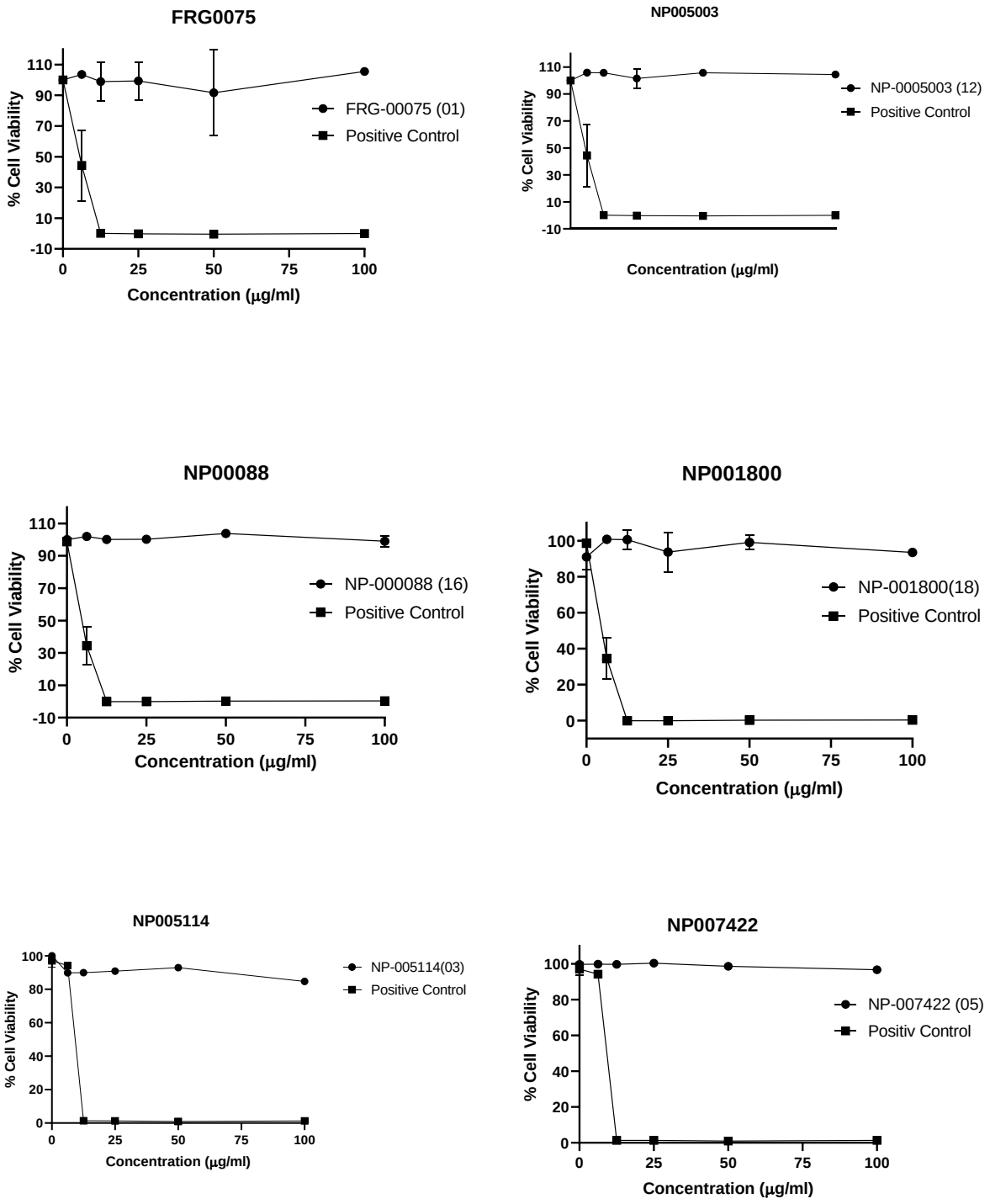

Figure 20. *Alamar blue cell viability assay shows tested compound had no cytotoxic effect on the TZM-bl cells. The positive control is ursolic acid, a known cytotoxic compound.*

4.2.5. Determination of 50% Cytotoxicity Concentration (CC_{50})

To determine the 50% cytotoxic concentration (CC_{50}) of compounds that had a cytotoxic effect on the TZM-bl cell (Figure 20). The assay was done in triplicate, and the mean values were calculated and used for the determination of the CC_{50}. Non-linear dose-response regression analysis was used to calculate CC_{50}. $CC_{50}$was defined as the concentration of the compound that is required to reduce viable cells by 50%. Compounds NP007382 had CC_{50} of 34.24µg/ml (Figure 21 C), while NP004255 and NP000945 had CC_{50} of 9.9µg/ml and 9.4µg/ml, respectively (Figure 21 A and B).

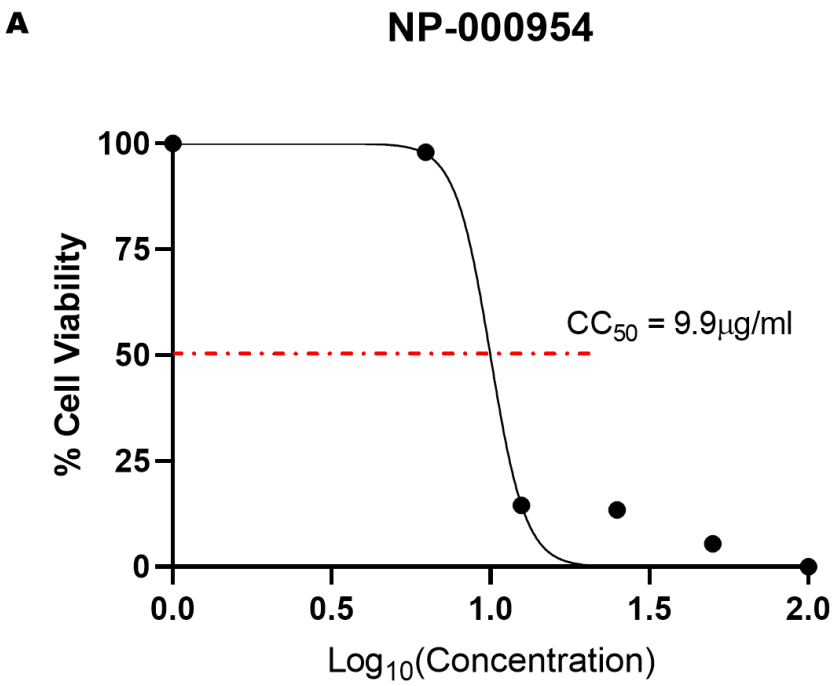

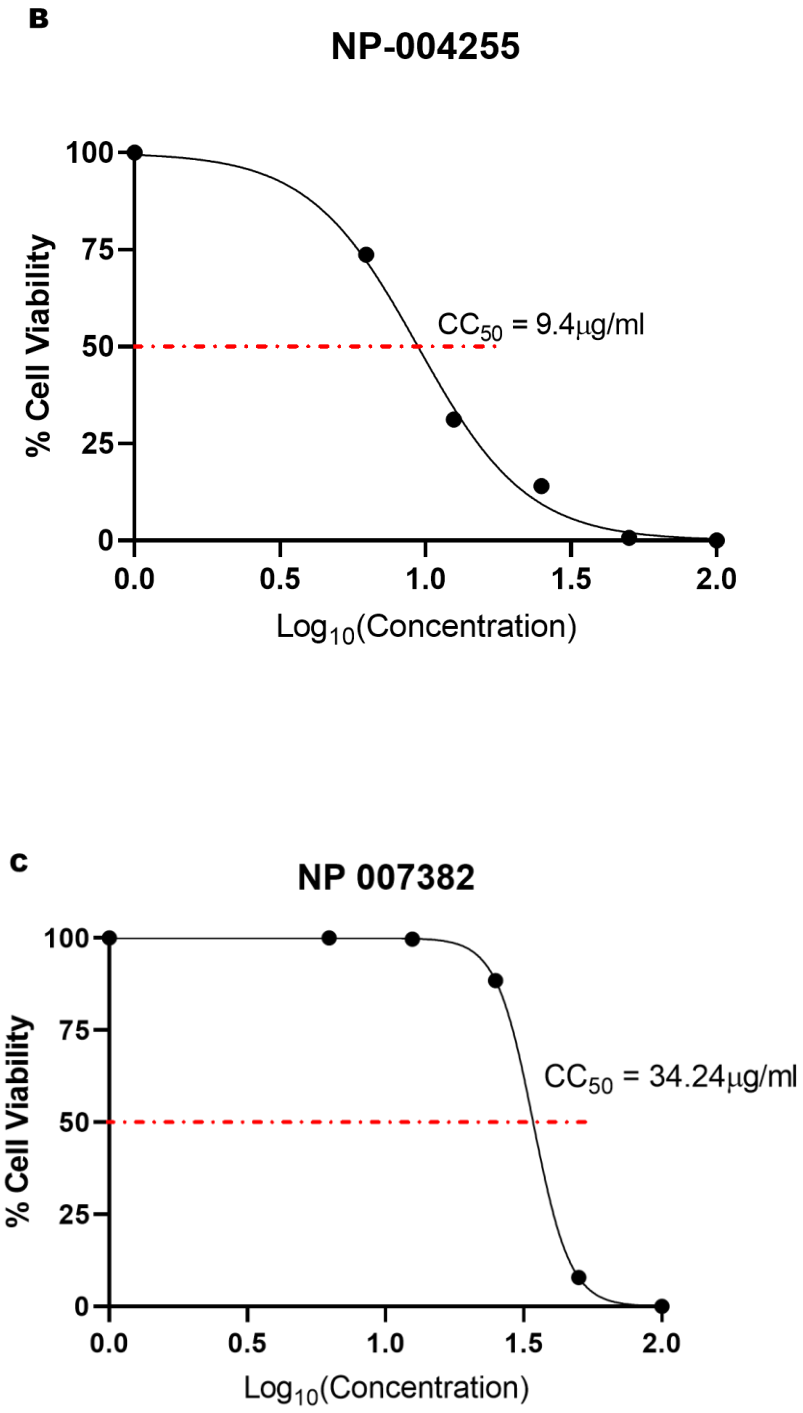

Figure 21. 50% Cytotoxicity Concentration (CC_{50}). *CC_{50} was determined using dose-response non-linear regression analysis. A) NP000945 with CC_{50} of 9.9µg/ml. B) NP004255 with CC_{50} of 9.4µg/ml. C) Compounds NP007382 with CC_{50} of 34.24µg/ml. All assay was carried out in triplicate*

4.2.6. Viral Infectivity Inhibition Assay

To determine the ability of the selected compounds to inhibit the transduction/infection of TZM-bl cell by HIV pseudotype. An infectivity inhibition assay was done by incubating the compounds, HIV pseudotype, and TZM-l cells, as described in methods (3.2.11), in duplicates. The relative light unit (RLU) was read with a luminometer, and the mean RLU was calculated. Non-linear regression dose-response analysis was used to analyse the results on GraphPad Prism as described by (Ferrara, Temperton, Ferrara, & Temperton, 2018), with slight modification. The modification done was by normalizing the Y-axis (response) to 0 = Pseudotype virus only control and 100% = Cell and pseudotype virus. The cell only control was set as the background RLU. All compounds were tested for viral inhibition, except for NP-000954.

50% inhibition concentration (IC_{50}) was defined as the concentration of the compound where the RLU (response) is reduced by 50% relative to the cell + Pseudotype virus control well. Only three compounds (NP-005114, NP-008297, and NP-007382) out of the nine tested compounds had dose response inhibition against viral infection/transduction of TZM-bl cells. NP-005114, NP-008297, and NP-007382 had IC_{50} of 10µg/ml, 15.5µg/ml and 13.1µg/ml respectively (Figure 21 A-C). Compounds NP-007422 and NP-004255 had some inhibition, but not a dose response kind (Figure 21 D). There was no observed inhibition for compounds FRG-00075, NP-005003, NP-000088, and NP-001800 (Figure 21 E).

A

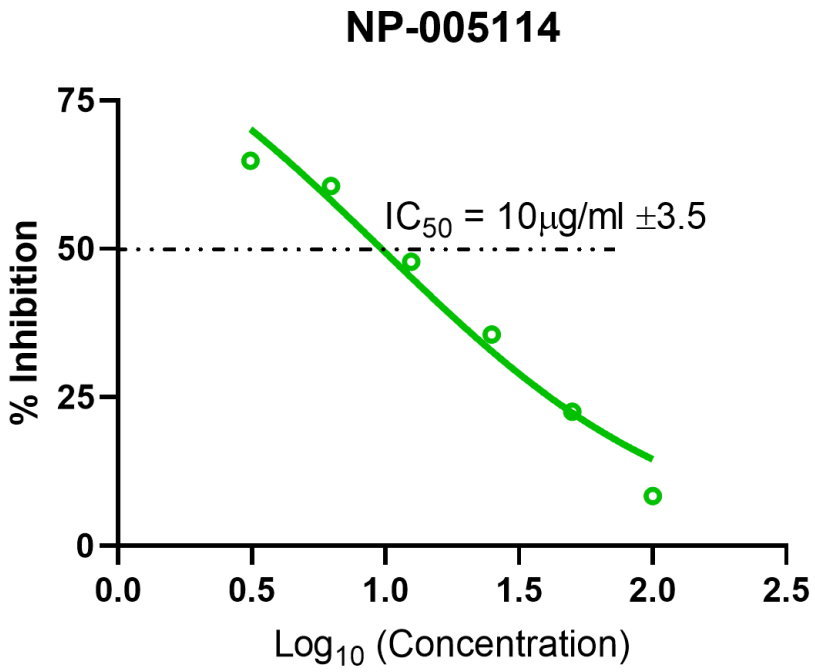

B

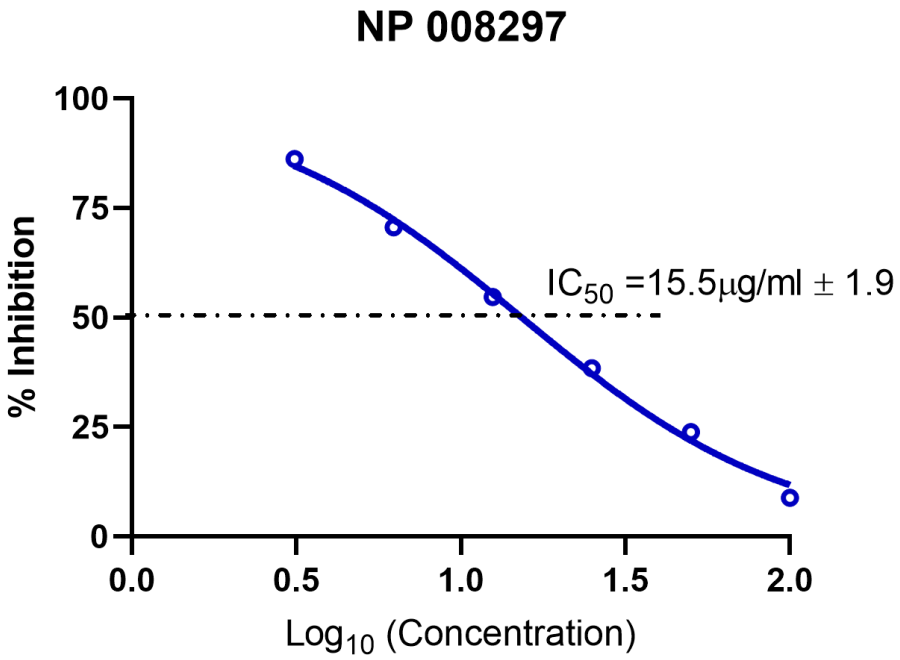

C

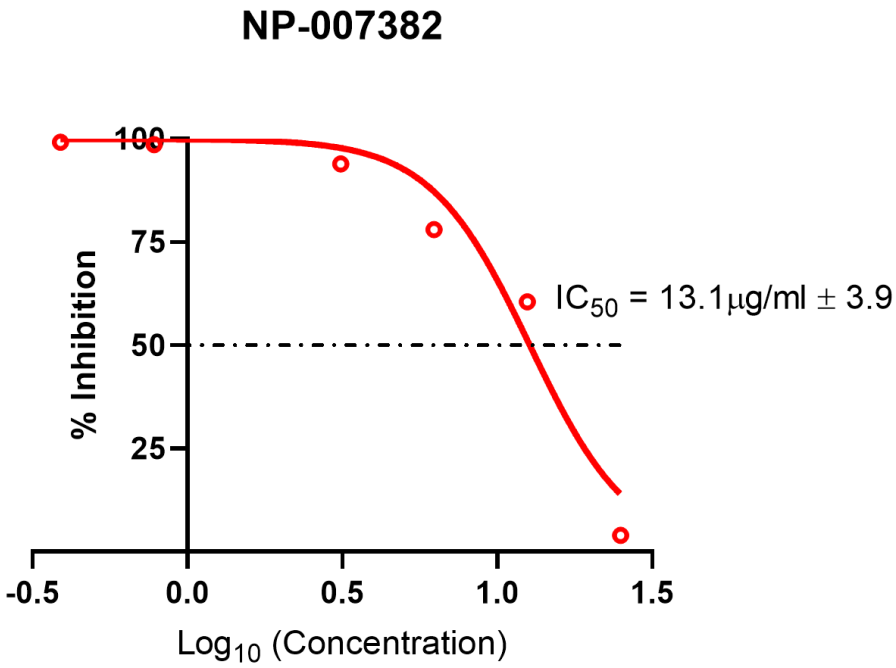

D

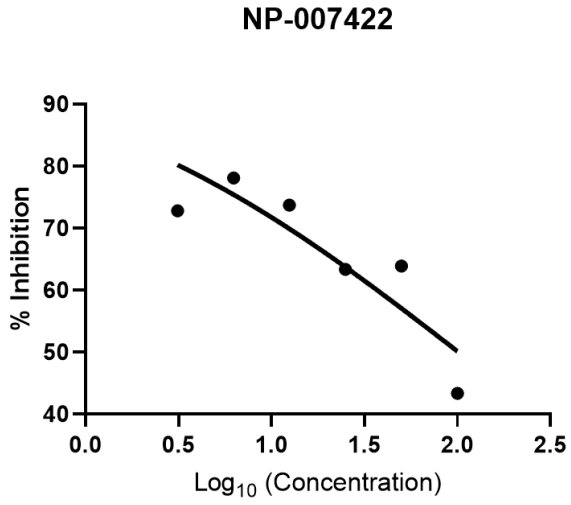

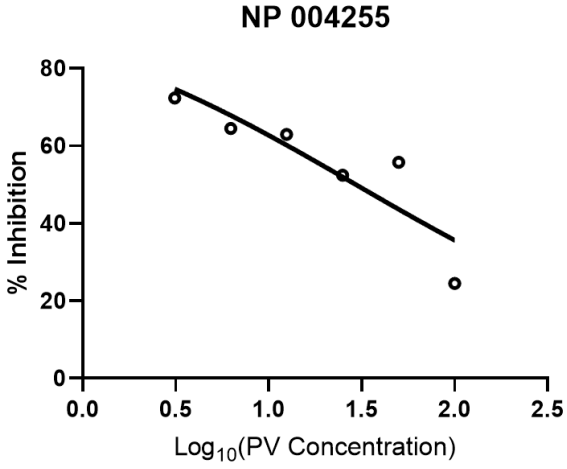

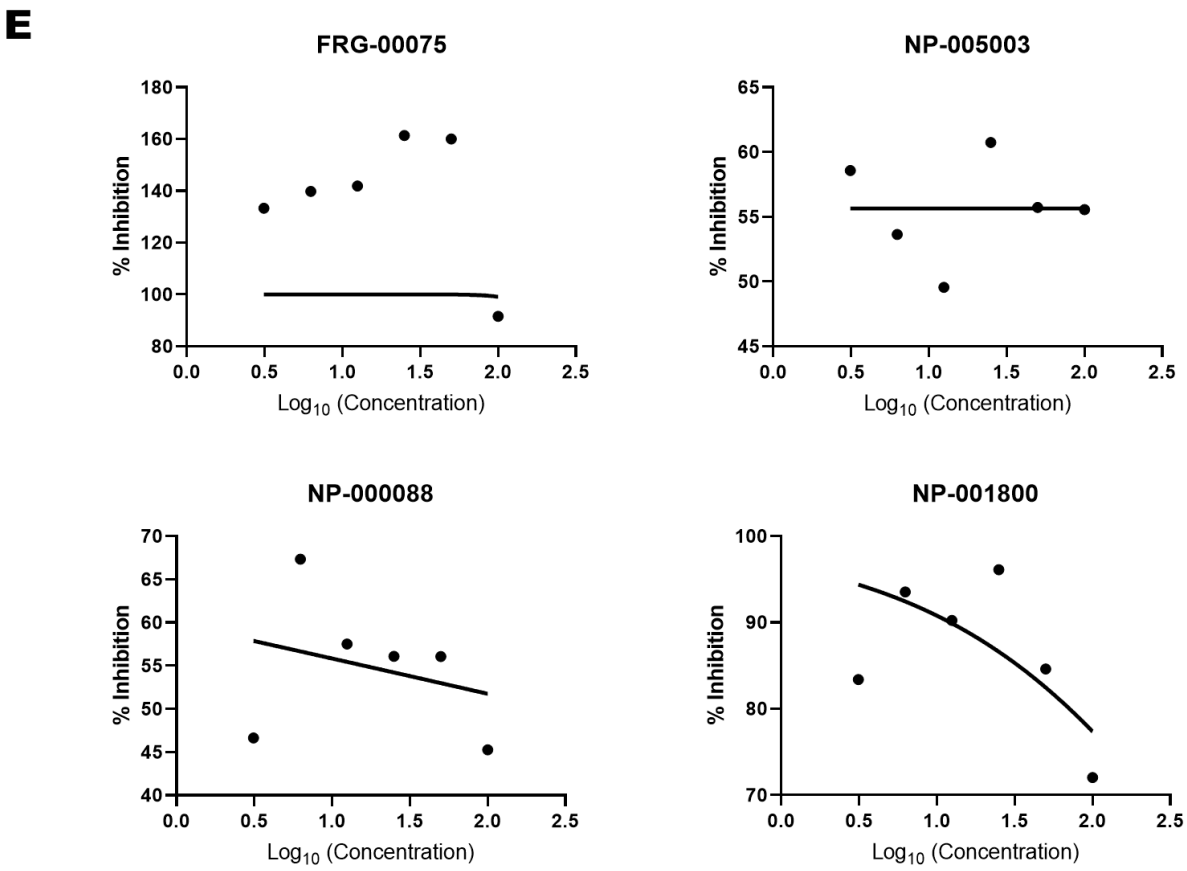

Figure 22. ***Cell-based Viral infectivity inhibition assay****. Nonlinear regression plot of Percentage inhibition (response) against the* Log_{10} *of compound concentration (dose) at a 95% confidence interval.* ***A)*** *NP-005114 had IC50 OF 10µg/ml.* ***B)*** *NP-008297 had* IC_{50} *of 15.5µg/ml.* ***C)*** *NP-007382 had* IC_{50} *of 13.1µg/ml.* ***D)*** *Some inhibition was observed for NP-007422 and NP-004255, but not a dose response inhibition.* ***E)*** *No inhibition was observed for Compounds FRG-00075, NP-0005003, NP-000088, and NP-001800. All assay was carried out in duplicates, mean values were used for the dose-response calculation.*

CHAPTER FIVE

5.0. DISCUSSION, CONCLUSION, AND RECOMMENDATION

5.1 DISCUSSION

This study used a pharmacoinformatic approach to identify compounds derived from natural products (plants and microorganism), that mimic VRC01 bNAb by interacting with similar binding site as VRC01 (CD4-bindng site) on the HIV gp120. The CD4-binding site (CD4-bs) is a conserved region on the HIV-1 gp120 that is crucial for the CD4-gp120 interaction required for successful HIV-1 infection. The compounds which interacted with the CD4-bs of gp120 *in silico* was confirmed *in vitro* using a cell-based assay to assess the inhibitory activity of these compounds against HIV-1 entry into the target cell using pseudotype virus technology. Three compounds comprising NP-005114, NP-008297 and NP-007382 were identified to have an inhibitory effect on HIV entry into target TZM-bl cells. *In silico* analysis showed that NP-005114, NP-008927 and NP-007382 had eight, ten and seven hydrogen bond interactions, respectively, with amino acid residues in the CD4-bs of the clade A/E recombinant 93TH057 HIV gp120 (Fig. 13). The Gibbs free binding energies (ΔG) of the interactions between the compounds and HIV gp120 were obtained as -9.1 kcal/mol, -10.3 kcal/mol and -9.6 kcal/mol for NP-005114, NP-008927 and NP-007382, respectively (Table 4). Corroboration of the interaction of the three compounds NP-005114, NP-008 927 and NP-007382 with the gp120 of the reference HIV strain, HIV Clade B clone 2 (HXB2), showed hydrogen bond interactions with eleven, four and five amino acids residues, respectively in the CD4-bs (Figure 16). The interactions of these compounds with gp120 of clades A/E and B indicate a possible conservation of the CD4-bs (T. Zhou et al., 2007), despite constant variation of the HIV envelope protein due to mutations caused by error-prone HIV reverse transcriptase. It is also indicative of the possibility of interactions with

gp120 from several strain of HIV, however, more work needs to be done to determine the interaction with other HIV clades. It is also worthy to note that the compounds NP-008297 and NP-007382 had biomolecular interactions with Asp368 and Asp425 residues, respectively, in the Phe43 cavity. Phe43 cavity is a functionally crucial and conserved pocket on HIV gp120, where CD4 binds (Kwong et al., 1998). Asp368 and Asp425 are critical amino acid residues in the cavity, alterations in the amino acid led to decrease in CD4-binding (Olshevsky et al., 1990). Many small compounds have been developed to target the CD4-bs of the HIV-1 gp120 (L. Lu et al., 2016), these compounds interact with the Phe43 cavity in the CD4-bs and have demonstrated broad activity against various strains of HIV-1 entry into target cells (L. Lu et al., 2016). Although, the *in silico* prediction is beneficial in identifying possible bioactive compounds, there is a need for further confirmation using experimental methods. Viral entry inhibition of the compounds was tested using molecularly cloned HXB2 pseudotype virus. NP-005114, NP-008297 and NP-007382 demonstrated dose-dependent inhibition of clade B (HXB2) env pseudotype viral entry into TZM-bl cells, with an IC_{50} value of 10 µg/ml., I5.5 µg/ml, and 13.1 µg/ml, respectively. The IC_{50} value of VRC01 in neutralizing panel of clade B HIV and Clade B Env pseudotype virus previously ranged from 0.1 – 50 µg/ml, the IC_{50} of the identified compounds fell within the range (Cohen et al., 2018; Magaret et al., 2019; Mayer et al., 2017; Walker et al., 2011). Of all the numerous small compound HIV-1 entry inhibitors discovered recently, only BMS-663068 and NBD-556 as well as their derivatives have shown good antiretroviral activity, and are in the preclinical and clinical trials of the drug development process (Lalezari et al., 2015; Meuser et al., 2018; Ray et al., 2013). BMS-663068 is a more potent derivative of BMS-626529, with inhibition to viral entry against a panel of pseudotype virus at IC_{50} of between 0.0001–9.5 µg/ml with varying sensitivity towards different clades of virus (Pancera et al., 2017). NBD-556 and derivative were shown to inhibit viral entry of HIV-1HXB2 pseudotype virus with IC_{50} between

20.0 µM (Zhao et al., 2005). Small compounds with the desired bioactivity are assessed for drug-likeness using the Lipinski's Rule of Five. Lipinski's rule uses the chemical structure of a bioactive compound to predict the pharmacokinetics properties and oral bioavailability. The rule includes not more than 5 and 10 hydrogen bond donors and acceptors, respectively; LogP ≤ 5; and molecular mass (MW) of ≤ 500 Daltons (Barret, 2018). Compounds NP-005114 and NP-00892 violated three of the Lipinski's rule (MW>500, H-bond donors and acceptors not more than 5 and 10, respectively), while compound NP-007382 violated only two rules (MW>500, H-bond acceptors >10) (Table 7). The implication of violating the Lipinski's rules is that the compounds are predicted to have poor pharmacokinetics properties (ADME) and oral bioavailability. However, Lipinski's rule does not predict pharmacological activity (Barret, 2018). The absorption, distribution, metabolism, and excretion (ADME) properties of the compounds describe their pharmacokinetics. Parameters including lipophilicity, solubility, gastrointestinal (GI) absorption, brain-blood barrier (BBB) permeant, P-glycoprotein (P-gp) substrate and Cytochrome 450 inhibitor are also used to predict pharmacokinetic properties. Lipophilicity is an indication of solubility, permeability, selectivity and promiscuity of a drug compound. Lipophilicity >5 has been associated with poor receptor selectivity, high metabolic turnover, low solubility and poor absorption. However, compounds with low lipophilicity value are also linked to poor ADME properties (Arnott, Kumar, & Planey, 2013). The ideal lipophilicity value lies between 1 and 3; only NP-008297 and NP-005114 fell within this range. All three compounds have low GI absorption, possibly due to the complex interplay of many factors like molecular weight, cell permeability and solubility of the compounds, however these properties can be optimized in the developmental stage of drug discovery (Amidon, Lennernäs, Shah, & Crison, 1995; Dahan & Miller, 2012). TPSA value is a metric used to define cell permeability by a drug compound. The ideal TPSA usually falls within 140 to 90 Å, above 140 Å indicates poor permeability

into cell (Pajouhesh & Lenz, 2005), and below 90 indicates penetration into the blood-brain-barrier (BBB) (Hitchcock & Pennington, 2006). None of the compounds fell within this range. The blood brain barrier (BBB) permeability index indicated the ability of the drug compound to be deposited into the central nervous system (CNS) (Pardridge, 2005); none of the compounds was BBB permeant (Table 8). P-glycoprotein (P-gp) is a transmembrane efflux pump that is important in the efflux and uptake of the drug compound (Heller, Voelker, Wacharamanotham, & Borchers, 2015). NP-008297 and NP-007382 were substrates of P-gp transporter. Cytochrome P450 (CYP450) enzymes play a significant role in drug metabolism, excretion and drug-drug interactions (McDonnell & Dang, 2013). Compounds that inhibit CYP enzymes interfere with the metabolism of other drugs that are activated by the enzyme. None of the compounds were inhibitors of CYP 450 enzyme. Compound NP-005114 was extracted from the seed of *Terminalia chebula*. *T. chebula* is a medicinal plant popularly referred to as the 'king of medicine,' due to a wide array of bioactivity of compounds extracted from the plant. Compounds extracted from *T. chebula* fruit have been shown to be HIV-1 integrase (Ahn et al., 2002) and reverse transcriptase inhibitors (Gambari & Lampronti, 2006). So far no compound extracted from *T. chebula* has been characterized as HIV-1 entry inhibitors (Salehi, Anil Kumar, et al., 2018; Singh, Bharate, & Bhutani, 2005). NP-005114 which was originally extracted from the seed of *T. chebula* has exhibited HIV-1 entry inhibitory property. NP-008297 was extracted from the leaf of *Ginkgo biloba, and* G. biloba crude extracts have shown activity against HIV-1 reverse transcriptase RNase H and protease (J. Lee, Hattori, & Kim, 2008; Salehi et al., 2018). This study has shown the HIV-1 entry inhibition activity of NP-008297. Unlike the others, NP-007382 was extracted from bacteria, microorganism have been source of active compounds against HIV-1 (Salehi, Kumar, et al., 2018).

5.2. CONCLUSION

The study report for the first time three natural product-derived compounds which mimic HIV-1 broadly neutralizing antibody VRC01, by interacting with the CD4-bs of HIV-1 gp120 of recombinant clades A/E and B. These compounds inhibit HIV-1 clade B (HXB2) entry into target TZM-BL cells. NP-005114 which is an extract from the seed of *T. chebula* had inhibitory activity at IC_{50} = 10µg/ml. NP-008297 which is an extract from the leaves of *G. biloba* exhibited entry inhibition at IC_{50} = 15.5µg/ml. NP-007382 was obtained from bacteria had inhibitory activity at IC_{50} = 13.1µg/ml. Characterisation of the binding mechanisms showed that these compounds formed hydrogen and hydrophobic bond interactions with essential amino acids residues in the CD4-bs. NP-005114 and NP-008297 formed intermolecular interactions with critical amino acid residues in the Phe43 cavity of the HIV-1 gp120 CD4-bs.

5.3. RECOMMENDATION

Based on the result obtained from this study, herein make these recommendations:

i. The interactions of compounds NP-005114, NP-008297 and NP-007382 with the HIV-1 gp120 from other clades should be evaluated *in silico*.
ii. The compounds showing inhibitory activity should be tested against HIV pseudotype virus bearing envelope protein from other clades.
iii. The structures of NP-005114, NP-008297 and NP-007382 could serve as skeletons for optimisation as more potent inhibitors.
iv. The entry inhibition of the compounds should be evaluated against a panel of HIV-1 primary isolate from HIV clades that are representative of the global circulating strains.

REFERENCES

Abdel-Rahman, H. M., Al-karamany, G. S., El-Koussi, N. A., Youssef, A. F., & Kiso, Y. (2002). HIV protease inhibitors: peptidomimetic drugs and future perspectives. *Current Medicinal Chemistry*. https://doi.org/10.2174/0929867023368890

Abraham, M. J., Murtola, T., Schulz, R., Páll, S., Smith, J. C., Hess, B., & Lindahl, E. (2015). GROMACS: High performance molecular simulations through multi-level parallelism from laptops to supercomputers. *SoftwareX*, *1–2*, 19–25. https://doi.org/10.1016/J.SOFTX.2015.06.001

Acharya, C., Coop, A., E. Polli, J., & D. MacKerell, A. (2011). Recent Advances in Ligand-Based Drug Design: Relevance and Utility of the Conformationally Sampled Pharmacophore Approach. *Current Computer Aided-Drug Design*. https://doi.org/10.2174/157340911793743547

Ahn, M. J., Chul, Y. K., Ji, S. L., Tae, G. K., Seung, H. K., Lee, C. K., … Kim, J. (2002). Inhibition of HIV-1 integrase by galloyl glucoses from Terminalia chebula and flavonol glycoside gallates from Euphorbia pekinensis. *Planta Medica*. https://doi.org/10.1055/s-2002-32070

Akram, O. N., DeGraff, D. J., Sheehan, J. H., Tilley, W. D., Matusik, R. J., Ahn, J.-M., & Raj, G. V. (2014). Tailoring Peptidomimetics for Targeting Protein-Protein Interactions. *Molecular Cancer Research*. https://doi.org/10.1158/1541-7786.MCR-13-0611

Akram, Omar N., DeGraff, D. J., Sheehan, J. H., Tilley, W. D., Matusik, R. J., Ahn, J. M., & Raj, G. V. (2014). Tailoring peptidomimetics for targeting protein-protein interactions. *Molecular Cancer Research*. https://doi.org/10.1158/1541-7786.MCR-13-0611

Ali, A., Bandaranayake, R. M., Cai, Y., King, N. M., Kolli, M., Mittal, S., … Schiffer, C. A.

(2010). Molecular basis for drug resistance in HIV-1 protease. *Viruses*. https://doi.org/10.3390/v2112509

Altfeld, M., Behrens, G., Berzow, D., & Boesecke, C. (n.d.). structure of HIV-1 | hivbook.com. Retrieved March 5, 2020, from https://www.hivbook.com/tag/structure-of-hiv-1/

Altfeld, M., Gale Jr, M., Borrow, P., Shattock, R. J., Vyakarnam, A., Working Group, E., … et al. (2015). Identification and specificity of broadly neutralizing antibodies against HIV. *Immunological Reviews*. https://doi.org/10.1111/imr.12484

Amidon, G. L., Lennernäs, H., Shah, V. P., & Crison, J. R. (1995). A theoretical basis for a biopharmaceutic drug classification: the correlation of in vitro drug product dissolution and in vivo bioavailability. *Pharmaceutical Research*, *12*(3), 413–420. Retrieved from http://www.ncbi.nlm.nih.gov/pubmed/7617530

Andrianov, A M, Kashyn, I. A., & Tuzikov, A. V. (2013). Computer-aided search for novel anti-HIV-1 agents presenting peptidomimetics of broadly neutralizing antibodies against the virus envelope GP120 V3 loop. *Journal of Biomolecular Structure and Dynamics*. https://doi.org/http://dx.doi.org/10.1080/07391102.2013.786434

Andrianov, Alexander M., Kashyn, I. A., & Tuzikov, A. V. (2014). Discovery of novel anti-HIV-1 agents based on a broadly neutralizing antibody against the envelope gp120 V3 loop: A computational study. *Journal of Biomolecular Structure and Dynamics*. https://doi.org/10.1080/07391102.2013.848825

Arnott, J. A., Kumar, R., & Planey, S. L. (2013). Lipophilicity Indices for Drug Development. In *Journal of Applied Biopharmaceutics and Pharmacokinetics*. Retrieved from https://pdfs.semanticscholar.org/a5e8/2211e5b5a96b2ffac3bfa4032b39dbfe3870.pdf

Artimo, P., Jonnalagedda, M., Arnold, K., Baratin, D., Csardi, G., de Castro, E., … Stockinger, H. (2012). ExPASy: SIB bioinformatics resource portal. *Nucleic Acids Research*, *40*(W1), W597–W603. https://doi.org/10.1093/nar/gks400

Avan, I., Dennis Hall, C., & Katritzky, A. R. (2014). Peptidomimetics via modifications of amino acids and peptide bonds. *Chemical Society Reviews*. https://doi.org/10.1039/c3cs60384a

Awi, N. J., & Teow, S.-Y. (2018). Antibody-Mediated Therapy against HIV/AIDS: Where Are We Standing Now? *Journal of Pathogens*. https://doi.org/10.1155/2018/8724549

Baeten, J. M., Donnell, D., Ndase, P., Mugo, N. R., Campbell, J. D., Wangisi, J., … Celum, C. (2012). Antiretroviral Prophylaxis for HIV Prevention in Heterosexual Men and Women. *New England Journal of Medicine*. https://doi.org/10.1056/NEJMoa1108524

Balla-Jhagjhoorsingh, S. S., Corti, D., Heyndrickx, L., Willems, E., Vereecken, K., Davis, D., & Vanham, G. (2013). The N276 Glycosylation Site Is Required for HIV-1 Neutralization by the CD4 Binding Site Specific HJ16 Monoclonal Antibody. *PLoS ONE*. https://doi.org/10.1371/journal.pone.0068863

Bar, K. J., Sneller, M. C., Harrison, L. J., Justement, J. S., Overton, E. T., Petrone, M. E., … Chun, T. W. (2016). Effect of HIV antibody VRC01 on viral rebound after treatment interruption. *New England Journal of Medicine*. https://doi.org/10.1056/NEJMoa1608243

Bar, Katharine J., Sneller, M. C., Harrison, L. J., Justement, J. S., Overton, E. T., Petrone, M. E., … Chun, T.-W. (2016). Effect of HIV Antibody VRC01 on Viral Rebound after Treatment Interruption. *New England Journal of Medicine*. https://doi.org/10.1056/NEJMoa1608243

Barret, R. (2018). Lipinski's Rule of Five. In *Therapeutical Chemistry*.

https://doi.org/10.1016/b978-1-78548-288-5.50006-8

Barrientos, L. G., Lasala, F., Otero, J. R., Sanchez, A., & Delgado, R. (2004). In Vitro Evaluation of Cyanovirin-N Antiviral Activity, by Use of Lentiviral Vectors Pseudotyped with Filovirus Envelope Glycoproteins. *The Journal of Infectious Diseases*, *189*(8), 1440–1443. https://doi.org/10.1086/382658

Basu, A., Li, B., Mills, D. M., Panchal, R. G., Cardinale, S. C., Butler, M. M., … Bowlin, T. L. (2011). Identification of a small-molecule entry inhibitor for filoviruses. *Journal of Virology*, *85*(7), 3106–3119. https://doi.org/10.1128/JVI.01456-10

Bertagnolio, S, Beanland, R. L., Jordan, M. R., Doherty, M., & Hirnschall, G. (2017). The World Health Organization's Response to Emerging Human Immunodeficiency Virus Drug Resistance and a Call for Global Action. *The Journal of Infectious Diseases*. https://doi.org/10.1093/infdis/jix402

Bertagnolio, Silvia, Beanland, R. L., Jordan, M. R., Doherty, M., & Hirnschall, and G. (2017). The World Health Organization's Response to Emerging Human Immunodeficiency Virus Drug Resistance and a Call for Global Action. *The Journal of Infectious Diseases*. https://doi.org/10.1093/infdis/jix402

Binley, J. M., Wrin, T., Korber, B., Zwick, M. B., Wang, M., Chappey, C., … Burton, D. R. (2004). Comprehensive cross-clade neutralization analysis of a panel of anti-human immunodeficiency virus type 1 monoclonal antibodies. *Journal of Virology*, *78*(23), 13232–13252. https://doi.org/10.1128/JVI.78.23.13232-13252.2004

Blattner, C., Lee, J. H., Sliepen, K., Derking, R., Falkowska, E., delaPeña, A. T., … Ward, A. B. (2014). Structural delineation of a quaternary, cleavage-dependent epitope at the gp41-gp120

interface on intact HIV-1 env trimers. *Immunity*. https://doi.org/10.1016/j.immuni.2014.04.008

Bonsignori, M., Scott, E., Wiehe, K., Easterhoff, D., Munir Alam, S., Hwang, K.-K., … Haynes, B. F. (2018). *Inference of the HIV-1 VRC01 Antibody Lineage Unmutated Common Ancestor Reveals Alternative Pathways to Overcome a Key Glycan Barrier*. https://doi.org/10.1016/j.immuni.2018.10.015

Broder, S. (2010). The development of antiretroviral therapy and its impact on the HIV-1/AIDS pandemic. *Antiviral Research*, Vol. 85, pp. 1–18. https://doi.org/10.1016/j.antiviral.2009.10.002

Burns, J. C., Friedmann, T., Driever, W., Burrascano, M., & Yee, J. K. (1993). Vesicular stomatitis virus G glycoprotein pseudotyped retroviral vectors: concentration to very high titer and efficient gene transfer into mammalian and nonmammalian cells. *Proceedings of the National Academy of Sciences*. https://doi.org/10.1073/pnas.90.17.8033

Burton, D. R., Ahmed, R., Barouch, D. H., Butera, S. T., Crotty, S., Godzik, A., … Wyatt, R. (2012). A blueprint for HIV vaccine discovery. *Cell Host and Microbe*. https://doi.org/10.1016/j.chom.2012.09.008

Calarese, D. A., Scanlan, C. N., Zwick, M. B., Deechongkit, S., Mimura, Y., Kunert, R., … Wilson, I. A. (2003). Antibody domain exchange is an immunological solution to carbohydrate cluster recognition. *Science*. https://doi.org/10.1126/science.1083182

Campbell, E. M., & Hope, T. J. (2008). Live cell imaging of the HIV-1 life cycle. *Trends in Microbiology*. https://doi.org/10.1016/j.tim.2008.09.006

Caskey, M., Klein, F., Lorenzi, J. C. C., Seaman, M. S., West, A. P., Buckley, N., … Nussenzweig, M. C. (2016). Corrigendum: Viraemia suppressed in HIV-1-infected humans by broadly neutralizing antibody 3BNC117. *Nature*, *535*(7613), 580–580. https://doi.org/10.1038/nature17642

Centers for Disease Control and Prevention. (2014). Preexposure Prophylaxis for the Prevention of HIV Infection in the United States – 2014 Clinical Practice Guideline. *Mmwr*.

Chen, L., Morrow, J. K., Tran, H. T., Phatak, S. S., Du-Cuny, L., & Zhang, S. (2012). From laptop to benchtop to bedside: structure-based drug design on protein targets. *Curr Pharm Des*.

Cherkasov, A., Muratov, E. N., Fourches, D., Varnek, A., Baskin, I. I., Cronin, M., … Tropsha, A. (2014). QSAR modeling: Where have you been? Where are you going to? *Journal of Medicinal Chemistry*. https://doi.org/10.1021/jm4004285

Chesney, M. A., Morin, M., & Sherr, L. (2000). Adherence to HIV combination therapy. *Social Science & Medicine*, *50*(11), 1599–1605. https://doi.org/10.1016/S0277-9536(99)00468-2

Cohen, Y. Z., Lorenzi, J. C. C., Seaman, M. S., Nogueira, L., Schoofs, T., Krassnig, L., … Nussenzweig, M. C. (2018). *Neutralizing Activity of Broadly Neutralizing Anti-HIV-1 Antibodies against Clade B Clinical Isolates Produced in Peripheral Blood Mononuclear Cells*. https://doi.org/10.1128/JVI

Corti, D., Langedijk, J. P. M., Hinz, A., Seaman, M. S., Vanzetta, F., Fernandez-Rodriguez, B. M., … Lanzavecchia, A. (2010). Analysis of Memory B Cell Responses and Isolation of Novel Monoclonal Antibodies with Neutralizing Breadth from HIV-1-Infected Individuals. *PLoS ONE*. https://doi.org/10.1371/journal.pone.0008805

Courter, J. R., Madani, N., Sodroski, J., Schön, A., Freire, E., Kwong, P. D., … Smith, A. B. (2014). Structure-based design, synthesis and validation of CD4-mimetic small molecule inhibitors of HIV-1 entry: Conversion of a viral entry agonist to an antagonist. *Accounts of Chemical Research*. https://doi.org/10.1021/ar4002735

Dahan, A., & Miller, J. M. (2012). The solubility-permeability interplay and its implications in formulation design and development for poorly soluble drugs. *The AAPS Journal*, *14*(2), 244–251. https://doi.org/10.1208/s12248-012-9337-6

Daina, A., Michielin, O., & Zoete, V. (2017). SwissADME: A free web tool to evaluate pharmacokinetics, drug-likeness and medicinal chemistry friendliness of small molecules. *Scientific Reports*. https://doi.org/10.1038/srep42717

Dallakyan, S., & Olson, A. J. (2015). Small-molecule library screening by docking with PyRx. *Methods in Molecular Biology*. https://doi.org/10.1007/978-1-4939-2269-7_19

Davis, A. M. (2017). Quantitative Structure-Activity Relationships. In *Comprehensive Medicinal Chemistry III*. https://doi.org/10.1016/B978-0-12-409547-2.12348-0

Dickinson, L., Khoo, S., & Back, D. (2010). Pharmacokinetics and drug-drug interactions of antiretrovirals: An update. *Antiviral Research*. https://doi.org/10.1016/j.antiviral.2009.07.017

Doores, K. J., Kong, L., Krumm, S. A., Le, K. M., Sok, D., Laserson, U., … Burton, D. R. (2015). Two Classes of Broadly Neutralizing Antibodies within a Single Lineage Directed to the High-Mannose Patch of HIV Envelope. *Journal of Virology*. https://doi.org/10.1128/JVI.02905-14

Doria-Rose, N. A., Georgiev, I., O'Dell, S., Chuang, G.-Y., Staupe, R. P., McLellan, J. S., … Mascola, J. R. (2012). A Short Segment of the HIV-1 gp120 V1/V2 Region Is a Major Determinant of Resistance to V1/V2 Neutralizing Antibodies. *Journal of Virology*. https://doi.org/10.1128/JVI.00696-12

Doria-Rose, Nicole A., Schramm, C. A., Gorman, J., Moore, P. L., Bhiman, J. N., DeKosky, B. J., … Mascola, J. R. (2014). Developmental pathway for potent V1V2-directed HIV-neutralizing antibodies. *Nature*. https://doi.org/10.1038/nature13036

Doro, F., Colombo, C., Alberti, C., Arosio, D., Belvisi, L., Casagrande, C., … Civera, M. (2015). Computational design of novel peptidomimetic inhibitors of cadherin homophilic interactions. *Organic and Biomolecular Chemistry*. https://doi.org/10.1039/c4ob02538e

Drag, M., & Salvesen, G. S. (2010). Emerging principles in protease-based drug discovery. *Nature Reviews Drug Discovery*. https://doi.org/10.1038/nrd3053

Drwal, M. N., Banerjee, P., Dunkel, M., Wettig, M. R., & Preissner, R. (2014). ProTox: A web server for the in silico prediction of rodent oral toxicity. *Nucleic Acids Research*. https://doi.org/10.1093/nar/gku401

Dunn, B. M., Goodenow, M. M., Gustchina, A., & Wlodawer, A. (2002). Retroviral proteases. *Genome Biology*. https://doi.org/10.1186/gb-2002-3-4-reviews3006

Duprez, W., Bachu, P., Stoermer, M. J., Tay, S., McMahon, R. M., Fairlie, D. P., & Martin, J. L. (2015). Virtual screening of peptide and peptidomimetic fragments targeted to inhibit bacterial dithiol oxidase DsbA. *PLoS ONE*. https://doi.org/10.1371/journal.pone.0133805

Durrant, J. D., & McCammon, J. A. (2011). Molecular dynamics simulations and drug discovery.

BMC Biology, *9*(1), 71. https://doi.org/10.1186/1741-7007-9-71

Eder, J., Hommel, U., Cumin, F., Martoglio, B., & Gerhartz, B. (2007). Aspartic proteases in drug discovery. *Current Pharmaceutical Design*. https://doi.org/10.2174/138161207779313560

Ekins, S., Mestres, J., & Testa, B. (2007). In silico pharmacology for drug discovery: Methods for virtual ligand screening and profiling. *British Journal of Pharmacology*. https://doi.org/10.1038/sj.bjp.0707305

Elshabrawy, H. A., Fan, J., Haddad, C. S., Ratia, K., Broder, C. C., Caffrey, M., & Prabhakar, B. S. (2014). Identification of a broad-spectrum antiviral small molecule against severe acute respiratory syndrome coronavirus and Ebola, Hendra, and Nipah viruses by using a novel high-throughput screening assay. *Journal of Virology*, *88*(8), 4353–4365. https://doi.org/10.1128/JVI.03050-13

Fairlie, D. P., Tyndall, J. D. A., Reid, R. C., Wong, A. K., Abbenante, G., Scanlon, M. J., … Burkett, B. A. (2000). Conformational selection of inhibitors and substrates by proteolytic enzymes: Implications for drug design and polypeptide processing. *Journal of Medicinal Chemistry*. https://doi.org/10.1021/jm990315t

Falkowska, E., Le, K. M., Ramos, A., Doores, K. J., Lee, J. H., Blattner, C., … Burton, D. R. (2014). Broadly neutralizing HIV antibodies define a glycan-dependent epitope on the prefusion conformation of gp41 on cleaved envelope trimers. *Immunity*. https://doi.org/10.1016/j.immuni.2014.04.009

Farhadi, T., & Hashemian, S. M. R. (2018). Computer-aided design of amino acid-based therapeutics: A review. *Drug Design, Development and Therapy*. https://doi.org/10.2147/DDDT.S159767

Fätkenheuer, G., Nelson, M., Lazzarin, A., Konourina, I., Hoepelman, A. I. M., Lampiris, H., … van der Ryst, E. (2008). Subgroup analyses of maraviroc in previously treated R5 HIV-1 infection. *The New England Journal of Medicine*, *359*(14), 1442–1455. https://doi.org/10.1056/NEJMoa0803154

Fernandes, J., & Gattass, C. R. (2009). Topological polar surface area defines substrate transport by multidrug resistance associated protein 1 (MRP1/ABCC1). *Journal of Medicinal Chemistry*. https://doi.org/10.1021/jm801389m

Ferrara, F., Temperton, N., Ferrara, F., & Temperton, N. (2018). Pseudotype Neutralization Assays: From Laboratory Bench to Data Analysis. *Methods and Protocols*, *1*(1), 8. https://doi.org/10.3390/mps1010008

Ferreira, L. G., Dos Santos, R. N., Oliva, G., & Andricopulo, A. D. (2015). Molecular docking and structure-based drug design strategies. *Molecules*. https://doi.org/10.3390/molecules200713384

Frecer, V., Berti, F., Benedetti, F., & Miertus, S. (2008). Design of peptidomimetic inhibitors of aspartic protease of HIV-1 containing -PheΨPro- core and displaying favourable ADME-related properties. *Journal of Molecular Graphics and Modelling*. https://doi.org/10.1016/j.jmgm.2008.06.006

Freed, E. O. (2015). HIV-1 assembly, release and maturation. *Nature Reviews Microbiology*, *13*(8), 484–496. https://doi.org/10.1038/nrmicro3490

Funke, S., Maisner, A., Mühlebach, M. D., Koehl, U., Grez, M., Cattaneo, R., … Buchholz, C. J. (2008). Targeted Cell Entry of Lentiviral Vectors. *Molecular Therapy*, *16*(8), 1427–1436. https://doi.org/10.1038/mt.2008.128

Gambari, R., & Lampronti, I. (2006). Inhibition of immunodeficiency type-1 virus (HIV-1) life cycle by medicinal plant extracts and plant-derived compounds. *Advances in Phytomedicine*. https://doi.org/10.1016/S1572-557X(05)02017-9

Garcia, J.-M., Gao, A., He, P.-L., Choi, J., Tang, W., Bruzzone, R., … Zuo, J.-P. (2009). High-throughput screening using pseudotyped lentiviral particles: A strategy for the identification of HIV-1 inhibitors in a cell-based assay. *Antiviral Research, 81*, 239–247. https://doi.org/10.1016/j.antiviral.2008.12.004

Gautam, R., Nishimura, Y., Pegu, A., Nason, M. C., Klein, F., Gazumyan, A., … Martin, M. A. (2016). A single injection of anti-HIV-1 antibodies protects against repeated SHIV challenges. *Nature*. https://doi.org/10.1038/nature17677

Gulick, R. M., Lalezari, J., Goodrich, J., Clumeck, N., DeJesus, E., Horban, A., … Mayer, H. (2008). Maraviroc for Previously Treated Patients with R5 HIV-1 Infection. *New England Journal of Medicine*, *359*(14), 1429–1441. https://doi.org/10.1056/NEJMoa0803152

Halper-Stromberg, A., Lu, C. L., Klein, F., Horwitz, J. A., Bournazos, S., Nogueira, L., … Nussenzweig, M. C. (2014). Broadly neutralizing antibodies and viral inducers decrease rebound from HIV-1 latent reservoirs in humanized mice. *Cell*, *158*(5), 989–999. https://doi.org/10.1016/j.cell.2014.07.043

Haqqani, A. A., & Tilton, J. C. (2013). Entry inhibitors and their use in the treatment of HIV-1 infection. *Antiviral Research*, Vol. 98, pp. 158–170. https://doi.org/10.1016/j.antiviral.2013.03.017

Heller, F., Voelker, S., Wacharamanotham, C., & Borchers, J. (2015). Transporters. *Proceedings of the 33rd Annual ACM Conference Extended Abstracts on Human Factors in Computing*

Systems - CHI EA '15. https://doi.org/10.1145/2702613.2732707

Henrich, T. J., & Kuritzkes, D. R. (2013). HIV-1 entry inhibitors: Recent development and clinical use. *Current Opinion in Virology*, Vol. 3, pp. 51–57. https://doi.org/10.1016/j.coviro.2012.12.002

Hessell, A. J., Rakasz, E. G., Poignard, P., Hangartner, L., Landucci, G., Forthal, D. N., … Burton, D. R. (2009). Broadly neutralizing human anti-HIV antibody 2G12 is effective in protection against mucosal SHIV challenge even at low serum neutralizing titers. *PLoS Pathogens*, *5*(5). https://doi.org/10.1371/journal.ppat.1000433

Hitchcock, S. A., & Pennington, L. D. (2006). Structure−Brain Exposure Relationships. *Journal of Medicinal Chemistry*, *49*(26), 7559–7583. https://doi.org/10.1021/jm060642i

Horwitz, J. A., Halper-Stromberg, A., Mouquet, H., Gitlin, A. D., Tretiakova, A., Eisenreich, T. R., … Nussenzweig, M. C. (2013). HIV-1 suppression and durable control by combining single broadly neutralizing antibodies and antiretroviral drugs in humanized mice. *Proceedings of the National Academy of Sciences*, *110*(41), 16538–16543. https://doi.org/10.1073/pnas.1315295110

Hraber, P., Seaman, M. S., Bailer, R. T., Mascola, J. R., Montefiori, D. C., & Korber, B. T. (2014). Prevalence of broadly neutralizing antibody responses during chronic HIV-1 infection. *Aids*. https://doi.org/10.1097/QAD.0000000000000106

Huang, J., Kang, B. H., Pancera, M., Lee, J. H., Tong, T., Feng, Y., … Connors, M. (2014). Broad and potent HIV-1 neutralization by a human antibody that binds the gp41-gp120 interface. *Nature*. https://doi.org/10.1038/nature13601

Huang, J., Ofek, G., Laub, L., Louder, M. K., Doria-Rose, N. A., Longo, N. S., … Connors, M. (2012). Broad and potent neutralization of HIV-1 by a gp41-specific human antibody. *Nature*. https://doi.org/10.1038/nature11544

Huang, S.-Y. (2017). Comprehensive assessment of flexible-ligand docking algorithms: current effectiveness and challenges. *Briefings in Bioinformatics*. https://doi.org/10.1093/bib/bbx030

Huang, S.-Y., Grinter, S. Z., & Zou, X. (2010). Scoring functions and their evaluation methods for protein–ligand docking: recent advances and future directions. *Physical Chemistry Chemical Physics*, *12*(40), 12899. https://doi.org/10.1039/c0cp00151a

Hughes, J. P., Rees, S. S., Kalindjian, S. B., & Philpott, K. L. (2011). Principles of early drug discovery. *British Journal of Pharmacology*. https://doi.org/10.1111/j.1476-5381.2010.01127.x

Humphrey, W., Dalke, A., & Schulten, K. (1996). VMD: Visual molecular dynamics. *Journal of Molecular Graphics*, *14*(1), 33–38. https://doi.org/10.1016/0263-7855(96)00018-5

Jackson, G. G., Perkins, J. T., Rubenis, M., Paul, D. A., Knigge, M., Despotes, J. C., & Spencer, P. (1988). Passive immunoneutralization of human immunodeficiency virus in patients with advanced AIDS. *Lancet*.

Janzen, W. P. (2014). Screening technologies for small molecule discovery: The state of the art. *Chemistry and Biology*. https://doi.org/10.1016/j.chembiol.2014.07.015

Jaworski, J. P., Vendrell, A., & Chiavenna, S. M. (2017). Neutralizing monoclonal antibodies to fight HIV-1: On the threshold of success. *Frontiers in Immunology*. https://doi.org/10.3389/fimmu.2016.00661

Jorgensen, W. L. (2004). The Many Roles of Computation in Drug Discovery. *Science*. https://doi.org/10.1126/science.1096361

Julien, J.-P., Lee, J. H., Cupo, A., Murin, C. D., Derking, R., Hoffenberg, S., … Ward, A. B. (2013). Asymmetric recognition of the HIV-1 trimer by broadly neutralizing antibody PG9. *Proceedings of the National Academy of Sciences*. https://doi.org/10.1073/pnas.1217537110

Julien, J. P., Cupo, A., Sok, D., Stanfield, R. L., Lyumkis, D., Deller, M. C., … Wilson, I. A. (2013). Crystal structure of a soluble cleaved HIV-1 envelope trimer. *Science*. https://doi.org/10.1126/science.1245625

Kapetanovic, I. M. (2008). Computer-aided drug discovery and development (CADDD): In silico-chemico-biological approach. *Chemico-Biological Interactions*. https://doi.org/10.1016/j.cbi.2006.12.006

Kaplan, W., & Littlejohn, T. G. (2001). Swiss-PDB Viewer (Deep View). *Briefings in Bioinformatics*. https://doi.org/10.1093/bib/2.2.195

Karpas, A., Hewlett, I. K., Hill, F., Gray, J., Byron, N., Gilgen, D., … Epstein, J. E. (1990). Polymerase chain reaction evidence for human immunodeficiency virus 1 neutralization by passive immunization in patients with AIDS and AIDS-related complex. *PROC NATL ACAD SCI U S A*.

Kaufmann, D. E., & Rosenberg, E. S. (2003). The value of preserving HIV-specific immune responses. *J HIV Ther*, *8*(1), 19–25. Retrieved from http://www.embase.com/search/results?subaction=viewrecord&from=export&id=L137604854

Keseru, G. M., & Makara, G. M. (2006). Hit discovery and hit-to-lead approaches. *Drug Discovery Today*. https://doi.org/10.1016/j.drudis.2006.06.016

Khetawat, D., & Broder, C. C. (2010). A functional henipavirus envelope glycoprotein pseudotyped lentivirus assay system. *Virology Journal*, *7*, 312. https://doi.org/10.1186/1743-422X-7-312

Kikelj, D. (2003). Peptidomimetic thrombin inhibitors. *Pathophysiology of Haemostasis and Thrombosis*. https://doi.org/10.1159/000083850

Kim, Y. B., Lee, M. K., Han, D. P., & Cho, M. W. (2001). Development of a Safe and Rapid Neutralization Assay Using Murine Leukemia Virus Pseudotyped with HIV Type 1 Envelope Glycoprotein Lacking the Cytoplasmic Domain. *AIDS Research and Human Retroviruses*, *17*(18), 1715–1724. https://doi.org/10.1089/08892220152741414

Kitchen, D. B., Decornez, H., Furr, J. R., & Bajorath, J. (2004). Docking and scoring in virtual screening for drug discovery: methods and applications. *Nature Reviews. Drug Discovery*. https://doi.org/10.1038/nrd1549

Klein, F, Halper-Stromberg, a, Horwitz, J. a, Gruell, H., Scheid, J. F., Bournazos, S., … Nussenzweig, M. C. (2012). HIV therapy by a combination of broadly neutralizing antibodies in humanized mice. *Nature*, *492*(7427), 118–122. https://doi.org/10.1038/nature11604

Klein, Florian, Halper-Stromberg, A., Horwitz, J. A., Gruell, H., Scheid, J. F., Bournazos, S., … Nussenzweig, M. C. (2012). HIV therapy by a combination of broadly neutralizing antibodies in humanized mice. *Nature*, *492*(7427), 118–122. https://doi.org/10.1038/nature11604

Kong, L., Lee, J. H., Doores, K. J., Murin, C. D., Julien, J. P., McBride, R., … Wilson, I. A. (2013).

Supersite of immune vulnerability on the glycosylated face of HIV-1 envelope glycoprotein gp120. *Nature Structural and Molecular Biology*. https://doi.org/10.1038/nsmb.2594

Kufareva, I., & Abagyan, R. (2012). Methods of protein structure comparison. *Methods in Molecular Biology (Clifton, N.J.), 857*, 231–257. https://doi.org/10.1007/978-1-61779-588-6_10

Kwong, P. D., Wyatt, R., Robinson, J., Sweet, R. W., Sodroski, J., & Hendrickson, W. A. (1998). Structure of an HIV gp120 envelope glycoprotein in complex with the CD4 receptor and a neutralizing human antibody. *Nature*, *393*(6686), 648–659. https://doi.org/10.1038/31405

Lalezari, J. P., Latiff, G. H., Brinson, C., Echevarría, J., Treviño-Pérez, S., Bogner, J. R., … AI438011 study team. (2015). Safety and efficacy of the HIV-1 attachment inhibitor prodrug BMS-663068 in treatment-experienced individuals: 24 week results of AI438011, a phase 2b, randomised controlled trial. *The Lancet HIV*, *2*(10), e427–e437. https://doi.org/10.1016/S2352-3018(15)00177-0

Laskowski, R. A., & Swindells, M. B. (2011). LigPlot+: Multiple ligand-protein interaction diagrams for drug discovery. *Journal of Chemical Information and Modeling*. https://doi.org/10.1021/ci200227u

Lazzarin, A., Clotet, B., Cooper, D., Reynes, J., Arasteh, K., Nelson, M., … Salgo, M. (2003). Efficacy of Enfuvirtide in Patients Infected with Drug-Resistant HIV-1 in Europe and Australia. *New England Journal of Medicine*, *348*(22), 2186–2195. https://doi.org/10.1056/NEJMoa035211

Lee, J. H., Ozorowski, G., Ward, A. B., Liu, J., Bartesaghi, A., Borgnia, M. J., … Frank, J. (2016). Cryo-EM structure of a native, fully glycosylated, cleaved HIV-1 envelope trimer. *Science*

(New York, N.Y.). https://doi.org/10.1126/science.aad2450

Lee, J., Hattori, M., & Kim, J. (2008). Inhibition of HIV-1 Protease and RNase H of HIV-1 Reverse Transcriptase Activities by Long Chain Phenols from the Sarcotestas of *Ginkgo biloba*. *Planta Medica*, *74*(5), 532–534. https://doi.org/10.1055/s-2008-1074497

Leelananda, S. P., & Lindert, S. (2016). Computational methods in drug discovery. *Beilstein Journal of Organic Chemistry*. https://doi.org/10.3762/bjoc.12.267

Liu, X., Shi, D., Zhou, S., Liu, H., Liu, H., & Yao, X. (2018). Molecular dynamics simulations and novel drug discovery. *Expert Opinion on Drug Discovery*, *13*(1), 23–37. https://doi.org/10.1080/17460441.2018.1403419

Loving, R., Sjoberg, M., Wu, S.-R., Binley, J. M., & Garoff, H. (2013). Inhibition of the HIV-1 Spike by Single-PG9/16-Antibody Binding Suggests a Coordinated-Activation Model for Its Three Protomeric Units. *Journal of Virology*. https://doi.org/10.1128/JVI.00530-13

Lü, J.-M., Yan, S., Jamaluddin, S., Weakley, S. M., Liang, Z., Siwak, E. B., … DeBakey, M. E. (n.d.). *Ginkgolic acid inhibits HIV protease activity and HIV infection in vitro*. Retrieved from http://www.medscimonit.com/fulltxt.php?ICID=883261

Lu, L., Yu, F., Cai, L., Debnath, A. K., & Jiang, S. (2016). Development of Small-molecule HIV Entry Inhibitors Specifically Targeting gp120 or gp41. *Current Topics in Medicinal Chemistry*, *16*(10), 1074–1090. Retrieved from http://www.ncbi.nlm.nih.gov/pubmed/26324044

Lu, Y., & Jiang, T. (2013). Pseudovirus-based neuraminidase inhibition assays reveal potential H5N1 drug-resistant mutations. *Protein & Cell*, *4*(5), 356–363.

https://doi.org/10.1007/s13238-013-2125-y

Maartens, G., Celum, C., & Lewin, S. R. (2014). HIV infection: Epidemiology, pathogenesis, treatment, and prevention. *The Lancet*, *384*(9939), 258–271. https://doi.org/10.1016/S0140-6736(14)60164-1

Madec, Y., Boufassa, F., Avettand-Fenoel, V., Hendou, S., Melard, A., Boucherit, S., … Rouzioux, C. (2009). Early control of HIV-1 infection in long-term nonprogressors followed since diagnosis in the ANRS SEROCO/HEMOCO cohort. *Journal of Acquired Immune Deficiency Syndromes*. https://doi.org/10.1097/QAI.0b013e31818ce709

Magaret, C. A., Benkeser, D. C., Williamson, B. D., Borate, B. R., Carpp, L. N., Georgiev, I. S., … Gilbert, P. B. (2019). Prediction of VRC01 neutralization sensitivity by HIV-1 gp160 sequence features. *PLOS Computational Biology*, *15*(4), e1006952. https://doi.org/10.1371/journal.pcbi.1006952

Mahmoud, K. A., Hrapovic, S., & Luong, J. H. T. (2008). Picomolar detection of protease using peptide/single walled carbon nanotube/gold nanoparticle-modified electrode. *ACS Nano*. https://doi.org/10.1021/nn8000774

Marshall, G. R. (1993). A hierarchical approach to peptidomimetic design. *Tetrahedron*. https://doi.org/10.1016/S0040-4020(01)90214-5

Mather, S. T., Wright, E., Scott, S. D., & Temperton, N. J. (2014). Lyophilisation of influenza, rabies and Marburg lentiviral pseudotype viruses for the development and distribution of a neutralisation -assay-based diagnostic kit. *Journal of Virological Methods*, *210*, 51–58. https://doi.org/10.1016/j.jviromet.2014.09.021

Mayer, K. H., Seaton, K. E., Huang, Y., Grunenberg, N., Isaacs, A., Allen, M., … and the NIAID HIV Vaccine Trials Network, and the N. H. V. T. (2017). Safety, pharmacokinetics, and immunological activities of multiple intravenous or subcutaneous doses of an anti-HIV monoclonal antibody, VRC01, administered to HIV-uninfected adults: Results of a phase 1 randomized trial. *PLoS Medicine*, *14*(11), e1002435. https://doi.org/10.1371/journal.pmed.1002435

Mayer, K. H., Seaton, K. E., Huang, Y., Grunenberg, N., Isaacs, A., Allen, M., … Montefiori, D. C. (2017a). Safety, pharmacokinetics, and immunological activities of multiple intravenous or subcutaneous doses of an anti-HIV monoclonal antibody, VRC01, administered to HIV-uninfected adults: Results of a phase 1 randomized trial. *PLoS Medicine*. https://doi.org/10.1371/journal.pmed.1002435

Mayer, K. H., Seaton, K. E., Huang, Y., Grunenberg, N., Isaacs, A., Allen, M., … Montefiori, D. C. (2017b). Safety, pharmacokinetics, and immunological activities of multiple intravenous or subcutaneous doses of an anti-HIV monoclonal antibody, VRC01, administered to HIV-uninfected adults: Results of a phase 1 randomized trial. *PLoS Medicine*. https://doi.org/10.1371/journal.pmed.1002435

McCoy, L. E. (2018, October 16). The expanding array of HIV broadly neutralizing antibodies 11 Medical and Health Sciences 1108 Medical Microbiology Marit van Gils, m.j.vangils@amc.uva.nl; Rogier W Sanders, rws2002@med.cornell.edu. *Retrovirology*, Vol. 15. https://doi.org/10.1186/s12977-018-0453-y

McCoy, L. E., & Burton, D. R. (2017). Identification and specificity of broadly neutralizing antibodies against HIV. *Immunological Reviews*, Vol. 275, pp. 11–20.

https://doi.org/10.1111/imr.12484

McDonnell, A. M., & Dang, C. H. (2013). Basic review of the cytochrome p450 system. *Journal of the Advanced Practitioner in Oncology*, *4*(4), 263–268. Retrieved from http://www.ncbi.nlm.nih.gov/pubmed/25032007

McGregor, M. J., Luo, Z., & Jiang, X. (2006). Virtual Screening in Drug Discovery. In *Drug Discovery Research: New Frontiers in the Post-Genomic Era*. https://doi.org/10.1002/9780470131862.ch3

McGuire, A. T., Hoot, S., Dreyer, A. M., Lippy, A., Stuart, A., Cohen, K. W., … Stamatatos, L. (2013). Engineering HIV envelope protein to activate germline B cell receptors of broadly neutralizing anti-CD4 binding site antibodies. *The Journal of Experimental Medicine*. https://doi.org/10.1084/jem.20122824

McInnes, C. (2007). Virtual screening strategies in drug discovery. *Current Opinion in Chemical Biology*. https://doi.org/10.1016/j.cbpa.2007.08.033

Meng, X.-Y., Zhang, H.-X., Mezei, M., & Cui, M. (2011). Molecular docking: a powerful approach for structure-based drug discovery. *Current Computer-Aided Drug Design*. https://doi.org/10.1016/j.biotechadv.2011.08.021.Secreted

Meuser, M. E., Murphy, M. B., Rashad, A. A., & Cocklin, S. (2018). Kinetic Characterization of Novel HIV-1 Entry Inhibitors: Discovery of a Relationship between Off-Rate and Potency. *Molecules (Basel, Switzerland)*, *23*(8). https://doi.org/10.3390/molecules23081940

Michelini, E., Cevenini, L., Mezzanotte, L., Coppa, A., & Roda, A. (2010). Cell-based assays: Fuelling drug discovery. *Analytical and Bioanalytical Chemistry*, *398*(1), 227–238.

https://doi.org/10.1007/s00216-010-3933-z

Montero, M., van Houten, N. E., Wang, X., & Scott, J. K. (2008). The Membrane-Proximal External Region of the Human Immunodeficiency Virus Type 1 Envelope: Dominant Site of Antibody Neutralization and Target for Vaccine Design. *Microbiology and Molecular Biology Reviews*. https://doi.org/10.1128/MMBR.00020-07

Moore, P. L., Williamson, C., & Morris, L. (2015). Virological features associated with the development of broadly neutralizing antibodies to HIV-1. *Trends in Microbiology*. https://doi.org/10.1016/j.tim.2014.12.007

Morris G.M., & Dallakyan S. (2013). AutoDock — AutoDock. *02-27*.

Mullard, A. (2014). New drugs cost US$2.6 billion to develop. *Nature Reviews Drug Discovery*, *13*(12), 877–877. https://doi.org/10.1038/nrd4507

Nachega, J. B., Mills, E. J., & Schechter, M. (2010). Antiretroviral therapy adherence and retention in care in middle-income and low-income countries: Current status of knowledge and research priorities. *Current Opinion in HIV and AIDS*. https://doi.org/10.1097/COH.0b013e328333ad61

Nichols, B. E., Boucher, C. A. B., & van de Vijver, D. A. M. C. (2011). HIV testing and antiretroviral treatment strategies for prevention of HIV infection: Impact on antiretroviral drug resistance. *Journal of Internal Medicine*. https://doi.org/10.1111/j.1365-2796.2011.02456.x

O'Boyle, N. M., Banck, M., James, C. A., Morley, C., Vandermeersch, T., & Hutchison, G. R. (2011). Open Babel: An Open chemical toolbox. *Journal of Cheminformatics*.

https://doi.org/10.1186/1758-2946-3-33

Obiako, O. R., & Muktar, H. M. (2010). Challenges of HIV treatment in resource-poor countries: a review. *Nigerian Journal of Medicine : Journal of the National Association of Resident Doctors of Nigeria*. https://doi.org/10.4314/njm.v19i4.69785

Okulicz, J. F., & Lambotte, O. (2011). Epidemiology and clinical characteristics of elite controllers. *Curr Opin HIV AIDS*. https://doi.org/10.1097/COH.0b013e328344f35e

Olshevsky, U., Helseth, E., Furman, C., Li, J., Haseltine, W., & Sodroski, J. (1990). Identification of individual human immunodeficiency virus type 1 gp120 amino acids important for CD4 receptor binding. *Journal of Virology*, *64*(12), 5701–5707. Retrieved from http://www.ncbi.nlm.nih.gov/pubmed/2243375

Pajouhesh, H., & Lenz, G. R. (2005). Medicinal chemical properties of successful central nervous system drugs. *NeuroRx : The Journal of the American Society for Experimental NeuroTherapeutics*, *2*(4), 541–553. https://doi.org/10.1602/neurorx.2.4.541

Pancera, M., Lai, Y.-T., Bylund, T., Druz, A., Narpala, S., O'Dell, S., … Kwong, P. D. (2017). Crystal structures of trimeric HIV envelope with entry inhibitors BMS-378806 and BMS-626529. *Nature Chemical Biology*, *13*(10), 1115–1122. https://doi.org/10.1038/nchembio.2460

Pancera, M., Zhou, T., Druz, A., Georgiev, I. S., Soto, C., Gorman, J., … Kwong, P. D. (2014). Structure and immune recognition of trimeric pre-fusion HIV-1 Env. *Nature*. https://doi.org/10.1038/nature13808

Panchal, R. G., Reid, S. P., Tran, J. P., Bergeron, A. A., Wells, J., Kota, K. P., … Bavari, S. (2012).

Identification of an antioxidant small-molecule with broad-spectrum antiviral activity. *Antiviral Research*, *93*(1), 23–29. https://doi.org/10.1016/j.antiviral.2011.10.011

Pardridge, W. M. (2005). The blood-brain barrier: Bottleneck in brain drug development. *NeuroRx*. https://doi.org/10.1602/neurorx.2.1.3

Paslay, J., Morin, J., & Harrison, R. (2010). High Throughput Screening in the Twenty-First Century. *Topics in Medicinal Chemistry*. https://doi.org/10.1007/7355

Pear, W. S., Nolan, G. P., Scott, M. L., & Baltimore, D. (1993). Production of high-titer helper-free retroviruses by transient transfection. *Proceedings of the National Academy of Sciences*, *90*(18), 8392–8396. https://doi.org/10.1073/pnas.90.18.8392

Pejchal, R., Doores, K. J., Walker, L. M., Khayat, R., Huang, P. S., Wang, S. K., … Wilson, I. A. (2011). A potent and broad neutralizing antibody recognizes and penetrates the HIV glycan shield. *Science*. https://doi.org/10.1126/science.1213256

Pelay-Gimeno, M., Glas, A., Koch, O., & Grossmann, T. N. (2015). Structure-Based Design of Inhibitors of Protein-Protein Interactions: Mimicking Peptide Binding Epitopes. *Angewandte Chemie - International Edition*. https://doi.org/10.1002/anie.201412070

Phillips, A. N., Stover, J., Cambiano, V., Nakagawa, F., Jordan, M. R., Pillay, D., … Bertagnolio, S. (2017). Impact of HIV drug resistance on HIV/AIDS-associated mortality, new infections, and antiretroviral therapy program costs in Sub-Saharan Africa. *Journal of Infectious Diseases*, *215*(9), 1362–1365. https://doi.org/10.1093/infdis/jix089

Postnikova, E., Cong, Y., DeWald, L. E., Dyall, J., Yu, S., Hart, B. J., … Jahrling, P. B. (2018a). Testing therapeutics in cell-based assays: Factors that influence the apparent potency of

drugs. *PLoS ONE*. https://doi.org/10.1371/journal.pone.0194880

Postnikova, E., Cong, Y., DeWald, L. E., Dyall, J., Yu, S., Hart, B. J., … Jahrling, P. B. (2018b). Testing therapeutics in cell-based assays: Factors that influence the apparent potency of drugs. *PLOS ONE*, *13*(3), e0194880. https://doi.org/10.1371/journal.pone.0194880

Pustil, R. (2016). Global AIDS. *Aids*, *17 Suppl 4*, S3-11. https://doi.org/10.1073/pnas.86.15.5781

Rasheed, M., Bettadapura, R., & Bajaj, C. (2015). Computational Refinement and Validation Protocol for Proteins with Large Variable Regions Applied to Model HIV Env Spike in CD4 and 17b Bound State. *Structure*. https://doi.org/10.1016/j.str.2015.03.026

Ray, N., Hwang, C., Healy, M. D., Whitcomb, J., Lataillade, M., Wind-Rotolo, M., … Hanna, G. J. (2013). Prediction of Virological Response and Assessment of Resistance Emergence to the HIV-1 Attachment Inhibitor BMS-626529 During 8-Day Monotherapy With Its Prodrug BMS-663068. *JAIDS Journal of Acquired Immune Deficiency Syndromes*, *64*(1), 7–15. https://doi.org/10.1097/QAI.0b013e31829726f3

Reese, H. R., Shanahan, C. C., Proulx, C., & Menegatti, S. (2020). Peptide science: A "rule model" for new generations of peptidomimetics. *Acta Biomaterialia*. https://doi.org/10.1016/j.actbio.2019.10.045

Rester, U. (2008). From virtuality to reality - Virtual screening in lead discovery and lead optimization: a medicinal chemistry perspective. *Current Opinion in Drug Discovery & Development*.

Ripka, A. S., & Rich, D. H. (1998). Peptidomimetic design. *Current Opinion in Chemical Biology*. https://doi.org/10.1016/S1367-5931(98)80119-1

Saeed, M. F., Kolokoltsov, A. A., & Davey, R. A. (2006). Novel, rapid assay for measuring entry of diverse enveloped viruses, including HIV and rabies. *Journal of Virological Methods*, *135*(2), 143–150. https://doi.org/10.1016/j.jviromet.2006.02.011

Salata, C., Calistri, A., Alvisi, G., Celestino, M., Parolin, C., & Palù, G. (2019). Ebola virus entry: From molecular characterization to drug discovery. *Viruses*, *11*(3). https://doi.org/10.3390/v11030274

Salazar, G., Zhang, N., Fu, T.-M., & An, Z. (2017). Antibody therapies for the prevention and treatment of viral infections. *Npj Vaccines*. https://doi.org/10.1038/s41541-017-0019-3

Salehi, B., Anil Kumar, N. V, Sharifi-Rad, M., Kılıç, M., Mahady, G. B., Vlaisavljevic, S., … Sharifi-Rad, J. (2018). Molecular Sciences Medicinal Plants Used in the Treatment of Human Immunodeficiency Virus. *Int. J. Mol. Sci*, *19*, 1459. https://doi.org/10.3390/ijms19051459

Salehi, B., Kumar, N. V. A., Şener, B., Sharifi-Rad, M., Kılıç, M., Mahady, G. B., … Sharifi-Rad, J. (2018). Medicinal Plants Used in the Treatment of Human Immunodeficiency Virus. *International Journal of Molecular Sciences*, *19*(5). https://doi.org/10.3390/ijms19051459

Scanlan, C. N., Pantophlet, R., Wormald, M. R., Ollmann Saphire, E., Stanfield, R., Wilson, I. A., … Burton, D. R. (2002). The broadly neutralizing anti-human immunodeficiency virus type 1 antibody 2G12 recognizes a cluster of alpha1-->2 mannose residues on the outer face of gp120. *Journal of Virology*. https://doi.org/10.1128/JVI.76.14.7306-7321.2002

Scharf, L., Scheid, J. F., Lee, J. H., West, A. P., Chen, C., Gao, H., … Bjorkman, P. J. (2014). Antibody 8ANC195 Reveals a Site of Broad Vulnerability on the HIV-1 Envelope Spike. *Cell Reports*. https://doi.org/10.1016/j.celrep.2014.04.001

Scheid, J. F., Mouquet, H., Ueberheide, B., Diskin, R., Klein, F., Oliveira, T. Y. K., … Nussenzweig, M. C. (2011). Sequence and Structural Convergence of Broad and Potent HIV Antibodies That Mimic CD4 Binding. *Science*. https://doi.org/10.1126/science.1207227

Schrodinger Software Release 2015-2. (2015). Induced Fit Docking. *Schrodinger Press*.

Scott, A. M., Wolchok, J. D., & Old, L. J. (2012). Antibody therapy of cancer. *Nat Rev Cancer*. https://doi.org/10.1038/nrc3236

Seelmeier, S., Schmidt, H., Turk, V., & von der Helm, K. (1988). Human immunodeficiency virus has an aspartic-type protease that can be inhibited by pepstatin A. *Proceedings of the National Academy of Sciences*. https://doi.org/10.1073/pnas.85.18.6612

Shaw, G. M., & Hunter, E. (2012). HIV transmission. *Cold Spring Harbor Perspectives in Medicine*. https://doi.org/10.1101/cshperspect.a006965

Shekhar, C. (2008). In Silico Pharmacology: Computer-Aided Methods Could Transform Drug Development. *Chemistry and Biology*. https://doi.org/10.1016/j.chembiol.2008.05.001

Shen, R., Raska, M., Bimczok, D., Novak, J., & Smith, P. D. (2014). HIV-1 Envelope Glycan Moieties Modulate HIV-1 Transmission. *Journal of Virology*. https://doi.org/10.1128/JVI.02164-14

Sherman, W., Beard, H. S., & Farid, R. (2006). Use of an induced fit receptor structure in virtual screening. *Chemical Biology and Drug Design*. https://doi.org/10.1111/j.1747-0285.2005.00327.x

Simek, M. D., Rida, W., Priddy, F. H., Pung, P., Carrow, E., Laufer, D. S., … Koff, W. C. (2009). Human Immunodeficiency Virus Type 1 Elite Neutralizers: Individuals with Broad and

Potent Neutralizing Activity Identified by Using a High-Throughput Neutralization Assay together with an Analytical Selection Algorithm. *Journal of Virology*, *83*(14), 7337–7348. https://doi.org/10.1128/JVI.00110-09

Singh, I. P., Bharate, S. B., & Bhutani, K. K. (2005). Anti-HIV natural products. *Current Science*.

Sliwoski, G., Kothiwale, S., Meiler, J., & Lowe, E. W. (2014a). Computational methods in drug discovery. *Pharmacological Reviews*. https://doi.org/10.1124/pr.112.007336

Sliwoski, G., Kothiwale, S., Meiler, J., & Lowe, E. W. (2014b). Computational methods in drug discovery. *Pharmacological Reviews*. https://doi.org/10.1124/pr.112.007336

Smith, R. L., de Boer, R., Brul, S., Budovskaya, Y., & van der Spek, H. (2013). Premature and accelerated aging: HIV or HAART? *Frontiers in Genetics*. https://doi.org/10.3389/fgene.2012.00328

Soneoka, Y., Cannon, P. M., Ramsdale, E. E., Griffiths, J. C., Romano, G., Kingsman, S. M., & Kingsman, A. J. (1995). A transient three-plasmid expression system for the production of high titer retroviral vectors. *Nucleic Acids Research*, *23*(4), 628–633. https://doi.org/10.1093/nar/23.4.628

Stephenson, K. E., & Barouch, D. H. (2016). Broadly Neutralizing Antibodies for HIV Eradication. *Current HIV/AIDS Reports*. https://doi.org/10.1007/s11904-016-0299-7

Stolk, L. M. L., & Lüers, J. F. J. (2004). Increasing number of anti-HIV drugs but no definite cure: Review of anti-HIV drugs. *Pharmacy World and Science*, Vol. 26, pp. 133–136. https://doi.org/10.1023/B:PHAR.0000026815.44214.83

Sundquist, W. I., & Kräusslich, H. G. (2012). HIV-1 assembly, budding, and maturation. *Cold*

Spring Harbor Perspectives in Medicine. https://doi.org/10.1101/cshperspect.a006924

Sung, V. M. H., & Lai, M. M. C. (2002). Murine retroviral pseudotype virus containing hepatitis B virus large and small surface antigens confers specific tropism for primary human hepatocytes: a potential liver-specific targeting system. *Journal of Virology*, *76*(2), 912–917. https://doi.org/10.1128/jvi.76.2.912-917.2002

Suthar, A. B., Ford, N., Bachanas, P. J., Wong, V. J., Rajan, J. S., Saltzman, A. K., … Baggaley, R. C. (2013). Towards Universal Voluntary HIV Testing and Counselling: A Systematic Review and Meta-Analysis of Community-Based Approaches. *PLoS Medicine*. https://doi.org/10.1371/journal.pmed.1001496

Talekar, A., Pessi, A., Glickman, F., Sengupta, U., Briese, T., Whitt, M. A., … Porotto, M. (2012). Rapid Screening for Entry Inhibitors of Highly Pathogenic Viruses under Low-Level Biocontainment. *PLoS ONE*, *7*(3), e30538. https://doi.org/10.1371/journal.pone.0030538

Taylor, B. S., Sobieszczyk, M. E., McCutchan, F. E., & Hammer, S. M. (2008). The Challenge of HIV-1 Subtype Diversity. *New England Journal of Medicine*. https://doi.org/10.1056/NEJMra0706737

Temperton, N. J., Chan, P. K., Simmons, G., Zambon, M. C., Tedder, R. S., Takeuchi, Y., & Weiss, R. A. (2005). Longitudinally profiling neutralizing antibody response to SARS coronavirus with pseudotypes. *Emerging Infectious Diseases*, *11*(3), 411–416. https://doi.org/10.3201/eid1103.040906

Temperton, N. J., & Wright, E. (2009). Retroviral Pseudotypes. In *Encyclopedia of Life Sciences*. https://doi.org/10.1002/9780470015902.a0021549

Temperton, N. J., Wright, E., & Scott, S. D. (2015). Retroviral Pseudotypes - From Scientific Tools to Clinical Utility. In *eLS*. https://doi.org/10.1002/9780470015902.a0021549.pub2

Towner, J. S., Paragas, J., Dover, J. E., Gupta, M., Goldsmith, C. S., Huggins, J. W., & Nichol, S. T. (2005). Generation of eGFP expressing recombinant Zaire ebolavirus for analysis of early pathogenesis events and high-throughput antiviral drug screening. *Virology*. https://doi.org/10.1016/j.virol.2004.10.048

Trott, O., & Olson, A. J. (2010). Software news and update AutoDock Vina: Improving the speed and accuracy of docking with a new scoring function, efficient optimization, and multithreading. *Journal of Computational Chemistry*. https://doi.org/10.1002/jcc.21334

Turner, B. G., & Summers, M. F. (1999). Structural biology of HIV. *Journal of Molecular Biology*. https://doi.org/10.1006/jmbi.1998.2354

Turner, P. (2005). XMGRACE, Version 5.1. 19. *Center for Coastal and Land-Margin Research, Oregon Graduate Institute of Science and Technology, Beaverton*. https://doi.org/10.1163/_q3_SIM_00374

U.S. Department of Health and Human Services. (2016). The HIV Life Cycle | Understanding HIV/AIDS | AIDSinfo. *AIDSinfo*.

UNAIDS. (2014). UNAIDS report | UNAIDS.

Vabenø, J., Haug, B. E., & Rosenkilde, M. M. (2015). Progress toward rationally designed small-molecule peptide and peptidomimetic CXCR4 antagonists. *Future Medicinal Chemistry*. https://doi.org/10.4155/fmc.15.64

Vagner, J., Qu, H., & Hruby, V. J. (2008). Peptidomimetics, a synthetic tool of drug discovery.

Current Opinion in Chemical Biology. https://doi.org/10.1016/j.cbpa.2008.03.009

Veber, D. F., Johnson, S. R., Cheng, H.-Y., Smith, B. R., Ward, K. W., & Kopple, K. D. (2002). Molecular Properties That Influence the Oral Bioavailability of Drug Candidates. *Journal of Medicinal Chemistry*, *45*(12), 2615–2623. https://doi.org/10.1021/jm020017n

Vergis, E. N., & Mellors, J. W. (2000). Natural history of HIV-1 infection. *Infectious Disease Clinics of North America*, *14*(4), 809–825, v–vi. Retrieved from http://www.ncbi.nlm.nih.gov/pubmed/11144640

Walker, L. M., Huber, M., Doores, K. J., Falkowska, E., Pejchal, R., Julien, J.-P., … Poignard, P. (2011). Broad neutralization coverage of HIV by multiple highly potent antibodies. *Nature*, *477*(7365), 466–470. https://doi.org/10.1038/nature10373

Walker, L. M., Huber, M., Doores, K. J., Falkowska, E., Pejchal, R., Julien, J. P., … Poignard, P. (2011). Broad neutralization coverage of HIV by multiple highly potent antibodies. *Nature*. https://doi.org/10.1038/nature10373

Wang, F., Liu, D., Wang, H., Luo, C., Zheng, M., Liu, H., … Jiang, H. (2011). Computational screening for active compounds targeting protein sequences: Methodology and experimental validation. *Journal of Chemical Information and Modeling*. https://doi.org/10.1021/ci200264h

Weber, I. T., & Agniswamy, J. (2009). HIV-1 Protease: Structural perspectives on drug resistance. *Viruses*. https://doi.org/10.3390/v1031110

Wensing, A. M. J., van Maarseveen, N. M., & Nijhuis, M. (2010). Fifteen years of HIV Protease Inhibitors: raising the barrier to resistance. *Antiviral Research*.

https://doi.org/10.1016/j.antiviral.2009.10.003

WHO. (2010). PMTCT strategic vision 2010–2015 : preventing mother-to-child transmission of HIV to reach the UNGASS and Millennium Development Goals. *World Health Organization*.

WHO. (2016). Millennium Development Goals (MDGs). Retrieved from WHO website: http://www.who.int/topics/millennium_development_goals/en/

Wibmer, C. K., Moore, P. L., & Morris, L. (2015). HIV broadly neutralizing antibody targets. *Current Opinion in HIV and AIDS*, *10*(3), 135–143. https://doi.org/10.1097/COH.0000000000000153

Wilen, C. B., Tilton, J. C., & Doms, R. W. (2012). HIV: Cell binding and entry. *Cold Spring Harbor Perspectives in Medicine*, *2*(8). https://doi.org/10.1101/cshperspect.a006866

Willett, P. (2006). Similarity-based virtual screening using 2D fingerprints. *Drug Discovery Today*. https://doi.org/10.1016/j.drudis.2006.10.005

Wolf, M. C., Freiberg, A. N., Zhang, T., Akyol-Ataman, Z., Grock, A., Hong, P. W., … Lee, B. (2010). A broad-spectrum antiviral targeting entry of enveloped viruses. *Proceedings of the National Academy of Sciences of the United States of America*, *107*(7), 3157–3162. https://doi.org/10.1073/pnas.0909587107

World Health Organisation. (2016). Consolidated guidelines on the use of antiretroviral drugs for treating and preventing HIV infection: recommendations for a public health approach - 2nd ed. *WHO Guidelines*.

Wu, X., Yang, Z.-Y., Li, Y., Hogerkorp, C.-M., Schief, W. R., Seaman, M. S., … Mascola, J. R. (2010). Rational Design of Envelope Identifies Broadly Neutralizing Human Monoclonal

Antibodies to HIV-1. *Science*, *329*(5993), 856–861. https://doi.org/10.1126/science.1187659

Wu, X., Yang, Z. Y., Li, Y., Hogerkorp, C. M., Schief, W., Seaman, M. S., … Nabel, G. J. (2011). Rational design of envelope surface identifies broadly neutralizing human monoclonal antibodies to HIV-1. *J ACQUIRED IMMUNE DEFIC SYNDR*.

Xiang, M. L., Cao, Y., Fan, W. J., Chen, L. J., & Mo, Y. R. (2012). Computer-aided drug design: Lead discovery and optimization. *Combinatorial Chemistry & High Throughput Screening*.

Xu, M., & Lill, M. A. (2013). Induced fit docking, and the use of QM/MM methods in docking. *Drug Discovery Today. Technologies*. https://doi.org/10.1016/j.ddtec.2013.02.003

Yang, S. Y. (2010). Pharmacophore modeling and applications in drug discovery: Challenges and recent advances. *Drug Discovery Today*. https://doi.org/10.1016/j.drudis.2010.03.013

Yuan, S., Chan, H. C. S., & Hu, Z. (2017). Using PyMOL as a platform for computational drug design. *Wiley Interdisciplinary Reviews: Computational Molecular Science*. https://doi.org/10.1002/wcms.1298

Zhao, Q., Ma, L., Jiang, S., Lu, H., Liu, S., He, Y., … Debnath, A. K. (2005). Identification of N-phenyl-N′-(2,2,6,6-tetramethyl-piperidin-4-yl)-oxalamides as a new class of HIV-1 entry inhibitors that prevent gp120 binding to CD4. *Virology*, *339*(2), 213–225. https://doi.org/10.1016/J.VIROL.2005.06.008

Zhou, T., Georgiev, I., Wu, X., Yang, Z. Y., Dai, K., Finzi, A., … Kwong, P. D. (2010). Structural basis for broad and potent neutralization of HIV-1 by antibody VRC01. *Science*. https://doi.org/10.1126/science.1192819

Zhou, T., Xu, L., Dey, B., Hessell, A. J., Van Ryk, D., Xiang, S. H., … Kwong, P. D. (2007).

Structural definition of a conserved neutralization epitope on HIV-1 gp120. *Nature*. https://doi.org/10.1038/nature05580

Zhou, T., Zhu, J., Wu, X., Moquin, S., Zhang, B., Acharya, P., … Kwong, P. D. (2013). Multidonor analysis reveals structural elements, genetic determinants, and maturation pathway for HIV-1 neutralization by VRC01-class antibodies. *Immunity*. https://doi.org/10.1016/j.immuni.2013.04.012

Zhou, Y., Agudelo, J., Lu, K., Goetz, D. H., Hansell, E., Chen, Y. T., … Simmons, G. (2011). Inhibitors of SARS-CoV entry--identification using an internally-controlled dual envelope pseudovirion assay. *Antiviral Research*, *92*(2), 187–194. https://doi.org/10.1016/j.antiviral.2011.07.016

APPENDICES

APPENDIX I

Molecular Docking Analysis of Ten Selected Compounds

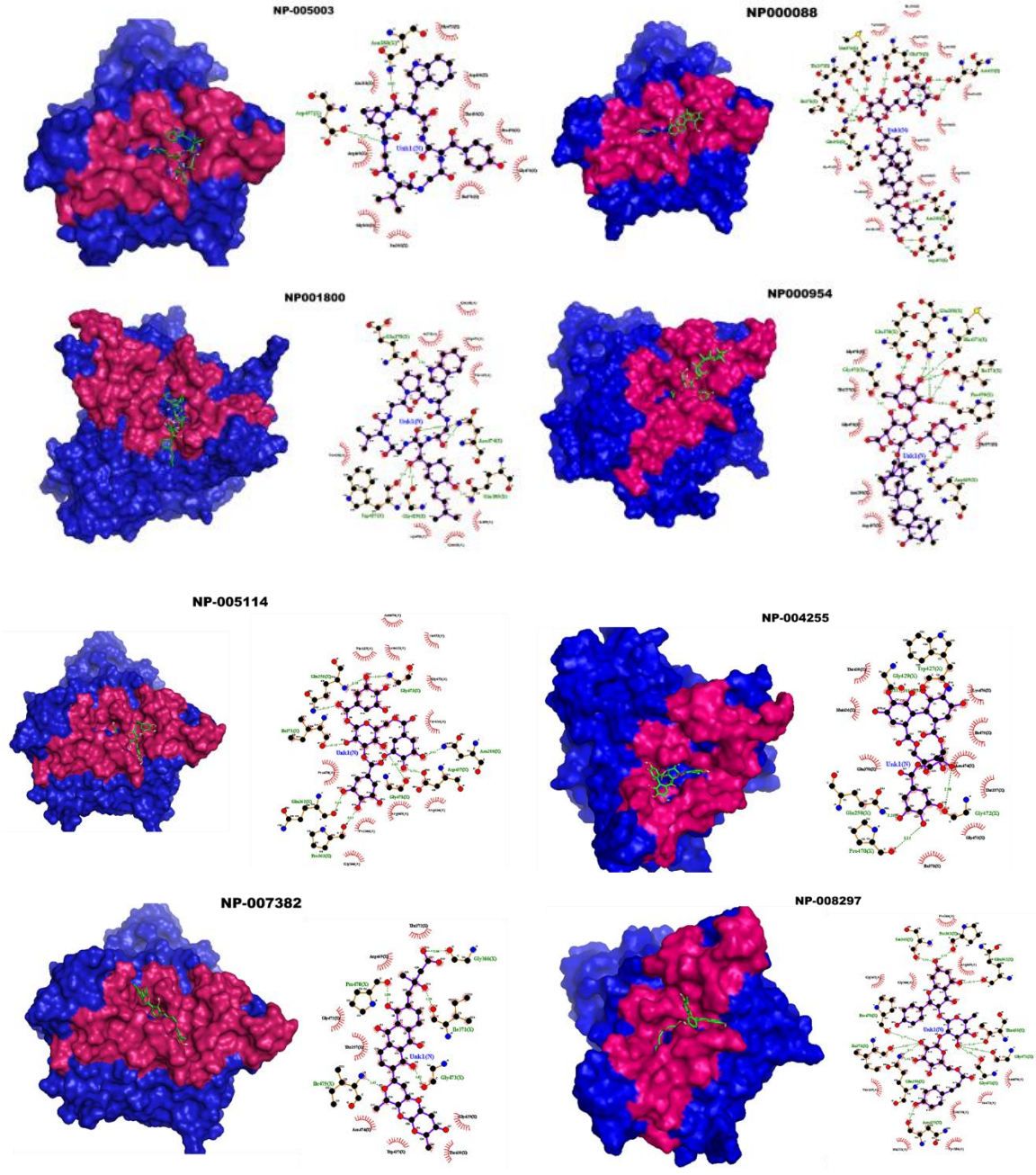

NP-007422

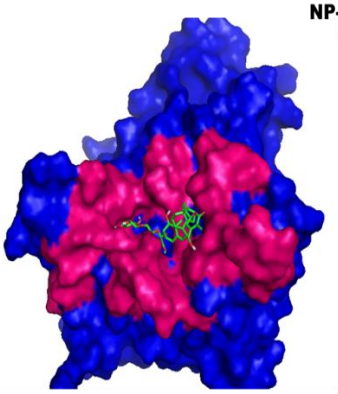

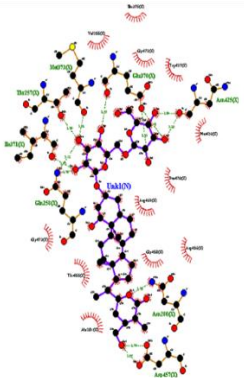

FRG-00075

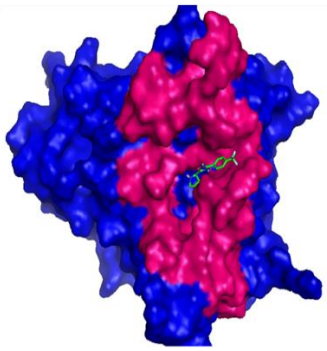

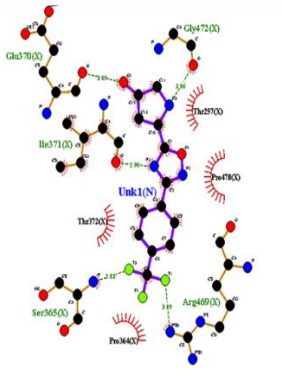

APPENDIX II

Chemical structure of the ten selected compounds

Chemical structure of the ten selected compounds	
Compound ID	**Chemical Structure**
NP-000088	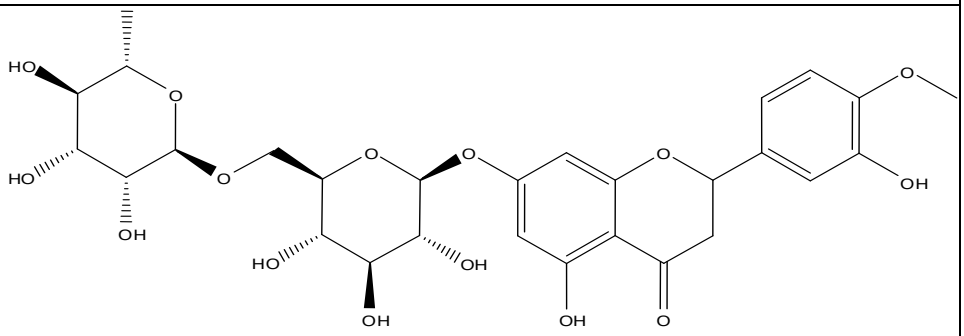
NP-000954	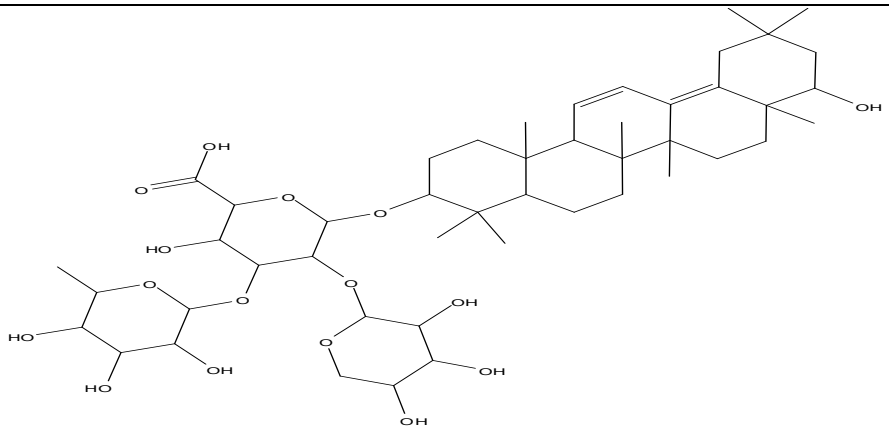
NP-004255	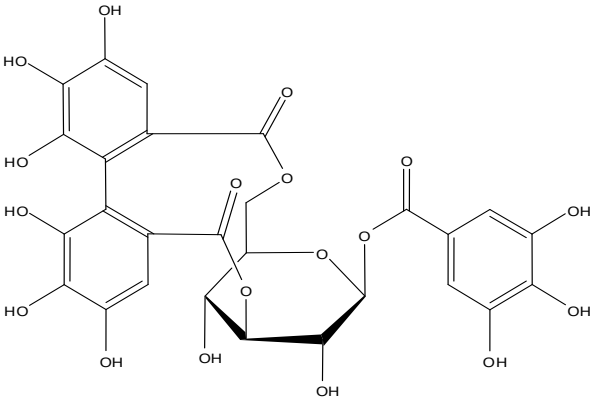

NP-005003	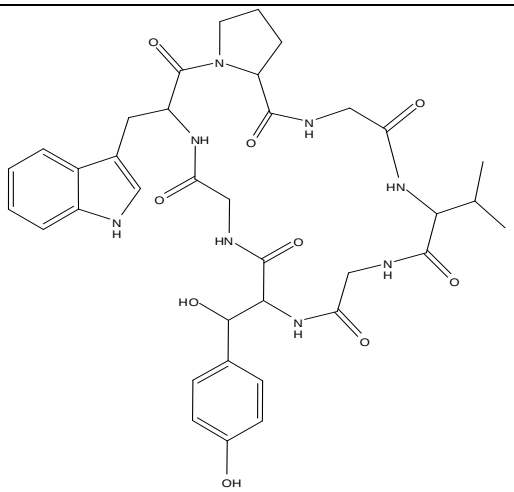
NP-005114	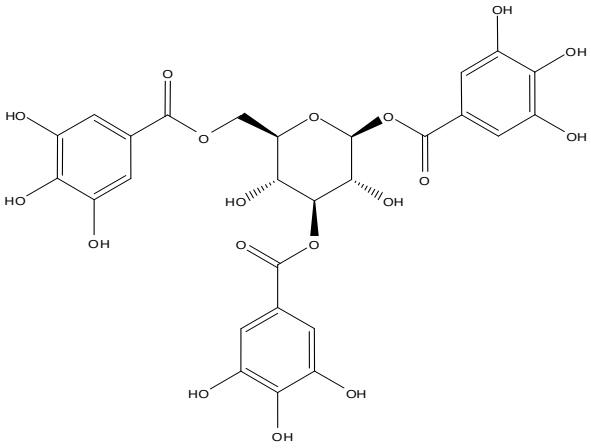
NP-007382	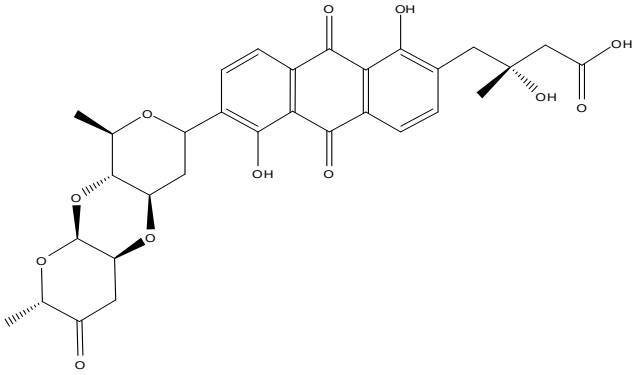

NP-007422	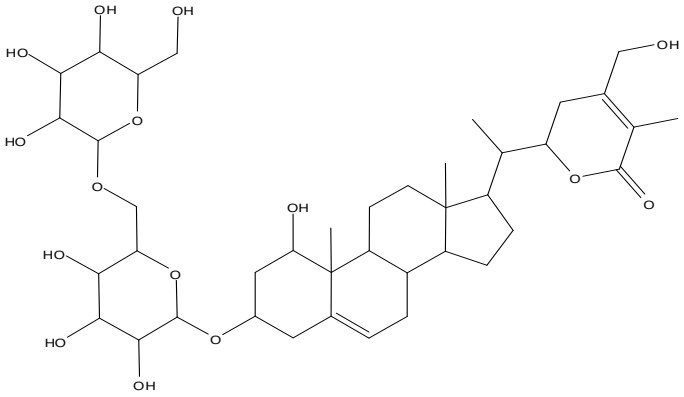
NP-008297	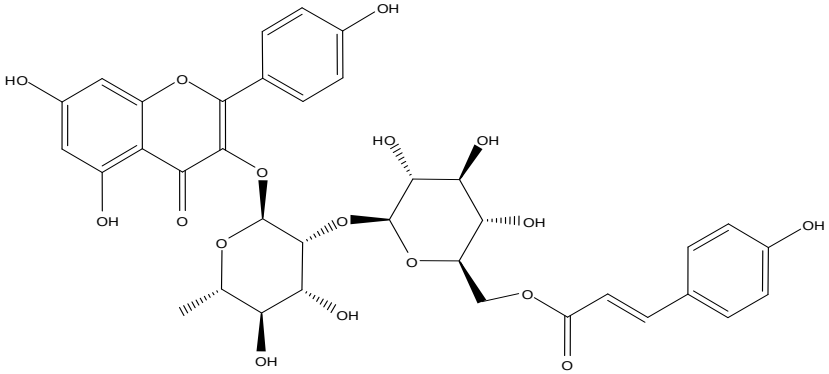
NP-001800	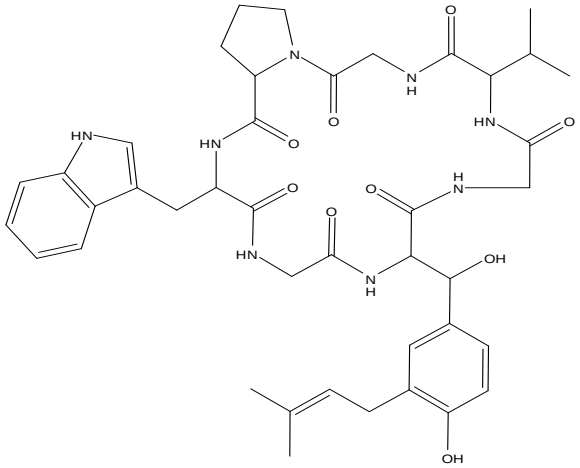

FRG-00075